

# The neural representation of abstract visual sequences

Nadira del R. Yusif Rodríguez

B. A. Psychology, University of Puerto Rico, Río Piedras 2016

A thesis dissertation submitted in partial fulfillment of the requirements for  
the degree of *Doctor of Philosophy*  
in the department of Neuroscience at Brown University

Providence, Rhode Island

February 2023

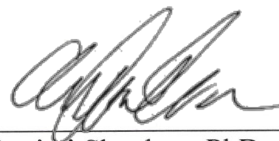
© Copyright 2023 by Nadira del R. Yusif Rodríguez

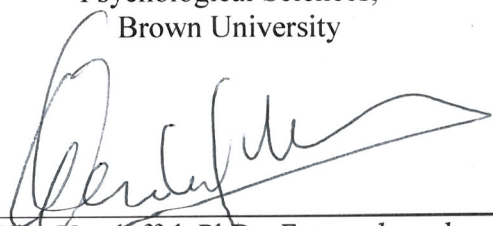
This dissertation by Nadira del R. Yusif Rodríguez is accepted in its present form by the Department of Neuroscience as satisfying the dissertation requirements for the degree of Doctor of Philosophy

Date: 1/11/2023   
Theresa M. Desrochers, PhD., *Advisor*  
Department of Neuroscience,  
Brown University

Recommended to the Graduate Council

Date: 1/10/2023   
David Sheinberg, PhD., *Reader, Committee Chair,*  
Department of Neuroscience,  
Brown University

Date: 1/10/2023   
Amitai Shenhav, PhD., *Reader*  
Department of Cognitive, Linguistic, and  
Psychological Sciences,  
Brown University

Date: January 10, 2023   
Wim Vanduffel, PhD., *External reader*  
Department of Neurosciences, KU Leuven

Approved by the Graduate Council

Date: \_\_\_\_\_  
Thomas A. Lewis, PhD.,  
Dean of Graduate School, Brown University

# Curriculum Vitae

**Nadira del R. Yusif Rodríguez**

nadira\_yusif\_rodriguez@brown.edu

Personal Website: <https://nyusif.github.io/>

Brown University, Neuroscience Graduate Program

---

## Education

<b>Brown University</b> , Neuroscience Department	Providence, RI
Doctoral candidate (PhD) in Neuroscience	2016 – Expected Winter 2022
University of Puerto Rico, Rio Piedras Campus	San Juan, PR
B.A. Psychology	2016

## Research Experience

<b>Graduate</b>	Providence, RI
Neuroscience, Brown University; Advisor: Dr. Theresa Desrochers	2016 – Present

### **Neural representation of abstract sequences in nonhuman primates**

Trained and scanned awake primates using fMRI while they complete computerized visual tasks developed using Tcl/Tk. Completed imaging and behavioral eye movement data analysis using Matlab/SPM.

### **Undergraduate**

University of Puerto Rico, Rio Piedras; Advisor: Dr. Carmen Maldonado-Vlaar	2014-2016
---	-----------

### **Blockade of FAAH/TRPV1 and Indirect Activation of CB1 Receptors in the NAcc Shell**

Intracranially microinjected rats in the Nucleus Accumbens shell. Used behavioral tasks, histological techniques, and biochemical assays like Western Blotting to examine the role of these receptors in the endocannabinoid system and anxiety-like states.

University of Puerto Rico, Rio Piedras; Advisor: Dr. Guillermo Bernal	2013-2016
---	-----------

### **Meta-analysis of Therapeutic Effectiveness in Hispanic/Latinos**

Examined studies containing therapeutic interventions for psychological conditions, with an emphasis on anxiety and depression. Completed a meta-analysis on selected studies that included therapeutic intervention in Hispanic and Latino populations.

Leadership Alliance SR-EIP, Brown University; Advisor: Joo-Hyun Song	Summer 2015
--	-------------

### **Interference Effect on Visuomotor Rotational Adaptation and Recall**

Tested human participants on a computerized behavioral task developed using Matlab code to study visuomotor learning interference and adaptation.

## Funding

Trainee, NSF-EPSCoR Neural Basis of Attention, #1632738	2018-2021
Trainee, NIGMS-NIH Initiative to Maximize Student Development (IMSD), #R25GM083270	2016-2018

## Publications

- Yusif Rodriguez, N.**, McKim, T. H., Basu, D., Ahuja, A., and Desrochers, T. M. (2022). Monkey dorsolateral prefrontal cortex monitors abstract visual sequences during a no-report task. Submitted for Publication. bioRxiv doi: <https://doi.org/10.1101/2022.09.19.508576>.
- Ahuja, A., & **Rodriguez, N. Y.** (2022). Is the Dorsolateral Prefrontal Cortex Actually Several Different Brain Areas?. *Journal of Neuroscience*, 42(33), 6310-6312.
- Desrochers, T. M., Ahuja, A., Maechler, M., Shires, J., **Yusif Rodriguez, N.**, & Berryhill, M. E. (2022). Caught in the ACTS: Defining Abstract Cognitive Task Sequences as an Independent Process. *Journal of Cognitive Neuroscience*, 1-12.
- Milham, M., Petkov, C., Belin, P., Hamed, S. B., Evrard, H., Fair, D., ... **Yusif Rodriguez, N.**, ... & Ortiz-Rios, M. (2022). Toward next-generation primate neuroscience: A collaboration-based strategic plan for integrative neuroimaging. *Neuron*, 110(1), 16-20.
- Pardo-García, T. R., **Yusif-Rodriguez, N.**, Yudowski, G., & Maldonado-Vlaar, C. S. (2020). Blockade of the endovanilloid receptor, TRPV1, and of the endocannabinoid enzyme, FAAH, within the nucleus accumbens shell elicits anxiolytic-like effects in male rats. *Neuroscience letters*, 732, 135023.
- Adames, C., Bernal, G., and **Yusif, N.** (2015). The Training Challenges in Evidence Based Psychological Treatments and Evidence Based Practice: Answer to Reflection on Training by Padilla-Martínez. *Ciencias de la Conducta*, 30(1), 192-199.

## Awards and Academic Achievements

Vanderbilt Integrated Training Alliance (VITA) Scholars Symposium	2021
Course Manager, Summer Program In Neuroscience Excellence and Success (SPINES), MBL	2019
Invited Participant, Summer Program In Neuroscience Excellence and Success (SPINES), MBL	2017
Invited Participant, Quantitative Methods Workshop (QMW), MIT	2016
Outstanding Presentation Award, Annual Biomedical Research Conference for Minority Students (ABRCMS)	2015
Research Assistantship, NIH-Research Initiative for Scientific Enhancement (RISE)	2015
International Honor Society in Psychology (PSI CHI)	2015
Puerto Rico House of Representatives Award for student led meta-analysis workshop	2015
Dean's List , University of Puerto Rico, Rio Piedras Campus	2013

## Mentoring and Teaching

### Mentees

Kyoko Leaman – Independent Research and Undergraduate Teaching and Research Award (UTRA)	2021-Present
Jay Vankawala - UTRA and honor's thesis	2019-2021
Ambar Delgado - Brown University Post-Baccalaurate Research Education Program (PREP)	2018-2019
Meghan Hershkowitz - UTRA	Summer 2018

### Teaching

Guest Lecturer, NEUR2050: Advanced Systems Neuroscience	Fall 2020, 2021
Experimental design session for BP-Endure Summer students	2019
CareerLab Panelist - Graduate School in the Sciences	2018
Teaching Assistant, NEUR1540: Neurobiology of learning and memory	Spring 2018

## Organizations and Memberships

Member, Society for the Advancement of Chicanos/Hispanics and Native Americans in Science (SACNAS), Brown University	2016- Present
Member, Graduate Women in Science & Engineering (GWISE), Brown University	2016- Present
Member, Society for Neuroscience (SfN)	2015- Present
Community Outreach Director of Brown University's SACNAS Chapter	2017- 2020
Neuroscience Scholars Program Associate, Society for Neuroscience (SfN)	2017-2019

## Community Service

Community outreach liaison, Rhode Island Museum for Science and Art (RIMOSA)	2018-2020
Big Bang Science Fair in Providence, RI science activity table	2019
Brain Week, Brown Brain fair activity table	2017-2019
Foo Fest Providence, RI science activity table	2018
Creation and presentation of a meta-analysis workshop for students	2015
Creation of a scientific poster workshop for student research initiative	2015

## Ad Hoc Journal Reviewer

Journal of Neuroscience • Cerebral Cortex • Journal of Cognitive Neuroscience

## Other Skills

**Programming:** Matlab (proficient), tcl/tk (intermediate), bash (intermediate), Python (beginner), R (beginner)

**Version Control:** Git

**Languages:** Spanish (native), English (fluent), Portuguese (beginner)

## Selected Abstracts and Presentations

**Yusif Rodriguez, N.,** McKim, T., Basu, D., Ahuja, A., and Desrochers, T. M. (July, 2022) No-response? No problem: Monkey DLPFC tracks abstract sequential information during a no-response task. Poster presented at the Neurobiology of Cognition, Gordon Research Conference in Newry, ME.

**Yusif, N.** and Desrochers, T.M. (July, 2017) Passive sequence viewing in non-human primates during awake fMRI. Oral presentations in SPINES at MBL in Woods Hole, MA and Neural Basis of Attention 2017 conference at Dartmouth in Hanover, NH.

**Yusif, N.,** Wang, T., and Song, J. H. (November, 2015). Interference Effect on Visuomotor Rotational Adaptation and Recall. Poster presented in the Annual Biomedical Research Conference for Minority Students (ABRCMS) in Seattle, WA.

Pardo, T., **Yusif, N.,** and Maldonado-Vlaar, C. (October, 2015). Modulation of the Endocannabinoid System Within the Nucleus Accumbens Shell Elicits Anxiolytic Effects. Poster presented at the Society for Neuroscience annual meeting in Chicago, IL.

Adames, C., Mariani, K., **Yusif, N.,** and Rivera, N. (October, 2015). Meta-Analysis Workshop: For Students, By Students. Workshop presented at the Institute of Psychological Research of the University of Puerto Rico, Rio Piedras Campus in San Juan, PR.

## Preface and Acknowledgements

Completing a thesis on monkey fMRI requires a specific sequence of steps. Much like the sequences I spent so many years studying, this monumental task has a specific set of rules and order that must be followed. Step one: befriend a monkey. You spend days in a quiet room, with this little individual you can't talk to, but you learn to communicate and understand each other. They probably think the same thing about you. Step two: learn to succeed, and then learn to fail. Eventually, succeed again. Step three: you are ready to run the experiment, the real deal. But then you realize that the entire time, you were missing the most important characteristic that was essential for the successful execution of this sequence: the people around you<sup>1</sup>.

There is no way I would have been able to complete any of the presented work without the people who surrounded me and provided support the entire way. I want to thank my mentors, who have supported me through this whole adventure. First, my amazing advisor, Dr. Theresa Desrochers. I remember seeing the lab go from being an empty space, to recognizing all the things we have built together. I could not have asked for a better mentor to build a lab from the ground up with. Dr. David Sheinberg, who has provided support and guidance even before I was a graduate student at Brown. I will always be grateful to this professor who took the time to meet with me, when I was just an undergraduate student doing a summer internship at Brown. The impact you had on my trajectory was life changing, I have achieved things I had never thought would be possible in my lifetime. Thank you and Dr. Amitai Shenhav all for being part of my committee, and for your endless patience throughout the years as my mentors.

---

<sup>1</sup> The MRI facilities require there to be at least one Level 3 and one Level 2 trained person to run an experiment.

This monumental effort would have been impossible without my amazing lab mates and the support of the school's facilities. Thank you, Aarit Ahuja, for your endless support as a peer and a friend. I cannot imagine how much more difficult this entire journey would have been without you. Thanks for always being the other half of my brain, together we will always make one functional graduate student. I would also like to thank the other current and former Desrochers lab members, including the "Monkey Team Magnet Force": Matthew Maestri, Debaleena Basu, and Theresa McKim. Without you there would have been no project, and no fun. With you helping me scan the monkeys it was never a dull time. Finally, I would like to thank Dr. Mike Worden, Lynn Fanella, Fabienne McEleney and the rest of the MRF staff for making all of this work possible.

I am grateful to have been a part of the amazing community that is the Neuroscience Graduate Program at Brown University. I want to thank my co-hort, for crying and laughing and studying together. This journey would have never been the same without you. I look forward to seeing all the amazing things you do in the future.

Thank you Dr. Carmen Maldonado-Vlaar, for being my forever mentor and for encouraging me to apply to this graduate program. Without you I would never have had the courage to be as bold as I have been. I can only aspire to become as amazing a mentor and scientist as you.

I also want to thank my family, and my friends who to me are simply an extension of my family. Thank you to Jaime Yusif, Aida Rodriguez, and Andrea Yusif for always answering my phone calls and being my home. I know I can always count on you to listen to me talk about science and even listen to my practice talks, whether you understand my ramblings or not. I love you all so much. I want to thank my friends Diana Burk, Sofia Melendez, and Brian Leon. We may not be related by blood but to me you are my family. Thank you for being such amazing friends, I know that no matter what happens you are always there in the good and the bad times. Finally, I want to

thank my partner, Marco Vilela. You are both a brilliant partner and a brilliant scientist. Thank you for listening to my crazy ideas and contributing your own, and for always being my number #1 cheerleader.

Like scanning a monkey, there is no way to complete a PhD alone. So many people have contributed to my success that I cannot name everyone. But I want to thank everyone else in my life who has helped me succeed in becoming the scientist I am today.

# Table of Contents

Contents	
Curriculum Vitae .....	iv
Preface and Acknowledgements .....	8
Table of Contents .....	11
List of Figures .....	15
List of tables .....	18
Abstract .....	19
1. Chapter 1. General Introduction: Sequential representation in the brain.....	21
1.1. What are sequences, and what can they tell us about how our brain organizes information? .....	21
1.1.1. Sequential tasks are prevalent in daily life .....	22
1.1.2. Sequences and their associated processes are a sub-set of cognitive control.....	22
1.2. Sequences can be defined in a variety of ways .....	24
1.2.1. Complex sequences .....	25
1.2.2. Simple sequences.....	27
1.3. The monitoring of abstract sequences .....	28
1.4. Sequential characteristics .....	30
1.4.1. Rule and what we know of its neural representations in the brain .....	30
1.4.2. Time and what we know of its neural representations in the brain .....	31

1.4.3.	How we define sequences in the following set of experiments.....	32
1.5.	Development of the proposed experiments and significance .....	33
2.	Chapter 2. Monkey dorsolateral prefrontal cortex represents abstract visual sequences during a no-report task .....	35
2.1.	Title Page .....	35
2.2.	Abstract.....	37
2.3.	Significance Statement .....	38
2.4.	Introduction .....	39
2.5.	Materials and Methods .....	42
2.5.1.	Subjects.....	42
2.5.2.	No-Report Abstract Visual Sequence Task .....	42
2.5.2.1.	Stimuli .....	42
2.5.2.2.	Sequence Types.....	43
2.5.2.3.	Block Structure.....	44
2.5.2.4.	Run Structure.....	45
2.5.2.5.	Reward .....	46
2.5.3.	FMRI Data Acquisition .....	46
2.5.4.	FMRI Data Analysis.....	48
2.5.4.1.	Models.....	49
2.5.4.2.	ROI Analyses .....	51

2.6.	Results.....	52
2.6.1.	Monkey DLPFC represents changes in abstract visual sequences.....	54
2.6.2.	Ramping activation reflects sequence monitoring in monkey DLPFC .....	60
2.7.	Discussion.....	70
2.8.	Extended Data.....	75
3.	Chapter 3: Sequence rule modulates DLPFC activity within our established no-response abstract sequential paradigm.....	78
3.1.	Abstract.....	78
3.2.	Introduction .....	79
3.3.	Materials and Methods .....	83
3.3.1.	Subjects.....	83
3.3.2.1.	Stimuli.....	83
3.3.3.	Sequence Rule Only Task.....	84
3.3.3.1.	Sequence Types.....	84
3.3.3.2.	Block Structure.....	84
3.3.3.3.	Run Structure.....	85
3.3.4.	Timing Only Task.....	85
3.3.4.1.	Timing Types .....	85
3.3.4.2.	Block Structure.....	88
3.3.4.3.	Run Structure.....	88

3.3.5.	Image Only Task.....	89
3.3.5.1.	Stimuli Types .....	89
3.3.5.2.	Block Structure.....	89
3.3.5.3.	Run Structure.....	89
3.3.6.	Pre-scan Fixation Period.....	90
3.3.7.	Reward .....	90
3.3.8.	FMRI Data Acquisition .....	91
3.3.9.	FMRI Data Analysis.....	92
3.3.9.1.	Models.....	93
3.3.9.2.	ROI Analyses .....	96
4.	Chapter 4: General Discussion and Final Remarks .....	139
4.1.	Overall Summary and Final Remarks .....	139
4.2.	Future Directions .....	140
	References.....	142

## List of Figures

Figure 1. Color shape task as illustrated in Desrochers et al., 2015. ....	26
Figure 2. Specific ramping dynamics support abstract visual sequence monitoring in humans (from Desrochers et al., 2019). ....	29
Figure 3. Awake behaving monkey fMRI setup and experimental task design. ....	34
Figure 4. No-report abstract sequence viewing task.....	53
Figure 5. Area 46 represents abstract visual sequences.....	56
Figure 6. Whole-brain deviant activity shows area 46 represents both rule and number deviants.....	58
Figure 7. Area 46 shows ramping activity for deviations to an established sequence rule .....	62
Figure 8. Area 46 shows greater unique ramping than unique last item activity during abstract sequence deviants.....	64
Figure 9. Area 46 shows unique ramping during abstract sequence deviants .....	66
Figure 10. DLPFC does not show significant responses to unique last items during abstract sequence deviants.....	67
Figure 11. Nearby regions of DLPFC show significantly different dynamics .....	69
Figure 12. Hypothesis summary and methodology .....	97
Figure 13. No response rule-only task .....	99
Figure 14. No response time-only task .....	102
Figure 15. No response random task.....	104
Figure 16. Isolated abstract rule modulates ramping activity in area 46 .....	108
Figure 17. No significant difference between unique ramping and unique last item activity for abstract rule in area 46 during Rule Only .....	110

Figure 18. Whole brain activity does not show significant unique ramping activity in Area 46 for Rule Only ..... 111

Figure 19. Whole brain activity for last position compared to first suggests that isolated rule modulates DLPFC activity for Rule Only ..... 112

Figure 20. DLPFC does not show significant activity for novel images when compared to habituation images in Time Only..... 116

Figure 21. Novelty responses in different brain areas suggest that animals are attending to visual stimuli during Time Only task ..... 117

Figure 22. Deviant timing structure does not affect DLPFC activity in Time Only ..... 119

Figure 23. There is no significant effect of image identity on area 46 activity in Time Only.... 120

Figure 24. Structured timing does not drive ramping activity in the DLPFC in Time Only ..... 122

Figure 25. No effect of deviant or novel image ramping activity when compared to habituation images with the same timing templates in Time Only..... 124

Figure 26. Responses related to detecting deviants and novel images indicate animals attend to task stimuli during Random task..... 126

Figure 27. Ramping pattern of activity is not present in the DLPFC in the absence of abstract rule or structured timing in Random task..... 127

Figure 28. No increase in activity at last position compared to first in area 46 for isolated image during Random task ..... 128

Figure 29. A parametric ramping novel supports the prediction that the DLPFC does not show ramping activity in different stimulus categories in the absence of abstract rule and structured timing during Random task..... 130

Figure 30. Comparison across position activity for Rule Only compared to Random is not significant..... 131

Figure 31. Left area 46 ramping activity across tasks suggests additive effect of abstract rule and structured timing..... 132

## List of tables

Table 1. Repeated measures ANOVAs comparing rule and number deviants to NISR in L46 and R46.....	57
Table 2. Repeated measures ANOVAs comparing deviant responses in L46 and R46. ....	57
Table 3. Rule and number deviants compared to NISR contrast activation coordinates. Area labels as in the NIMH NMT v02 Macaque Atlas.....	59
Table 4. Repeated measures ANOVAs comparing unique ramping activity during rule and number deviants to NISR in L46 and R46. ....	63
Table 5. Repeated measures ANOVAs comparing unique ramping deviant responses in L46 and R46.....	63
Table 6. Repeated measures ANOVAs comparing unique ramping activity to unique last item activity during rule and number deviants to NISR in L46 and R46. ....	64
Table 7. Unique ramp rule and number deviants compared to NISR contrast activation coordinates. ....	66
Table 8. Unique last item rule and number deviants compared to NISR contrast activation coordinates. ....	68
Table 9. Percentage of excluded data using fixation and motion criteria and total included data across tasks and animals. ....	93
Table 10. Repeated measures ANOVAs comparing position activity in L46 and R46.....	108
Table 11. Last position compared to first position contrast activation coordinates.....	112
Table 12. Repeated measures ANOVAs comparing position activity in left ramp ROI and right ramp ROI .....	128

# Abstract

Everyday tasks often require to be completed following a specific set of steps or sequentially. Oftentimes, these sequential tasks are abstract, meaning that they are not defined by their specific contents, but instead by the higher order rule which can be used to describe them. As an example, consider taking a daily commute. When taking a bus, you may track a familiar sequence of buildings (three houses, then a library). Additionally, variables like timing and rule could affect sequential monitoring such as when a delay occurs, or when there is a route deviation. Despite its ubiquity, little is known about the neural underpinnings of this tracking process also known as sequential monitoring nor how specific task variables can influence relevant neural responses.

Previous work in both human and non-human primates has identified brain areas involved in sequential tasks. In humans, the rostralateral prefrontal cortex (RLPFC) exhibits a specific pattern of increasing neural activity (i.e., “ramping”) during abstract sequences. Work in non-human primates has identified the dorsolateral prefrontal cortex (DLPFC) as a key area for the representation of sequential information. Furthermore, the monkey DLPFC contains a sub-region, area 46, with homologous functional connectivity to human RLPFC. However, much of this work has yet to directly test the representation of abstract sequences.

The work presented in this thesis aims to test the following predictions: First, that the nonhuman primate DLPFC may represent abstract sequence information with parallel dynamics to those found in humans. Second, that these dynamics may be modulated by different sequential characteristics such as abstract sequential rule or structured timing. To investigate these predictions, we conducted functional magnetic resonance imaging (fMRI) in awake monkeys. When monkeys performed no-report abstract sequence viewing, we found that left and right area 46 responded to abstract sequential changes. Interestingly, responses to rule and number changes

overlapped in right area 46 and left area 46 exhibited responses to abstract sequence rules with changes in ramping activation, similar to that observed in humans.

To further test what specific characteristics of sequences modulated the response observed in area 46, animals did variations of the no-response task which contained either only abstract rule, only structured timing or neither. Our findings suggest that abstract rule and structured timing in combination elicit ramping neural dynamics in area 46. Together, these results indicate that monkey DLPFC monitors abstract visual sequential information. Additionally, these ramping dynamics are elicited by characteristics such as abstract rule and structured timing. More generally, these results show that abstract sequences are represented in functionally homologous regions across monkeys and humans.

# Chapter 1. General Introduction: Sequential representation in the brain

## 1.1. What are sequences, and what can they tell us about how our brain organizes information?

Information that is serially organized, having a particular set of rules or order surrounds us daily. There is, of course, an easier way to refer to these types of stimuli. Commonly referred to as sequences, these have been defined as a problem of neuroscience and behavior since at least the 50's by Lashley (Lashley, 1951). Although some of the ideas in this text may now be outdated, it is true that understanding the “problem of serial order” as Lashley puts it, would provide great insight into the underlying machinations of the brain. Specifically, what can we learn about how the brain parses information in our environment from how it processes sequential information? Additionally, what is identified as being relevant for sequential stimuli to be considered as such? Despite the formal definition of sequences being introduced for well over half a decade at the time this text is being written, our knowledge regarding the neural representations of sequences in the brain remains limited.

This chapter aims to lay the groundwork and motivation for the study of sequences in the monkey prefrontal cortex. We will review the existing literature on sequential processing, ranging from concrete sequences across different sensory modalities, up to abstract sequences. In these sections we will elaborate on the behavioral and physiological evidence that suggesting specific brain areas are essential for sequential processing. Additionally, we discuss the possible neural dynamics that are associated with these cognitive computations. We provide a thorough summary of the current literature, while highlighting the existing gaps in our understanding of abstract sequential

processing in the brain. In the final segment of this chapter, we will outline the experiments carried out to elucidate the brain areas involved in the monkey brain during sequential processing, and the neural dynamics present throughout.

### **1.1.1. Sequential tasks are prevalent in daily life**

This work aims to understand a very specific sub-set of sequences known as abstract sequences. What do we mean by *abstract sequences*? Let's consider the example of a specific but very well-known piece of music, Beethoven's 5<sup>th</sup> symphony in C minor. This iconic piece of music can be described in a variety of ways. A musical piece contains visual, auditory, and motor components after all. However, a particularly outstanding feature of this piece that makes it instantly recognizable, is its first fifteen seconds. Specifically, the repeating pattern of *three of the same, one different* (dun dun dun dunnnnnn). This sequence, which can be used to describe the structure of these first few seconds of the song is known as an *abstract sequence*. Abstract sequences are defined not by the specific components of the sequence, but instead by the higher order structure that can be used to describe them (in this case three of the same, one different). In this case, even changing the key of the song, or playing it on a different instrument still makes it distinct and recognizable. Therefore, abstract sequential representations are not specific to a particular sensory modality, are generalizable, and flexible higher order representations of a sequential structure. In the following sections we discuss the literature relevant to sequential tasks and abstract sequences with their associated neural dynamics in both humans and non-human primates.

### **1.1.2. Sequences and their associated processes are a sub-set of cognitive control**

Cognitive control refers to the capacity of action selection that allows for goal selection, flexible modification of this behavior, and completion of these goals (Badre & Nee, 2018). Cognitive control tasks often demand that individuals maintain information across multiple levels of rules.

These tasks often result in having to maintain internal sub-goals as one pursues a higher order goal. A classic example of these tasks are response selection tasks. This task contains multiple nested tasks, going from simpler to more complex rules, each requiring different responses depending on feature level that had to be attended to (Badre et al., 2009; Badre & D'Esposito, 2007a). Individuals are then capable of completing this complex task successfully, keeping track of the nested structures to complete the higher order goal. As in these cognitive control tasks, sequential tasks often demand similar maintenance of higher order goals as one continues through a sequence of steps.

Similar brain areas have also been identified as being necessary for both cognitive control and sequential processing. In humans, it has been shown that the PFC contains a rostral to caudal progression, in which more rostral areas respond to increasing levels of abstraction across the cognitive hierarchy (Badre & D'Esposito, 2007a). The PFC has been shown to support cognitive control function and goal directed behavior. (Badre & D'Esposito, 2007a; Badre & Nee, 2018; Miller & Cohen, 2001). Generally, frontal areas support more abstract control than caudal areas (shown in humans) starting with more caudal areas (PMD, pre-PMD) and going rostrally towards mid-DLPFC and RLPFC. Human RLPFC has been implicated to be necessary not just in higher levels of abstraction but specifically in tasks that share characteristics of sequential hierarchical control (Badre & D'Esposito, 2007a; Badre & Nee, 2018; Desrochers et al., 2016). Therefore, we can consider sequential tasks to demand similar cognitive resources as cognitive control, being represented as more abstract higher order structures requiring the involvement of the frontal cortex. Due to the similarities shared with cognitive control, sequential tasks can be considered to be a subset of this cognitive process. As mentioned in the beginning of this section, cognitive control tasks often require maintaining and tracking sub-goals that serve a higher order goal. Sequences

are distinct from other cognitive control tasks in that they have an order and contain temporal dependencies (Desrochers et al., 2016; Ninokura et al., 2004; Schapiro, Rogers, et al., 2013). However, sequential tasks being abstract higher order cognitive processes tend to necessitate similar brain areas observed to be involved in cognitive control. Some of these brain areas include lower level processing regions such as the supplementary motor area SMA, the pre-SMA, and motor cortex which are recruited for the completion of motor sequential tasks (Carpenter et al., 2018; Clower & Alexander, 1998; Dahms et al., 2020; Hoshi et al., 1998). Similar to the identification of lower-level task features or simple task demands during cognitive control, these brain are implicated in sequences that require the completion of simple motor sequences or very specifically defined and learned sequences. Work studying abstract sequences suggests that higher order cortical areas such as the pre-frontal cortex and associated sub-regions, may be responsible and necessary for the execution and processing of sequential tasks (Averbeck et al., 2006; Averbeck & Lee, 2007; Desrochers et al., 2016; L. Wang et al., 2019). Overall, sequential tasks require similar brain areas and cognitive demands as cognitive control tasks but are considered to be a distinct cognitive process within the umbrella of cognitive control.

## **1.2. Sequences can be defined in a variety of ways**

Thus far, we have defined the relationship between cognitive control and sequential tasks and begun to discuss the brain areas that are involved in the processing of different types of sequences. However, in this initial discussion a variety of sequence types were highlighted. Some of the studies mentioned were motor sequential tasks, while others were abstract sequential tasks. As implied by these studies, sequential tasks have a variety of elements that distinguish them not only from other cognitive processes but also from each other. In the following sections, we will discuss these differences. Specifically, we will classify sequences as being either complex sequences or

simple sequences and the different ways these have been studied in the literature. Because the focus of this thesis is simple abstract sequences, we will provide a brief description of complex sequences and their related neural dynamics. Afterwards we will provide a thorough review of the literature related to simple abstract sequences and the relationship to the completed sets of experiments.

### 1.2.1. Complex sequences

For this thesis, we will define complex sequences as sequences containing a higher order abstract rule, demand a behavioral response, have a higher order goal with sub-goals, and require sequential monitoring. Complex sequences can be encountered across a variety of sensory modalities including visual (Desrochers et al., 2015; Trach et al., 2021), motor (Averbeck et al., 2003, 2006), and even olfactory sequences (Allen et al., 2014). Oftentimes these complex sequences will require that subjects track a higher order rule in order to complete the sequential task. As an example, a complex sequential task in humans required that they respond to a four item sequence of visual stimuli based on the sequence color shape shape color, or color color shape shape (**Figure 1**, Desrochers et al., 2015). Stimuli containing both color and shape features (e.g. a blue circle, a red square) were serially presented. Individuals were then asked to make a color or shape judgement based on the abstract sequence, and not the specific stimulus information. To complete such a task it is necessary for subjects to keep track or monitor the higher order sequential structure (color color shape shape), and track individual sequence steps producing responses at each one (sub-goals). This process of tracking and maintaining an internal representation of the higher order abstract sequential structure is known as *sequential monitoring*. Therefore, while complex sequences can have a variety of task demands, they are characterized by having abstract higher ordered rules and require keeping one's place through sequential monitoring.

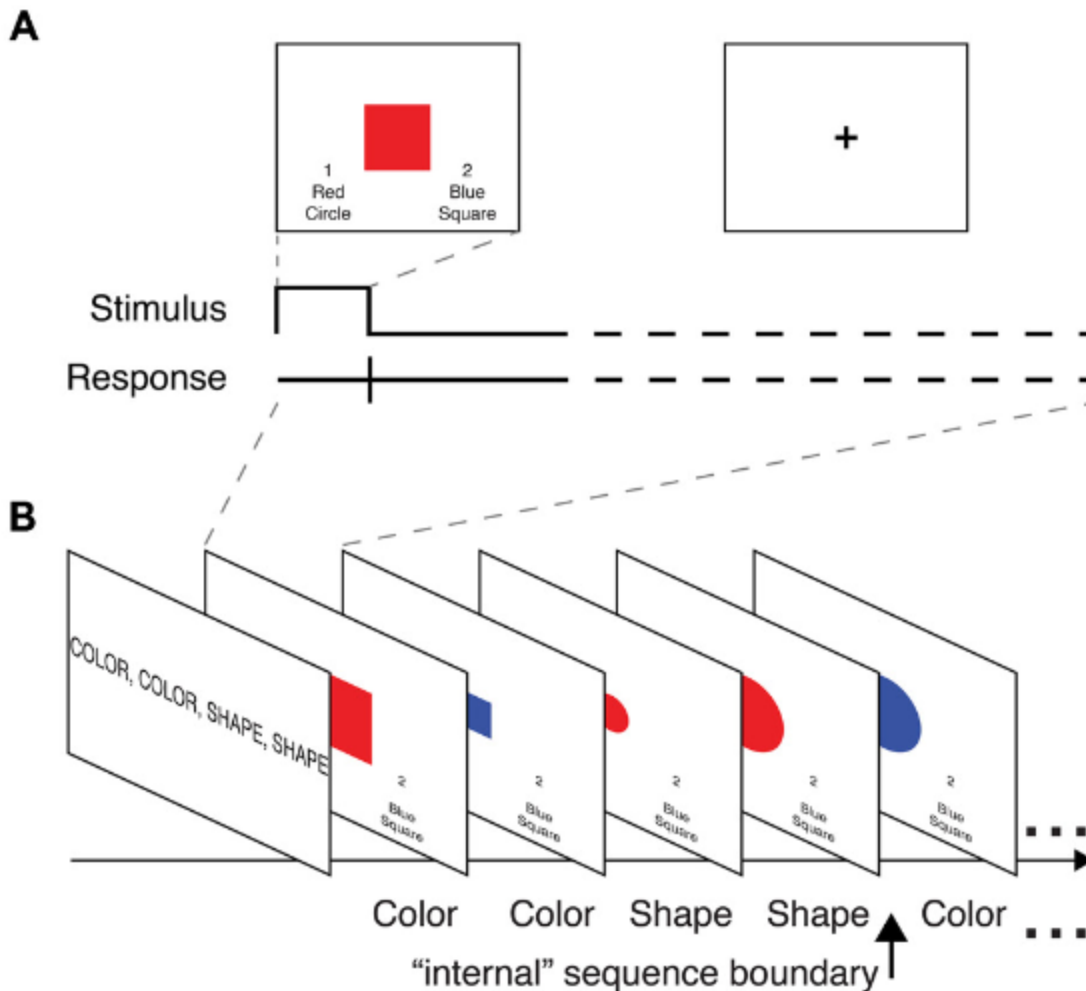


**Figure 1. Color shape task as illustrated in Desrochers et al., 2015.**A. Individuals are asked to make a color or shape judgement on each trial. **B.** Each block starts by indicating the sequence rule, in this case color, color, shape, shape. Subjects must keep track of the rule and make a color or shape judgement accordingly depending on the stimuli.

Because complex sequences tend to recruit higher order cognitive processes, they are similarly represented in higher order brain areas. Tasks in humans have identified the PFC as being necessary for the completion of complex sequential tasks (L. Wang et al., 2019; Wen et al., 2020), and the rostral LPFC such as in the color shape task mentioned in the previous paragraph (Desrochers et al., 2015). Complex sequential tasks in monkeys testing the processing of serial order across a variety of sequences have identified neural responses related to rank ordering across

a variety of prefrontal and fronto-cortical areas including SMA, pre-SMA, supplementary eye field (SEF), and dorsal LPFC (Berdyeva & Olson, 2010; Farooqui et al., 2012). Overall, most complex sequential information seems to be represented in the prefrontal cortex and its associated network, making these regions key for the understanding of sequential tasks.

### **1.2.2. Simple sequences**

Unlike complex sequences, simple sequences may not always demand a behavioral response, do not require higher order abstract rule, but may still similarly demand sequential monitoring. Some examples of these simple sequences include oddball tasks (Bodnar et al., n.d.; and reviewed in Garrido et al., 2009), statistical sequences (Conway & Christiansen, 2005; Fiser & Aslin, 2002; Schapiro, Greogry, et al., 2013; Schapiro, Rogers, et al., 2013; Turk-Browne et al., 2009), and tasks containing fixed sequences (Allen et al., 2014; Desrochers et al., 2019; Ninokura et al., 2004; Tanji & Shima, 1994). The oddball task can be considered to be the simplest of these sequences. Oddball tasks are characterized by a repeating stream of serially presented stimuli, with an eventual deviant stimuli presentation termed an “oddball”, making their construction a very simple sequence. Statistical learning sequences, while still simple sequences are slightly more complex than oddball tasks. In these tasks in that a series of stimuli are serially presented, such that individuals must extract regularities from the stream. Within the stream, there are statistical probabilities embedded for the stimuli, making the co-occurrence of certain stimuli more likely. Finally, tasks with fixed sequences simply require that subjects remember a specific set of stimuli in a particular order (ABCD, etc.) and track it through time. Despite the apparent simplicity of these sequences these sequences still demand cognitive resources such as attention for the proper detection of sequential organization and require monitoring sequential steps. These simple sequences elicit neural responses in a variety of sensory and domain general brain areas. This is

precisely the case for the mismatch negativity (MMN) response in the oddball task. The MMN occurs as a novelty detection response for the stimulus deviation, characterized by a negative deflection in activity usually observed in EEG responses (May & Tiitinen, 2010). These MMN responses occur in visual oddballs as well (reviewed in Pazo-Alvarez et al., 2003), and can be observed in monkeys (Boehnke et al., 2011). In the case of statistical learning sequences, we can also observe neural responses across sensory domains (Henin et al., 2021). Neural responses related to statistical sequences occur in areas including the hippocampus in humans (Cerreta et al., 2018; Schapiro, Greogry, et al., 2013; Schlichting et al., 2013) and visual areas such as inferotemporal cortex in monkeys (Meyer, Ramachandran, et al., 2014; Meyer, Walker, et al., 2014; Vergnieux & Vogels, 2020). Similarly, fixed order tasks also elicit neural responses in both sensory specific and domain general areas. However, these tasks can also drive neural responses in the prefrontal cortex, with cells encoding specific stimuli order in monkeys (Shima et al., 2007). In humans, sequence tasks having a fixed order have been shown to elicit similar neural dynamics in the rostral LPFC as those observed during more complex sequential tasks (Desrochers et al., 2019). Findings from these types of simple sequential tasks show that even very simple sequences can elicit robust neural responses that indicate the detection of sequential regularities and task engagement.

### **1.3. The monitoring of abstract sequences**

Whether sequential tasks are simple or complex, to successfully complete them it is necessary to engage in sequential monitoring to maintain our place in the sequence. Work studying abstract sequences has identified specific brain areas and neural dynamics that are essential for sequential monitoring. A specific increasing neural dynamic or *ramping* is required for sequential monitoring in humans. Activity in the human rostral lateral prefrontal cortex (LPFC) continuously increases

(“ramps”) throughout sequence position (**Figure 2**) and is necessary for sequential monitoring (Desrochers et al., 2015, 2019; McKim & Desrochers, 2022a). Few studies have suggested similar neural mechanisms associated with sequential tasks in the monkey brain. Work in monkeys have identified the LPFC as being involved in abstract sequential tasks. Cells in the monkey LPFC have been shown to respond during multi step motor sequence tasks (Averbeck et al., 2003, 2006; Averbeck & Lee, 2007). LPFC responses in the monkey brain during motor sequences also generalize to novel sequences, indicating an encoding of the higher order sequential structures (Bernardi et al., 2020; Xie et al., 2022). Additionally, while the existence of ramping dynamics during complex sequences in the monkey LPFC have not been tested it is known that the monkey LPFC shows similar neural activity during other cognitive tasks (Ding, 2015). Therefore, determining whether ramping underlies sequence monitoring in the monkey brain is essential for improved cross-species models and establishing a better understanding of the macaque LPFC and its similarities to the human LPFC.

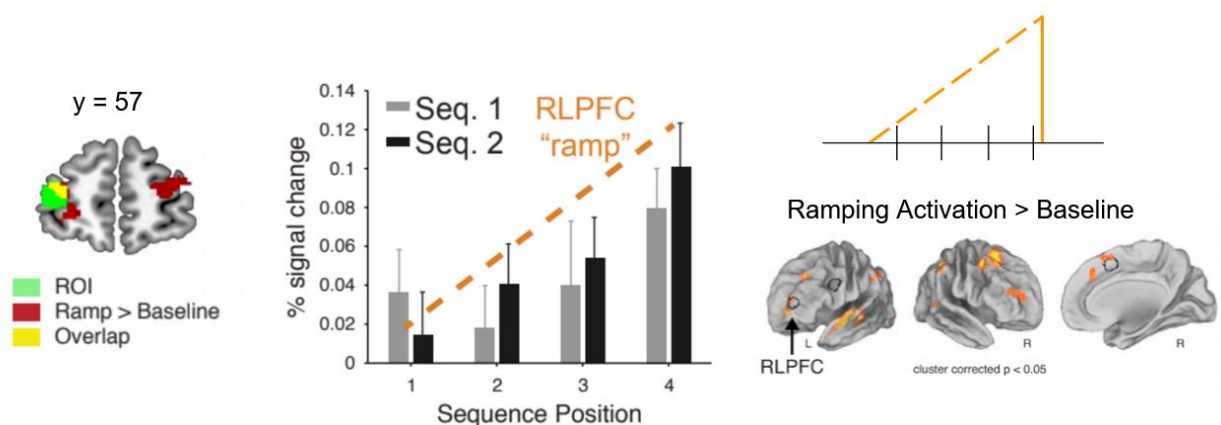


**Figure 2. Specific ramping dynamics support abstract visual sequence monitoring in humans (from Desrochers et al., 2019).**

## **1.4. Sequential characteristics**

Abstract sequences require a variety of characteristics to be defined as such. We saw that while oddball and statistical tasks can be described as sequences, they are not necessarily abstract. In order for a serially presented set of stimuli to be considered an abstract sequence, we believe it must contain certain characteristics. First, it must have an abstract rule, allowing the sequences to have a generalizable structure that does not depend on individual stimulus identity. Additionally, they must have a well-defined beginning and an end, allowing individuals to detect the sequential boundary during monitoring. Coupled with rule, a characteristic such as structured timing can enable the grouping of sequential information perceptually making the sequence boundaries more distinct. In the following sections we discuss the literature that supports rule and timing representations in the LPFC, and how these are relevant characteristics for the construction of abstract visual sequences. At the end of this section, we describe in detail how we specifically defined abstract visual sequences in the following chapters, and how we proceeded to test their neural representation and dynamics in the macaque LPFC.

### **1.4.1. Rule and what we know of its neural representations in the brain**

The LPFC processes different types of regularities or higher order rule structures. One of these types of structures are perceptual or algebraic patterns. Algebraic patterns include repetitions (AAAA, BBBB), alternations (ABAB, CDCD), and pairs (AABB, CCDD) across different sequences. Importantly, algebraic patterns are independent of the specific constituent items. They are well defined (Dehaene et al., 2015; Endress et al., 2009; Marcus et al., 1999, 2007), and elicit neural responses unique to the rule structure (J. Saffran et al., 2008; Shima et al., 2007; L. Wang et al., 2015). The following experiments use sequences with algebraic patterns for the following reasons: 1) Sequential studies in monkeys showed neural responses to algebraic patterns in the

LPFC (Averbeck et al., 2006; Shima et al., 2007), 2) Responses to algebraic pattern changes require global pattern recognition and do not follow adaptation and prediction error patterns that typify oddball tasks (Bekinschtein et al., 2009; Strauss et al., 2015), 3) In contrast to statistical learning, studies in humans indicate that neural responses to algebraic patterns require attention (Bekinschtein et al., 2009; Chennu et al., 2013). Neurons in the monkey LPFC are selective to algebraic patterns and ordinal position in sequential tasks (Averbeck et al., 2003, 2006; Averbeck & Lee, 2007). In fMRI and electrophysiology studies LPFC responds differentially to regularities or algebraic patterns including repetitions across different sequences, independent of sensory modality or specific item (Dehaene et al., 2015). Changes to established algebraic patterns elicit activity in the monkey brain suggesting animals actively monitor these sequences (L. Wang et al., 2015), as such effects disappear with inattention (Bekinschtein et al., 2009; Chennu et al., 2013; Musz et al., 2015). The inclusion of these simple sequential structures allow us to create the simplest version of a visual sequence possible, while ensuring neural activity when animals attend to the higher order structure that does not require a behavioral response.

#### **1.4.2. Time and what we know of its neural representations in the brain**

Neural activity in the LPFC has been implicated as a neural mechanism associated with multiple processes including time and progression towards a goal (Ma et al., 2014; Peters et al., 2005). There are a variety of ways in which timing has been studied including dwell-time, event anticipation, the timing of specific intervals or even rhythmic timing (reviewed in A. C. Nobre & van Ede, 2018). Work across different timing modalities suggests that a wide variety of timing associated dynamics may be key modulators of ramping activity in the LPFC. Human studies from our lab showed that time modulates sequence-related ramping in rostral LPFC (“dwell time”; Desrochers et al., 2019). Populations of neurons can be tuned to specific timing intervals, and

timing anticipation of temporal patterns (Coull & Nobre, 2008; Ekman et al., 2017; A. C. Nobre & van Ede, 2018). Firing irregularities occur in the LPFC as monkeys get closer to a goal (Tiganj et al., 2018). The variables that modulate LPFC activity have also been associated with ramping dynamics elsewhere in the brain. Neurons that show ramping dynamics in the PFC and medial FC respond to the passage of time (Emmons et al., 2017; J. Kim et al., 2013; Y.-C. Kim et al., 2017; Narayanan, 2016; Niki & Watanabe, 1979; J. Wang et al., 2018), and anticipation (Paton & Buonomano, 2018; Schall, 2019; Schultz, 2000), both of which likely modulate sequence monitoring. Elapsed time modulates neural activity in the monkey LPFC (Niki & Watanabe, 1979) and adding temporal sequence to serial reaction time tasks with a spatial sequences results in enhanced task performance (Coull & Nobre, 2008; A. C. Nobre & van Ede, 2018; Shin & Ivry, 2002). Utilizing structured timing will allow us to test whether this characteristic modulates responses in LPFC when paired with abstract sequences and in isolation.

### **1.4.3. How we define sequences in the following set of experiments**

We define sequence monitoring as an active not implicit process, requiring awareness and attention to detect the sequential patterns in the proposed task (REFS). In sum, there is a need to separate monitoring from commonly associated processes when determining its neural correlates. Specifically, our abstract sequences contain *abstract rule* and *structured timing*. Because this work does not directly test for the generalizability of how abstract rules overall are processed by the DLPFC, we specifically define abstract rule as two of the simplest possible sequences we could design. These sequences specifically followed the format of 3 of the same, and one different image (AAAB), or four of the same image (AAAA). Additionally, to further distinguish the sequences we include structured timing, which allows them to be perceptually grouped by assigning image sequences distinct timing categories depending on the sequence type. Afterwards, we isolate each

of these sequential characteristics to identify which specifically modulate neural responses related to abstract sequential processing.

### **1.5. Development of the proposed experiments and significance**

In the following chapters, we will show how we utilized awake behaving monkey fMRI to test the representation of abstract sequences in the DLPFC. To achieve this work, it was necessary to first develop the methods necessary to do so at the institution. As such, this is the first set awake behaving monkey fMRI experiments carried out at Brown University. FMRI provides a whole brain view, while minimizing the need for invasive procedures. This type of method is rare, in that few other institutions have the resources and expertise to conduct awake monkey fMRI experiments, carrying with it a special set of challenges.

Awake monkey fMRI requires the development of specialized tools and analysis pipelines. Animals must be trained to perform tasks under conditions imitating the MRI facilities, to ensure good behavior during experimental data collection sessions. This is in addition to the special considerations that must be taken to minimize movement, while also making sure that there is not a great amount of discomfort to the animals. Other measures to keep animals engaged, such as providing juice during the task, can directly introduce noise into the dataset. Because of this, besides the necessary custom analysis pipelines, the addition of regressor that take into consideration correlations to movement and reward delivery must be included. Additional challenges can also arise from the limited signal to noise ratio, making the use of contrast agent imperative (Leite et al., 2002). Finally, it is also necessary to use custom head coils that can be placed proximal to the animal's skull (**Figure 3**). A detailed account of the methods utilized to acquire this data can be found in the methods section of this text. Additional resources detailing methods used to acquire this data have been previously published (Leite et al., 2002; Vanduffel et

al., 2001; Vanduffel & Farivar, 2014), but we hope to elaborate in the improvement of the methods used through this text and future work (Yusif Rodriguez et al., 2022).

Most information of the functional organization of the DLPFC during sequential and cognitive tasks is derived from electrophysiology studies, which are limited to specific cell sub-population and sub-region sampling of the LPFC. Behaving monkey fMRI provides the unique benefit of observing the sum of activity across multiple PFC sub-regions and other brain areas with similar neural responses. This method thus provides the opportunity to delineate activity across multiple DLPFC sub-regions during sequential monitoring. To this end, I will employ a no-response abstract visual sequence task and task variants that isolate rule, time, and image variables to determine the neural mechanisms that underlie sequential monitoring in the DLPFC. The following experiments show the work completed to test the hypotheses that sequence monitoring elicits ramping in the monkey DLPFC, and that this neural activity is modulated by the variables of rule and timing.

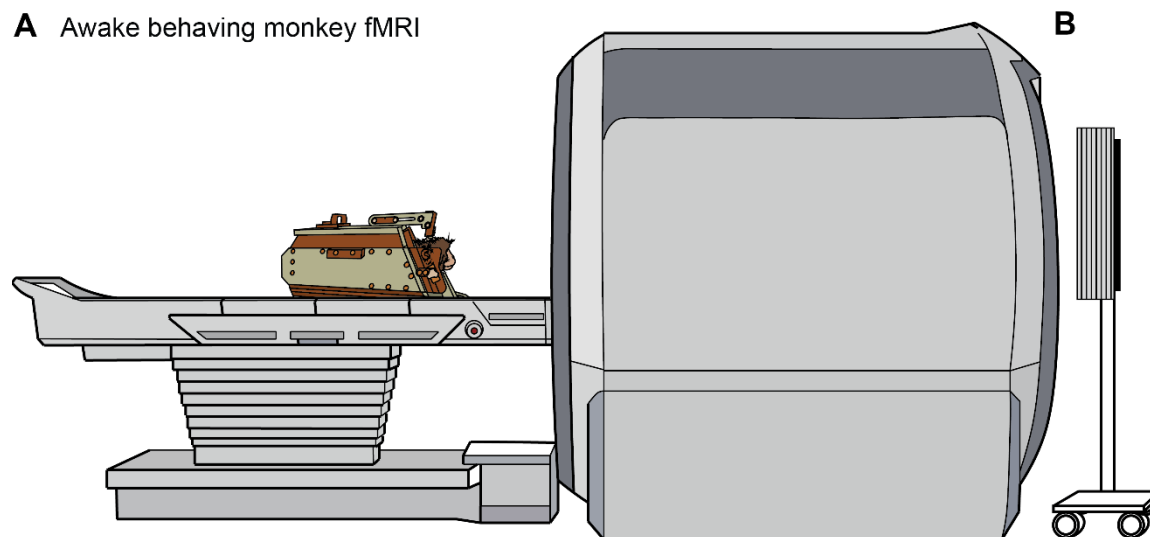


**Figure 3. Awake behaving monkey fMRI setup and experimental task design.** **A.** Monkeys complete tasks in an MRI safe chair seated in the sphinx position. **B.** A BOLD screen displaying stimuli is at the end of the scanner bore.

# **Chapter 2. Monkey dorsolateral prefrontal cortex represents abstract visual sequences during a no-report task**

## **2.1. Title Page**

\*This chapter is presented in the form in which it was submitted for publication in 2022.

**Authors:** Nadira Yusif Rodriguez<sup>1,2</sup>, Theresa H. McKim<sup>1^</sup>, Debaleena Basu<sup>1</sup>, Aarit Ahuja<sup>1,2</sup>, and Theresa M. Desrochers<sup>1,2,3\*</sup>

### **Affiliations:**

1. Department of Neuroscience, Brown University
2. Robert J. and Nancy D. Carney Institute for Brain Science

^ current address: Department of Child and Adolescent Psychiatry, Psychosomatics and Psychotherapy, University Hospital Würzburg, Germany

3. Department of Psychiatry and Human Behavior

\* Corresponding Author: Theresa M. Desrochers, [theresa\\_desrochers@brown.edu](mailto:theresa_desrochers@brown.edu)

Abbreviated title: Monkey DLPFC represents abstract visual sequences

**Conflict of Interest Statement:** The authors declare no competing financial interests.

**Acknowledgements:** We thank Matthew Maestri for his assistance with animal training and data collection. We would also like to thank Dr. Michael Worden, Lynn Fanella, Fabienne McEleney and Brown University's MRI Facilities staff for their support and guidance throughout this project. We also thank Dr. David Sheinberg, Dr. Amitai Shenhav, Dr. Katherine Conen, and Dr. Diana Burk for their continued support throughout this project and preparation of this publication, as well as members of both the Sheinberg and the Desrochers Labs for many helpful discussions and contributions. This study was supported by the NSF-EPSCoR Neural Basis of Attention 1632738 (N.Y.R, T.M.D.), the NIGMS-NIH Initiative to Maximize Student Development IMSD R25GM083270 (N.Y.R.), the NIH-NIGMS COBRE P20GM103645-07, and the Carney Institute for Brain Science Innovation Award (T.M.D.). Part of this research was conducted using computational resources and services at the Center for Computation and Visualization, Brown University, S10 OD016366.

## **2.2. Abstract**

Monitoring sequential information is an essential component of our daily lives. Many of these sequences are abstract, in that they do not depend on the individual stimuli, but do depend on an ordered set of rules (e.g., chop then stir when cooking). Despite the ubiquity and utility of abstract sequential monitoring, little is known about its neural mechanisms. Human rostralateral prefrontal cortex (RLPFC) exhibits specific increases in neural activity (i.e., “ramping”) during abstract sequences. Monkey dorsolateral prefrontal cortex (DLPFC) has been shown to represent sequential information in motor (not abstract) sequence tasks, and contains a sub-region, area 46, with homologous functional connectivity to human RLPFC. To test the prediction that area 46 may represent abstract sequence information, and do so with parallel dynamics to those found in humans, we conducted functional magnetic resonance imaging (fMRI) in monkeys. When monkeys performed no-report abstract sequence viewing, we found that left and right area 46 responded to abstract sequential changes. Interestingly, responses to rule and number changes overlapped in right area 46 and left area 46 exhibited responses to abstract sequence rules with changes in ramping activation, similar to that observed in humans. Together, these results indicate that monkey DLPFC monitors abstract visual sequential information, potentially with a preference for different dynamics in the two hemispheres. More generally, these results show that abstract sequences are represented in functionally homologous regions across monkeys and humans.

### **2.3. Significance Statement**

Daily, we complete sequences that are “abstract” because they depend on an ordered set of rules (e.g., chop then stir when cooking) rather than the identity of individual items. Little is known about how the brain tracks, or monitors, this abstract sequential information. Based on previous human work showing abstract sequence related dynamics in an analogous area, we tested if monkey dorsolateral prefrontal cortex (DLPFC), specifically area 46, represents abstract sequential information using awake monkey fMRI. We found that area 46 responded to abstract sequence changes, with a preference for more general responses on the right and dynamics similar to humans on the left. These results suggest that abstract sequences are represented in functionally homologous regions across monkeys and humans.

## 2.4. Introduction

Sequential tasks that require monitoring are prevalent in daily life. For example, taking a bus requires tracking familiar sequences of buildings (e.g., three houses then a library), enabling the detection of deviations from this sequence (e.g., if there is a detour). Similarly, many cognitive processes occur serially, and often demand that we maintain an internal representation of the previous steps to complete the next. Even in tasks that are not explicitly sequential, a system for tracking transitions between steps, such as when completing a mathematical operation, may be essential.

*Sequence monitoring* is this active process of tracking the order of subsequent “states” or steps. Monitoring is distinct from other well-studied sequence processes, such as explicit memorization, or potentially more automatic behaviors, such as a series of motor outputs (e.g., playing the piano) or statistical sequence learning (Desrochers et al., 2019). Such sequential processes likely contain monitoring operations within them but are also comprised of other cognitive computations. *Abstract sequences* are sequences that are not dependent on the individual stimuli but can instead be described by the rule they follow (e.g., three same, one different or AAAB) (Desrochers et al., 2022). Therefore, *abstract sequence monitoring* entails sequences of sensory stimuli that possess abstract structure and active monitoring of this structure. While it may be assumed that abstract sequence monitoring underlies many aforementioned sequence types (including motor sequences), it is rarely studied in isolation and the neural underpinnings of abstract sequence monitoring remain largely unknown.

Multiple modes of evidence in humans indicate that activity in rostralateral prefrontal cortex (RLPFC) is crucial to sequence monitoring (Desrochers et al., 2015, 2019; McKim & Desrochers, 2022b). Functional magnetic resonance imaging (fMRI) revealed systematic increasing activity

(“ramping”) from the beginning to the end of each sequence in human RLPFC. Across studies, this activity occurs either bilaterally, or in the left RLPFC. Further, noninvasive transcranial magnetic stimulation (TMS) showed that the left RLPFC was necessary for sequential tasks in humans. Other studies have also demonstrated the involvement of RLPFC as part of a frontoparietal network active during complex sequential tasks (Farooqui et al., 2012; L. Wang et al., 2019; Wen et al., 2020). While consistent with the findings discussed above, these studies frequently involve other cognitive phenomena, like decision-making, leaving open their specific role of sequence monitoring.

Studies in nonhuman primates also suggest a role of lateral prefrontal cortex in abstract visual sequence monitoring. Motor sequence studies show that neurons in the dorsolateral prefrontal cortex (DLPFC) are selective for serial position (Averbeck et al., 2006; Barone & Joseph, 1989; Berdyeva & Olson, 2010; Shima et al., 2007) and sequence boundaries (Fujii & Graybiel, 2003), and include neural dynamics that could underlie the ramping observed in human BOLD activation (Desrochers et al., 2015, 2019; McKim & Desrochers, 2022b). Neurons in the DLPFC also show ordinal selectivity during visual object sequences (Naya et al., 2017; Ninokura et al., 2004; Warden & Miller, 2010). A rich literature also supports the involvement of DLPFC in representing non-sequential abstract rules (Eiselt & Nieder, 2013; Hoshi et al., 1998; Wallis et al., 2001; White & Wise, 1999). Responses in the DLPFC can also selectively represent sequential regularities (Vergnienx & Vogels, 2020). Together, these physiological studies suggest that the monkey DLPFC is well-positioned to monitor abstract visual sequences.

We hypothesized that a specific sub-region of monkey DLPFC (area 46) monitors visual abstract sequential information. In humans, abstract sequence monitoring has been localized to the RLPFC, which is distinct from the rostromedial prefrontal cortex (Burgess et al., 2003; Du et al., 2020;

Gilbert et al., 2010; Henssen et al., 2016; Koechlin et al., 2000; Moayedi et al., 2015). While rostromedial prefrontal cortex has similar connectivity in monkeys and humans, anatomical evidence suggests that monkey area 46 contains the most similar connectivity patterns to human RLPFC (Neubert et al., 2014; Sallet et al., 2013), and overlapping high-level visual representations (R. Xu et al., 2022). Therefore, we predicted that abstract visual sequence monitoring would be supported by monkey area 46, and that similar ramping dynamics, as observed in humans, would localize to this same area.

To directly test these predictions, we conducted event-related fMRI in awake nonhuman primates, and used deviations from established abstract visual sequences during a no-report task to index abstract sequence monitoring. We found that nonhuman primate DLPFC distinctly represents abstract visual sequence information, independent from other task constraints. Additionally, we find that these abstract sequences elicit ramping dynamics similar to those observed in humans during abstract sequence performance. Intriguingly, deviant responses with differing primary dynamics were observed in the two hemispheres: an onset-based signal on the right, and ramping on the left. These findings indicate that a specific sub-region of DLPFC preferentially supports abstract sequence monitoring in monkeys and may be functionally homologous to humans. Further, these results establish an important connection between human and monkey complex cognition and the neural substrates that mediate it, providing a foundation for understanding more complex behaviors across species in the future.

## **2.5. Materials and Methods**

### **2.5.1. Subjects**

We tested three adult male rhesus macaques (ages spanning 6-12 years during data collection, 9-14 kg). All procedures followed the NIH Guide for Care and Use of Laboratory Animals and were approved by Institutional Animal Care and Use Committee (IACUC) at Brown University.

### **2.5.2. No-Report Abstract Visual Sequence Task**

All visual stimuli used in this study were displayed using an OpenGL-based software system developed by Dr. David Sheinberg at Brown University. The experimental task was controlled by a QNX real-time operating system using a state machine. Eye position was monitored using video eye tracking (Eyelink 1000, SR Research). Stimuli were displayed at the scanner on a 24-inch BOLDscreen flat-panel display (Cambridge Systems). The general design of the visual sequence paradigm was based on a similar auditory sequence task (L. Wang et al., 2015).

#### **2.5.2.1. Stimuli**

Each image presentation consisted of fractal stimulus (approximately 8° visual angle) with varying colors and features. Fractals were generated using MATLAB for each scanning session using custom scripts based on stimuli from (H. F. Kim & Hikosaka, 2013) following the instructions outlined in (Miyashita et al., 1991). For each scan session, new, luminance matched, fractal sets were generated. All stimuli were presented on a gray background, with a fixation spot that was always present on the screen superimposed on the images. To provide behavioral feedback, the fixation spot was yellow when the monkey was successfully maintaining fixation and red if the monkey was not fixating. Stimuli were displayed for 0.1 to 0.3 s each, depending on the sequence type and timing template, detailed as follows.

#### 2.5.2.2. Sequence Types

There are five sequence types in this task (**Figure 4**): habituation sequences and four deviant sequence types. Across these sequence types, there were a total of nine different timing templates used. These templates were included to counterbalance for stimulus and sequence duration across the sequence types and to provide a greater variety of sequential timings during habituation. The inter-sequence interval was jittered to decorrelate across timing templates (mean 2 s, 0.25-8 s).

##### *Habituation Sequences*

Habituation sequences were composed of images drawn from a pool of four possible fractals. We will refer to the habituation image pool as [A, B, C, D]. Sequences were composed from these images in one of two possible rules: three the same, one different (e.g., AAAB, DDDC) and four the same (e.g., AAAA, CCCC). All sequences contained four images and followed one of three possible general timings based on the total duration of the sequence: short (1.1 s), medium (1.7 s), and long (2.3 s). Each total sequence duration, in turn, had two possible timing templates within it, one with longer stimulus durations and one with shorter stimulus durations: short 0.1 s and 0.2 s, medium 0.1 s and 0.3 s, long 0.2 s and 0.3 s. Inter-stimulus intervals were arranged to evenly space the four stimulus presentations within the total sequence duration.

##### *Deviant Sequences*

Deviant sequences were composed of images drawn from a different pool of three possible fractals. We will refer to the deviant image pool as [E, F, G]. All deviant images were displayed for 0.2 s, regardless of deviant type. Across deviant types, the total sequence durations were matched to the short, medium, and long habituation timing templates. There were four deviant types, detailed as follows:

*New Items, Same Rule (NISR)*: These deviants use images that come from the deviant pool of images, but do not differ from the habituation rule. For example, if the habituation rule was three the same, one different then NISR sequences would follow the same rule with new images (e.g., GGGF and FFFE) Alternatively, if the habituation rule was four same, an example NISR would be EEEE. All sequences were four items and had a total duration of 1.7 s.

*Rule deviants*: These deviants do not follow the same rule as habituation, but instead follow the alternate rule. If the habituation rule was three the same, one different, example deviants would follow the four the same rule, e.g., EEEE and GGGG. All deviants contained four images and had a total sequence duration of 1.7 s, the same as medium habituation sequences.

*Number Deviants*: These deviants follow the same rule as habituation but contain a different number of images (either two or six). If the habituation rule was three the same, one different, example deviants would be EG and FFFFFE. Two-item deviants had a total sequence duration of 1.1 s, the same as short habituation sequences, and six-item deviants had a total sequence duration of 2.3 s, the same as long habituation sequences.

*Double Deviants*: These deviants combine Rule and Number deviant types. If the habituation rule was three the same, one different, example deviants would be EE and GGGGGG. The timing was the same as number deviants.

### **2.5.2.3. Block Structure**

Each block contained 30 sequences and lasted approximately 112 s on average. Habituation blocks contained equal numbers of the six possible timing templates (two of each: short, medium, and long). Habituation sequences were presented in pseudo-random order such that a sequence could not begin with the same fractal as the final fractal of the previous sequence. Deviant blocks were

composed of 24 habituation sequences and six deviant sequences. All deviant sequences within a block were of the same sequence type. The six deviant sequences were pseudo-randomly interspersed throughout the block such that deviant sequences did not occur in the first 6 sequences of the block (to avoid block initiation confounds), and deviant sequences were not presented consecutively to each other. If deviant sequences contained a variable number of items (i.e., number deviants and double deviants), then an equal number of two- and six-item sequences were included within a single block. The 24 habituation sequences within deviant blocks were presented in the same manner as in habituation blocks (i.e., evenly distributed timing templates and avoiding between-sequence fractal image repeats).

#### 2.5.2.4. Run Structure

Each run was composed of five blocks, interleaved with 14 s fixation blocks (**Figure 4**). The first block of each run contained only habituation sequences. The four subsequent blocks were one of each of the four possible deviant types, with their order counterbalanced across runs. The same habituation rule was used for the entirety of a single run. Runs lasted approximately 10.5 min. The sequence rule (*three same, one different* or *four same*) used for each run was counterbalanced across each scanning session so as to have an equal number of runs for each rule. Monkeys typically completed 4-8 runs of this task (among other tasks not reported on here) in a single scanning session (one day).

Runs were initiated according to the monkey's fixation behavior to ensure that the monkey was not moving and engaged in the task before acquiring functional images. During this pre-scan period, a fixation spot was presented. Once the monkey successfully acquired this fixation spot and received approximately four liquid rewards (12 – 16 s), functional image acquisition and the first habituation block were initiated.

#### **2.5.2.5. Reward**

The timing of liquid rewards was not contingent upon sequential events, only on the monkey maintaining fixation. Rewards were delivered on a graduated schedule such that the longer the monkey maintained fixation, the more frequent rewards were administered (Leite et al., 2002). The first reward was given after 4 s of continuous fixation. After two consecutive rewards of the same fixation duration, the fixation duration required to obtain reward was decreased by 0.5 s. The minimum duration between rewards that the monkey could obtain was 0.5 s. Fixation had to be maintained within a small window (typically 3° of visual angle) around the fixation spot to not break fixation. The only exception was a brief time window (0.32 s) provided for blinks. If the monkey's eyes left the fixation window and returned within that time window, it would not trigger a fixation break. If fixation was broken, the reward schedule would restart at the maximum 4 s duration required to obtain reward.

#### **2.5.3. FMRI Data Acquisition**

Monkeys were trained to sit in the “sphinx” position in a custom MR-safe primate chair (Applied Prototype, Franklin, MA or custom-made by Brown University). The monkey's head was restrained from moving via a plastic “post” (PEEK, Applied Prototype, Franklin, MA) affixed to the monkeys' head and the primate chair. Monkeys were habituated to contrast agent injection procedures, recorded MRI sounds, wearing earplugs (Mack's Soft Moldable Silicone Putty Ear Plugs, Kid's size), and transportation to the scanner prior to MRI scanning sessions. Monkeys were trained on the behavioral task with different images that were never used during scanning.

Prior to each scanning session, monkeys were intravenously injected with a contrast agent: monocryalline iron oxide nanoparticle (MION, Feraheme (ferumoxytol), AMAG Pharmaceuticals, Inc., Waltham, MA, 30 mg per mL or BioPal Molday ION, Biophysics Assay

Lab Inc., Worcester, MA, 30 mg per mL). MION to improves the contrast-to-noise ratio ~3-fold (Leite et al., 2002; Vanduffel et al., 2001) and enhances spatial selectivity of MR signal changes (Zhao et al., 2006). MION was injected, approximately 30-60 min before scanning, into the saphenous vein below the knee (7 mg/kg), then flushed with a volume of sterile saline approximately double the volume of the MION injected. No additional MION was added during scanning, as MION has a long blood half-life (15.3 +/- 3.5 hr) (Leite et al., 2002).

A Siemens 3T PRISMA MRI system with a custom six-channel surface coil (ScanMed, Omaha, NE) at the Brown University MRI Research Facility was used for whole-brain imaging. Anatomical scans consisted of a T1-MPRAGE (repetition time, TR, 2700 ms; echo time, TE, 3.16 ms; flip angle, 9°; 208 sagittal slices; 0.5 x 0.5 x 0.5 mm), a T2 anatomical (TR, 3200 ms; TE 410 ms; variable flip angle; 192 interleaved transversal slices; 0.4 x 0.4 x 0.4 mm), and an additional high resolution T2 anatomical (TR, 8020 ms; TE 44 ms; flip angle, 122°; 30 interleaved transversal slices; 0.4 x 0.4 x 1.2 mm). Functional images were acquired using a fat-saturated gradient-echo planar sequence (TR, 1.8 s; TE, 15 ms; flip angle, 80°; 40 interleaved axial slices; 1.1 x 1.1 x 1.1 mm).

The target sample size (number of runs per monkey) was calculated using pilot data from a previous version of this task not included in the current data set. A region of interest was constructed from a cluster of deviant > NISR activation and the number of runs calculated for a significant effect in this region (using the beta values of the onset GLM, see below) at 80% power and alpha = 0.05 (G-Power). Guided by this power analysis and similar studies (L. Wang et al., 2015), we estimated a total of 200 runs across the three animals would be necessary.

#### 2.5.4. FMRI Data Analysis

The majority of the following analyses were performed in Matlab using SPM 12 (<http://www.fil.ion.ucl.ac.uk/spm>). Prior to analysis, data were preprocessed using the following steps: reorienting (to ensure proper assignment of the x,y,z planes), motion correction (realignment), normalization, and spatial smoothing (2 mm isotropic Gaussian kernel separately for gray matter and white matter). All steps were performed on individual runs separately. The T1-MPRAGE anatomical image was skull stripped using FSL BET brain extraction tool (<http://www.fmrib.ox.ac.uk/fsl/>) to facilitate normalization. All images were normalized to the 112-RM SL macaque atlas (McLaren et al., 2009).

Runs were included for analysis only if they met the following criteria: the monkey had to be performing well and a sufficient number of acquisition volumes within the run had to pass data quality checks. The monkey's performance was evaluated by calculating the percentage of time within a run that fixation was maintained. Runs were excluded if the monkey was fixating < 80% of the time (similar criteria as in (Leite et al., 2002; Vanduffel et al., 2001; L. Wang et al., 2015)). Approximately 20% of runs were excluded due to poor fixation: 10% from monkey J, 3% from monkey W and 7% from monkey B. To evaluate data quality, we used the ART toolbox (Artifact Detection Tools, [https://www.nitrc.org/projects/artifact\\_detect](https://www.nitrc.org/projects/artifact_detect)) to detect outlier volumes. Any volumes that had motion greater than one voxel (1.1 mm) in any direction were excluded. Any run with greater than 12% of volumes excluded was excluded from analysis (0% runs excluded for monkey J, 0.5% of runs excluded for monkey W, and 15% of runs excluded for monkey B). Runs with poor image quality due to artifact or banding to pre-process or analyze were also excluded. These accounted for 2% of the data for monkey J, 5% for monkey W, and 0.5% for monkey B. After applying these criteria, a total of 232 runs (average of 340 volumes per run for all animals,

93 sessions in total across animals) were included for analysis from 3 monkeys: monkey W: 97 runs (32 sessions); monkey J: 65 runs (32 sessions), and monkey B: 70 runs (32 sessions).

#### 2.5.4.1. Models

Within-subject statistical models were constructed under the assumptions of the general linear model (GLM) in SPM 12 for each pseudo-subject bin. For all models, data were binned into approximately 10-run pseudo-subject bins. Each bin contained data from only one monkey. Runs were pseudo-randomly assigned to bins to balance the number of runs which followed each of the two sequential rules (three same one different or four same) and the distribution of runs from earlier and later scanning sessions. Condition regressors were all convolved with a gamma function (shape parameter = 1.55, scale parameter = 0.022727) to model the MION hemodynamic response function (Vanduffel & Farivar, 2014). The first six sequences in a run and reward times were included as nuisance conditions. Additional nuisance regressors were included for the six motion estimate parameters (translation and rotation), outlier volumes, and image variability (standard deviation of within run image movement variability, calculated using the ART toolbox). Outlier volumes were determined using the ART toolbox (standard global mean; global signal detection outlier detection threshold = 4.5; motion threshold = 1.1mm; scan to scan motion and global signal change for outlier detection) and one additional regressor with a “1” at only that volume was included for each volume to be “scrubbed”.

Regressors were estimated using a bin-specific fixed-effects model. Whole-brain estimates of bin-specific effects were entered into second-level analyses that treated bin as a random effect. One-sample t-tests (contrast value vs zero,  $p < 0.005$ ) were used to assess significance. These effects were corrected for multiple comparisons when examining whole-brain group voxelwise effects using extent thresholds at the cluster level to yield false discovery rate (FDR) error correction ( $p$

< 0.05). Group contrasts were rendered on an inflated MNI canonical brain using Caret (Van Essen et al., 2001). Prior to selecting GLM's we used the model assessment, comparison, and selection toolbox (MACS, <https://github.com/JoramSoch/MACS>, (Soch & Allefeld, 2018) to determine models that would be the best fit. Three GLMs were applied to the data as follows:

*Onsets Model:* To assess the univariate effects of deviant sequences, we constructed a model using instantaneous stimulus onset regressors for the first item in each sequence with the following nine condition regressors for different sequence types: short, medium, and long habituation sequence timing templates; NISR; rule deviants; two- and six-item number deviants; and two- and six-item rule and number deviants.

*Parametric Last Item versus Unique Ramp Model:* To directly test whether variance could be better accounted for by a phasic response at the last item in the sequence or ramping activation, we constructed a pair of models to allow last item and ramp regressors to compete for variance within the same model. Onset regressors were constructed with an instantaneous stimulus onset regressor at each position in the sequence with the same nine condition regressors for the different sequence types as in the Onsets Model: short, medium, and long habituation sequence timing templates; NISR; rule deviants; two- and six-item number deviants; and two- and six-item rule and number deviants. Including an onset at each position effectively modeled sustained activation throughout the sequence and enabled the inclusion of the following parametric regressors. The last item parametric was added as ones at the first sequence positions and an arbitrarily larger value (6) at the last item. The ramp parametric was entered as the sequence position (1-4, 1-2, or 1-6) for each sequence. Parametric regressors were implemented hierarchically in the GLM. Therefore, variance explained by the last parametric regressor (in this case, ramping), is above and beyond what could be explained by the onsets or last item regressors.

*Parametric Ramp versus Unique Last Item Model:* This second model of the pair sought to identify variance uniquely explained by the last item regressor, above and beyond variance explained by the onsets or ramping regressors. All other aspects of the model were the same as the unique ramp model above.

#### **2.5.4.2. ROI Analyses**

The primary bilateral regions of interest were constructed from the coordinates of a seed region centered in macaque monkey area 46d. These coordinates were determined, using diffusion weighted and functional MRI, to be most similar to the lateral portion of human area 10 (Gilbert et al., 2010; Sallet et al., 2013). Human lateral area 10 overlaps with areas of ramping activation observed in human RLPFC in previous studies (Desrochers et al., 2015, 2019; McKim & Desrochers, 2022b). A 5 mm sphere was created around the center coordinate for the seed region in macaque Montreal Neurological Institute (MNI) space. The sphere was then transformed into 112RM-SL space using RheMap (Simpilatz & Klink, 2020, resulting in a sphere centered at  $xyz = 12.7, 32.6, 22.5$  in 112RM-SL space. For identification of brain areas we also utilized the NIMH Macaque Template (NMT v02, Macaque Atlas, Jung et al., 2021; Seidlitz et al., 2018).

Additional ROIs were constructed with the explicit purpose of comparing nearby regions in DLPFC that were significant clusters of activation last item versus ramping models. Specifically, the significant left DLPFC cluster of activation for Unique Ramp, Rule Deviants > NISR in the unique ramp model (center  $xyz = -12.2, 36, 23$ ) and the significant left DLPFC cluster of activation for Unique Last, Rule Deviants > NISR in the unique last item model (center  $xyz = -12.3, 42.9, 21.8$ ) were taken for comparison.

To compare activation within and across ROIs in a manner that controlled for variance, we extracted t-values from the condition of interest over baseline using the Marsbar toolbox (Jean-

Baptiste Poline, 2002). T-values (one for each pseudo-subject bin,  $n = 22$  bins) were entered into RM-ANOVAs with the identity of the monkey entered as a covariate.

## 2.6. Results

Three monkeys (*macaca mulatta*) performed no-report abstract sequence viewing while undergoing awake fMRI scanning. The monkeys were trained to fixate on a central spot while viewing a stream of fractal images arranged into four-item visual sequences (based on Wang, et al., **Figure 4**). This task did not require responses, only fixation, and thus was termed “no-report”. The task was performed in runs (~10 min each), that each contained five blocks. For each run, the first block habituated animals to one of two possible sequential rules AAAB, or AAAA (A and B represent different images drawn from a pool of four possible images; 30 sequences in total per block). Habituation sequences each had one of six possible timing templates to balance stimulus and sequence durations across sequence types. Each subsequent block contained rare deviants (6 of the 30 sequence repetitions per block) of one of the following four possible types: new images following the same rule, number deviants (2 or 6 items), rule deviants (e.g., AAAA), or double deviants. All deviant images were drawn from a separate three-image pool. The five total blocks were interleaved with 16 s fixation blocks. To encourage animals to maintain fixation throughout, reward was administered on a graduated schedule not correlated with sequence presentation: the longer they maintained fixation, the shorter the duration between rewards. Reward was thus decorrelated from the four-item visual sequences. A total of 232 runs were analyzed (97 monkey W, 65 monkey J, 70 monkey B). Monkeys performed the task well and fixated for 95% of the time in included runs (see Methods for those excluded).

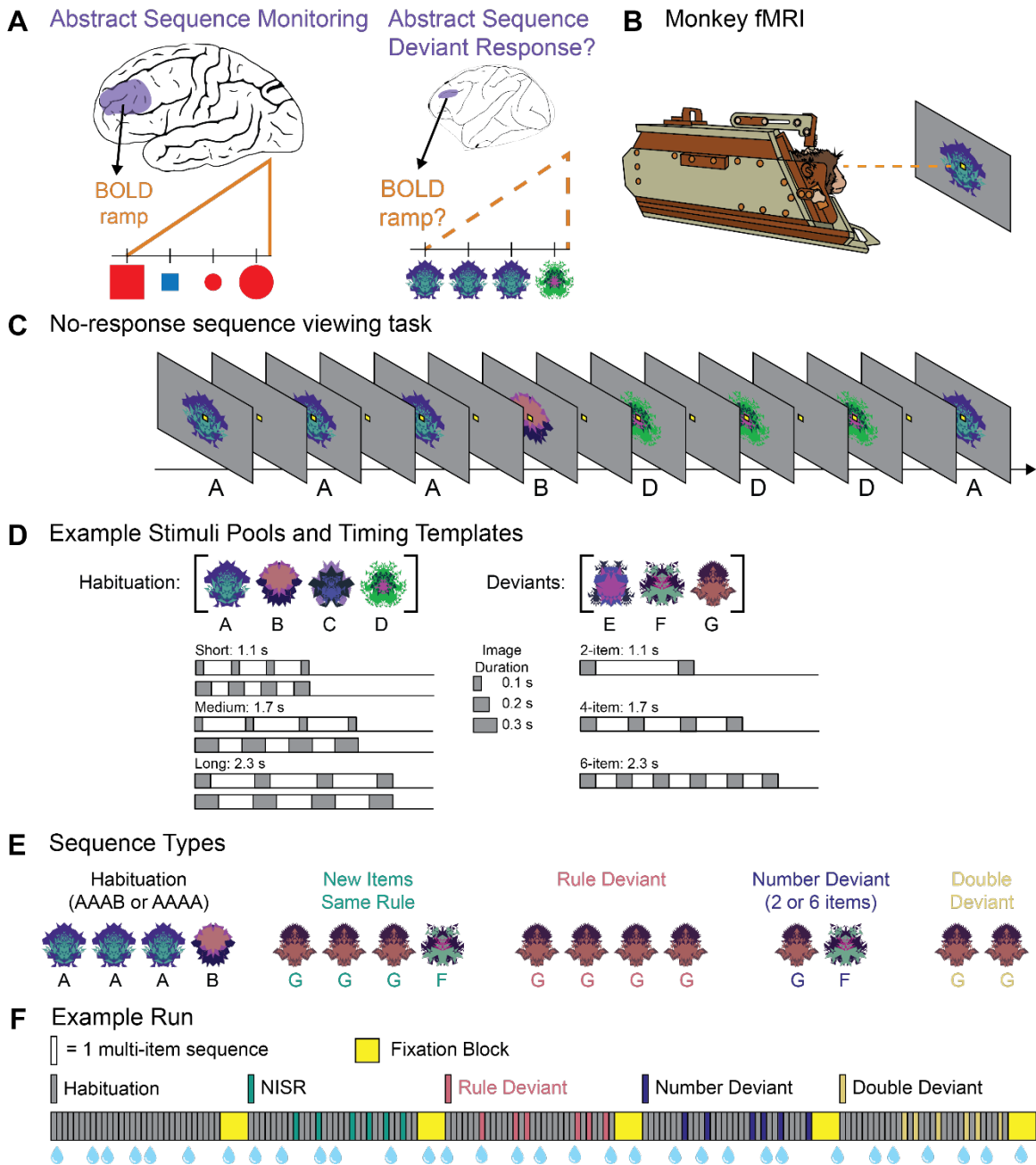


**Figure 4. No-report abstract sequence viewing task.** **A.** Schematic representation of human rostralateral prefrontal cortex (RLPFC; left) and monkey dorsolateral prefrontal cortex (DLPFC; right) depicting the main questions that were the focus of this study: Does monkey DLPFC monitor abstract sequences, as shown by responses to deviant sequences? and does monkey DLPFC exhibit ramping activation, as found in human RLPFC during sequence monitoring? **B.** Monkeys only fixate throughout runs. Scanning is performed in the “sphinx” position. **C.** Example partial habituation block for sequence rule *three same, one different* (AAAB). **D.** Example stimulus pools (top) show

a set of images that would be used in a single scanning session. New images are used each session. Six possible timing templates for habituation sequences (bottom, left) and deviant sequences (bottom, right) illustrated with gray rectangles indicating single images. Total sequence durations are listed for each template type. **E.** Examples of the five sequence types if the sequence rule in use is *three same, one different*. **F.** Example run, with each bar indicating one multi-image sequence: four images in habituation, new items same rule (NISR), and rule deviants; two or six images in number and double deviants. The first block contains only habituation sequences and subsequent blocks contain only one of the four deviant types. Sequence blocks alternate with fixation blocks. Blue water droplets schematize reward delivery, which is decoupled from sequence viewing and delivered on a graduated schedule based on the duration the monkey has maintained fixation.

### **2.6.1. Monkey DLPFC represents changes in abstract visual sequences**

Our first goal was to test whether area 46 differentially responds when there is a change in the abstract visual sequence. Because this task is no-report, we examined this question using neural responses (BOLD) to deviant sequences. Previous work has shown that such deviant responses disappear with inattention and are robust in brain areas processing sequence related information (Bekinschtein et al., 2009; Dehaene et al., 2015). These results suggest that deviant neural responses indicate that individuals are attending to the sequences, even in the absence of a report. Therefore, we used neural responses to rare deviant sequences to indicate awareness of changes to an established abstract sequence, as is in similar auditory tasks (Uhrig et al., 2014; L. Wang et al., 2015). To specifically query the responses to abstract sequence changes, we could not simply compare habituated sequences to deviant sequences, as the deviant sequences were composed from a different pool of images than the habituation sequences, and any differences observed between habituation and deviant sequences could have resulted from differences in image identity. Therefore, to specifically examine changes in abstract sequence structure, we compared new items of the same rule (NISR) to number deviants and rule deviants. All images in this comparison were

drawn from the same pool of (deviant) images. Double deviants were not included in analyses because of the inability to dissociate between changes due to rule and number.

We first constructed an unbiased region of interest (ROI) for monkey area 46 in each hemisphere to compare activity between rule and number deviants and NISR. Monkey area 46 has many potential functional subdivisions (Borra et al., 2011, 2019; Gerbella et al., 2010, 2013; Saleem et al., 2014); therefore, we created a 5 mm sphere centered on a seed region identified as having the most similar connectivity with human RLPFC in monkey diffusion and functional MRI (Sallet et al., 2013, center  $xyz = 12.7, 32.6, 22.5$  in area 46d, see Methods). The resulting sphere spanned a small region of area 46 that encompassed 46d, 46f, and 46v (NIMH Macaque Template, NMT v2.0 Macaque Atlas, Jung et al., 2021; Seidlitz et al., 2018). Because sequence related activity in human RLPFC was observed in both hemispheres, we used identical spheres (mirrored coordinates) in the left and right hemispheres (referred to as L46 and R46, respectively) throughout. To compare activity between rule and number deviants and NISR in these ROIs, we created a model that included separate regressors for each habituation timing and deviant type, modeled as zero-duration onsets. Statistical testing was performed on  $\sim 10$  run bins ( $n = 22$ ), each consisting of data from a single monkey (see Methods). We compared t-values from the contrast of each condition over baseline (e.g., Rule Deviants  $>$  Baseline vs. NISR  $>$  Baseline) to account for potential differences in variance across conditions. This type of comparison was used to examine ROI activity throughout, and we refer to comparisons by the conditions of interest (without listing the contrast over baseline, e.g., Rule Deviants  $>$  NISR). All statistical tests on ROIs were performed on binned data and included a covariate for monkey identity ( $n = 3$ ). While we report the effect of monkey in the following analyses, the main focus of the study was not on individual differences, and our discussion focuses on condition effects.

We found that R46 represented abstract sequence changes, showing greater deviant activation across both deviant types (**Figure 5; Table 1**). Responses were reliably greater for rule deviants compared to NISR (sequence type:  $F(1, 19) = 4.6, p = 0.046, \eta_p^2 = 0.19$ ) and marginally greater for number deviants compared to NISR (sequence type:  $F(1, 19) = 3.9, p = 0.062, \eta_p^2 = 0.17$ ). Even though deviant responses compared to NISR in L46 did not reach statistical significance (**Table 1**), there were no reliable differences between responses in R46 and L46 (**Table 2**). These results suggest that a specific region of monkey DLPFC, area 46, monitors abstract visual sequence structure.

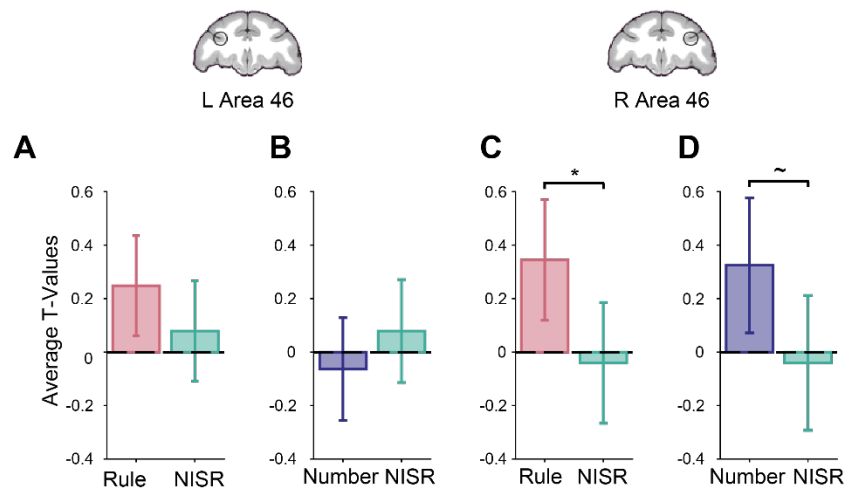


**Figure 5. Area 46 represents abstract visual sequences.** T-values for the condition of interest > baseline are shown. The locations of area 46 regions of interest (ROIs), L46 and R46, are outlined in black on coronal sections ( $y = 33$ ). **A.** Rule deviants compared to new items, same rule (NISR) in L46. **B.** Number deviants compared to NISR in L46. **C.** Rule deviants compared to NISR in R46 showed a reliable difference. **D.** Number deviants compared to NISR in R46 showed a marginal difference. Comparisons in L46 showed similar trends as in R46. Error bars are 95% confidence intervals (1.96 x standard error of the within-bin mean).

**Table 1.** Repeated measures ANOVAs comparing rule and number deviants to NISR in L46 and R46.

Factor	dfs	L46			R 46		
		F	p	$\eta_p^2$	F	p	$\eta_p^2$
<i>Rule Deviants &gt; NISR</i>							
Sequence Type	1, 19	0.39	0.54	0.02	4.6	0.046	0.19
Monkey	2, 19	3.55	0.049	0.27	1.4	0.28	0.13
Monkey x Sequence Type	2, 19	1.15	0.34	0.11	2.9	0.078	0.24
<i>Number Deviants &gt; NISR</i>							
Sequence Type	1, 19	0.51	0.48	0.03	3.9	0.062	0.17
Monkey	2, 19	3.8	0.041	0.29	0.76	0.48	0.074
Monkey x Sequence Type	2, 19	0.098	0.91	0.01	5.15	0.016	0.35
<i>Habituation &gt; NISR</i>							
Sequence Type	1, 19	0.0053	0.94	0.0003	1.6233	0.33	0.051
Monkey	2, 19	4.35	0.028	0.31	3.37	0.48	0.26
Monkey x Sequence Type	2, 19	0.45	0.64	0.05	1.6	0.22	0.15

**Table 2.** Repeated measures ANOVAs comparing deviant responses in L46 and R46.

Factor	dfs	Rule Deviants > NISR			Number Deviants > NISR		
		F	p	$\eta_p^2$	F	p	$\eta_p^2$
<i>R46 &gt; L46</i>							
Sequence Type	1, 40	3.6	0.07	0.08	0.85	0.36	0.02
Monkey	2, 40	4.15	0.02	0.17	1.14	0.33	0.05
Brain Area	1,40	0.005	0.94	0.0001	0.67	0.42	0.016
Monkey x Sequence Type	2, 40	0.54	0.6	0.026	2.88	0.07	0.13
Brain Area x Sequence Type	1,40	0.51	0.48	0.012	2.7	0.11	0.06

As a control, we also examined conditions where the pool of images differed, but the abstract sequential structure did not. If area 46 was responding specifically to a change in the abstract sequential structure, then a change in the images should not change its activation level. We examined the difference in contrast t-values between NISR and habituation trials with comparable stimulus durations (“medium” timing, as in **Figure 4D**). We did not find any significant differences between these conditions in either R46 or L46 (**Table 1**), indicating that changes in activation in area 46 were specific to changes in abstract sequential structure.

Results from area 46 ROIs were supported by whole-brain contrasts examining responses to number and rule deviants. Contrasts of Rule Deviants > NISR and Number Deviants > NISR both showed significant clusters of activation in right area 46 (**Figure 6, Table 3, Extended Data Figure 3-1**). Other significant clusters of activation were located in areas such as the caudate nucleus, high-level auditory cortex (rostromedial belt region), and dorsal premotor cortex, areas also observed in a similar auditory sequence task (L. Wang et al., 2015). Further, deviant responses in earlier sensory areas (e.g., V2) may be analogous to responses in auditory cortex previously observed. Though we could not address the question of sensory generality within the current experiment, these results raise the intriguing possibility that these previously indicated areas could be sensory-modality general in their responses to abstract sequential structure.

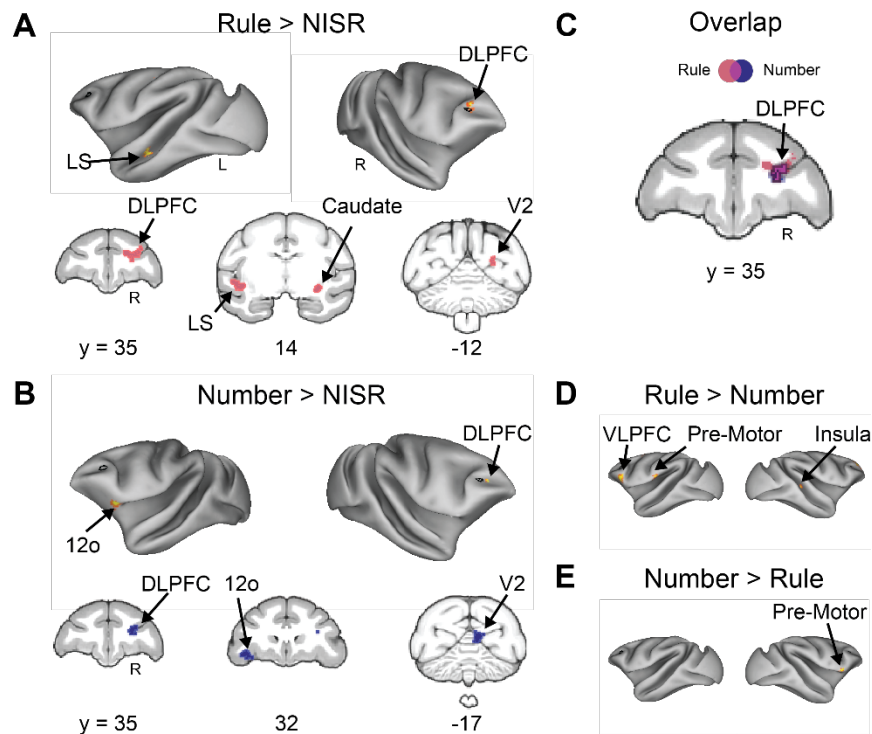


**Figure 6. Whole-brain deviant activity shows area 46 represents both rule and number deviants.** A. Voxel wise contrast of Rule Deviants > NISR false discovery rate (FDR) error cluster corrected for multiple comparisons (FDRc < 0.05, height  $p < 0.005$  unc., extent = 130) are shown. Individual monkey data shown in **Extended Data Figure 3-**

**1A. B.** Voxelwise contrast of Number Deviants > NISR (FDRc < 0.05, height  $p < 0.005$  unc., extent = 132). Individual monkey data shown in **Extended Data Figure 3-1B**. **C.** Overlap of Rule Deviants > NISR and Number Deviants > NISR contrasts showed significant, unique conjunction (violet outlined in black) only in the DLPFC. **D.** Voxelwise contrast of Rule Deviants > Number Deviants showing no significant clusters of activation in area 46 (FDRc < 0.05, height  $p < 0.005$  unc., extent = 102). **E.** As in (C) for Number Deviants > Rule Deviants (FDRc < 0.05, height  $p < 0.005$  unc., extent = 111). Black outline on inflated brains indicates location of L46 or R46 (depending on the hemisphere shown) for reference. Lateral Sulcus (LS), Dorsal Lateral Pre-frontal Cortex (DLPFC), Ventral Lateral Pre-frontal Cortex (VLPFC), Secondary Visual Cortex (V2), Orbital Prefrontal Area (12o).

**Table 3.** Rule and number deviants compared to NISR contrast activation coordinates. Area labels as in the NIMH NMT v02 Macaque Atlas.

Contrast Location	Extent (voxels)	x	y	z	Peak t-val
<b>Rule Deviant &gt; NISR</b>					
Dorsolateral Prefrontal Cortex (46d)	282	10.5 14	34.5 36	21.5 26	4.24 3.88
Medial Prefrontal Cortex (10mr)	195	0	47.5	17	5.96
Dorsal Pre-motor Cortex(6DR)		13	21	25	
Motor Cortex (F1)	213	-11	16.5	32	5.58
Caudate Nucleus (cd)	130	14.5	13	8	3.88
	138	-14.5	11.5	7.5	4.09
Lateral Sulcus/Auditory Cortex (RM)	282	-21	13.5	9	5.59
Secondary Visual Cortex (V2)	207	8.5	-15	21	4.34
Cerebellum					
<b>Number Deviants &gt; NISR</b>					
Dorsolateral Prefrontal Cortex (Area 46d)	168	9	35	21.5	6.44
Orbital Prefrontal Area (12o)	162	-16	32	9.5	5.13
Secondary Visual Cortex (V2)	132	4.5	-16.5	18.5	4.96

To determine if the observed responses to number and rule deviants were similar in area 46, we directly examined whether these responses generalized across deviant types. The t-values in R46 were not different between rule and number deviants (sequence type:  $F(1,19) = 0.0011$ ,  $p = 0.92$ ,

$\eta_p^2 = 0.11$ , monkey:  $F(2, 19) = 2.5$ ,  $p = 0.11$ ,  $\eta_p^2 = 0.21$ ; monkey x sequence type:  $F(2, 19) = 1.15$ ,  $p = 0.34$ ,  $\eta_p^2 = 0.11$ ). Next, we performed a conjunction analysis to determine the areas of activation that overlapped in the Rule Deviants > NISR and Number Deviants > NISR contrasts. We found that the only cluster of significant overlap between the deviant contrasts was in right area 46 (**Figure 6C**). In support of this finding, whole-brain direct contrasts of rule and number deviants showed significant activation clusters in VLPFC, insula, and pre-motor cortex, but no significant clusters in area 46 (**Figure 6D, E**). In summary, these results suggest that abstract visual sequential structure is monitored in area 46, and that this monitoring is both unique to area 46 and general across different kinds of deviations.

### **2.6.2. Ramping activation reflects sequence monitoring in monkey DLPFC**

We next tested the prediction that area 46 would display similar dynamics to those observed in humans during abstract sequences. Specifically, previous experiments in humans showed that BOLD activity increased (“ramped”) from the beginning to the end of sequences in the RL PFC (Desrochers et al., 2015, 2019; McKim & Desrochers, 2022b). Given the similarity in connectivity between monkey area 46 and human RL PFC, we hypothesized that changes in abstract sequence structure would also produce changes in ramping activation in area 46 if abstract sequence monitoring underlies this dynamic.

To test if ramping dynamics were present in area 46 during this task, we first designed a model to isolate these dynamics. This model included regressors for the three dominant potential dynamics (**Figure 7A, Extended Data Figures 4-1 and 4-2**, see also Materials and Methods). First, instantaneous onsets were included for each image presentation, effectively modeling sustained activation throughout each sequence. Then, two parametric regressors were included: last item change and ramping. The ramping regressor parallels the analysis that revealed ramping in human

RLPFC: it increases linearly from the first to the last item in the sequence, and resets at each new sequence. The last item change regressor is low at the first three positions of each sequence, and high at the last item in the sequence. This regressor was designed to account for the fact that differences in the rule that the sequence followed would occur at the last item (e.g., the difference between AAAA and AAAB occurs at the fourth item), and a dynamic associated with this change could have variance mistakenly assigned to a ramping regressor.

These parametric regressors were orthogonalized in a stepwise fashion and only absorbed variance above and beyond variance accounted for by the onset regressor. The last regressor, therefore, contained “unique” variance. A pair of models, one with unique variance assigned to ramp and one with it assigned to last item, were created to examine these dynamics. The correlation between the resulting regressors was, as expected, low. For example, in one bin of this parametric model with the unique variance assigned to ramp, the average correlation coefficient between last item change and ramp regressors was 0.00005 ( $\pm 0.0001$  standard deviation). While there are likely nearly infinite variations of dynamics possible that lie across a spectrum between the last item change and ramping (e.g., exponential), our purpose in designing these models was not to explore the space of all possible dynamics, but to test for ramping dynamics in area 46.

We found ramping dynamics in monkey area 46 related to abstract sequence monitoring. When comparing t-values of contrasts between deviants and baseline using the same spherical area 46 ROIs described above, we observed significant, unique variance ascribed to ramping activation in L46 during rule deviants compared to NISR (sequence type:  $F(1, 19) = 5.03, p = 0.037, \eta_p^2 = 0.21$ ; **Table 4; Figure 7B**). Unique ramping activation showed a numerical trend in the same direction for number deviants compared to NISR in L46, but it did not reach statistical significance (**Table**

4). Activity in L46 was not reliably different between the two deviant types (sequence type:  $F(1,19) = 2.06, p = 0.17, \eta_p^2 = 0.098$ , monkey:  $F(2, 19) = 0.57, p = 0.64, \eta_p^2 = 0.06$ ; monkey x sequence type:  $F(2, 19) = 2.01, p = 0.16, \eta_p^2 = 0.17$ ). In R46, changes in unique ramping activation during rule and number deviants were not significant (**Table 4**). Despite apparent differences between L46 and R46, unique ramping was not reliably different between these ROIs (**Table 5**). These results suggest that area 46 shows ramping dynamics for sequential rule changes. Interestingly, ramping may be preferentially present in L46, suggesting that while both hemispheres detect abstract sequence deviations, they may do so with different dynamics. Further, these results suggest similar sequential monitoring processes may be present across species in analogous areas.

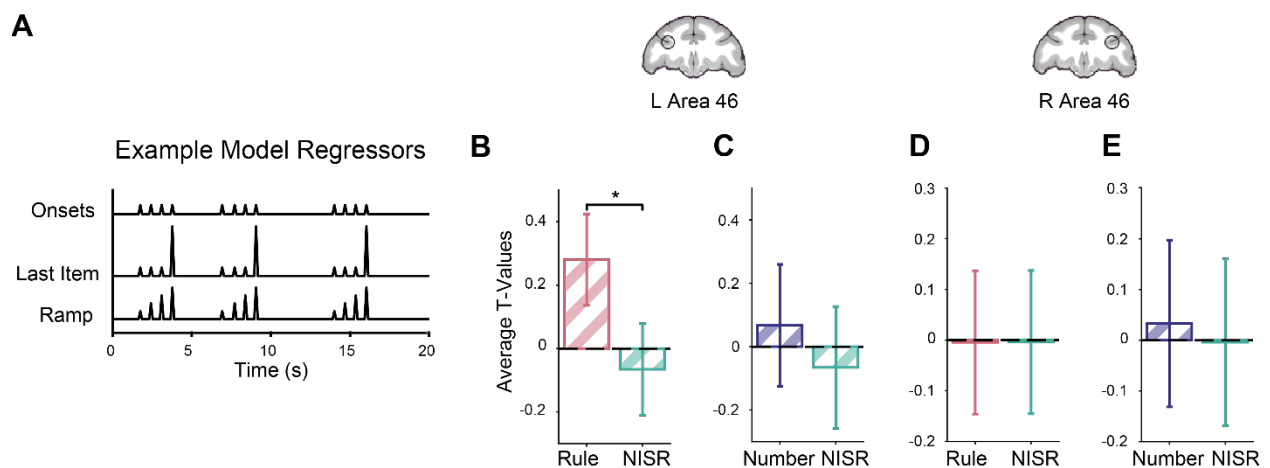


**Figure 7. Area 46 shows ramping activity for deviations to an established sequence rule.** Parametric models and T-values for the condition of interest > baseline shown. Coronal brain slices ( $y = 33$ ) show locations of area 46 ROIs, L46 and R46, outlined in black. **A.** Example of regressors used to model parametric ramp and parametric last item. Example regressors through the orthogonalization process shown in **Extended Data Figures 4-1 and 4-2**. **B.** Unique ramping during rule deviants compared to NISR in L46 showed a reliable difference. **C.** Unique ramping during number deviants compared to NISR in L46. **D.** Unique ramp number deviants compared to NISR in R46. **E.** Unique ramping during number deviants compared to NISR in R46. Comparisons that were not reliably different showed similar trends. Error bars are 95% confidence intervals (1.96 x standard error of the within-bin mean).

**Table 4.** Repeated measures ANOVAs comparing unique ramping activity during rule and number deviants to NISR in L46 and R46.

Factor	dfs	L46			R 46		
		F	p	$\eta_p^2$	F	p	$\eta_p^2$
<i>Unique Ramp, Rule Deviants &gt; NISR</i>							
Sequence Type	1, 19	5.03	0.037	0.21	0.01	0.91	0.00075
Monkey	2, 19	0.82	0.45	0.08	0.64	0.54	0.63
Monkey x Sequence Type	2, 19	0.23	0.8	0.0235	0.81	0.46	0.08
<i>Unique Ramp, Number Deviants &gt; NISR</i>							
Sequence Type	1, 19	0.42	0.52	0.02	0.03	0.86	0.0016
Monkey	2, 19	2.39	0.12	0.2	0.24	0.45	0.08
Monkey x Sequence Type	2, 19	5.15	0.63	0.047	5.15	0.84	0.0235

**Table 5.** Repeated measures ANOVAs comparing unique ramping deviant responses in L46 and R46.

Factor	dfs	Unique Ramp, Rule Deviants > NISR			Unique Ramp, Number Deviants > NISR		
		F	p	$\eta_p^2$	F	p	$\eta_p^2$
<i>R46 &gt; L46</i>							
Sequence Type	1, 40	0.38	0.54	0.009	2.4	0.13	0.06
Monkey	2, 40	1.62	0.21	0.07	1.5	0.24	0.07
Brain Area	1, 40	0.02	0.89	0.0005	1.5	0.25	0.03
Monkey x Sequence Type	2, 40	0.64	0.53	0.03	0.12	0.89	0.006
Brain Area x Sequence Type	1, 40	0.14	0.71	0.003	2.7	0.11	0.06

Because variance due to changes at the last item of the sequence could be misattributed to ramping regressors, we directly compared activity in area 46 that could be accounted for by ramping and last item change regressors. In this control analysis, we found that activity was significantly greater for unique ramping than unique last item change during rule deviants in L46 (regressor type:  $F(1, 19) = 9.53, p = 0.006, \eta_p^2 = 0.33$ ; **Table 6; Figure 8A**). Number deviants in L46 and both deviants in R46 showed similar numerical trends for unique ramping accounting for greater variance than last item change but did not reach statistical significance (**Figure 5B-D; Table 6**). These results

suggest that area 46 dynamics during abstract sequence monitoring are best accounted for by a ramping function, rather than a last item change.

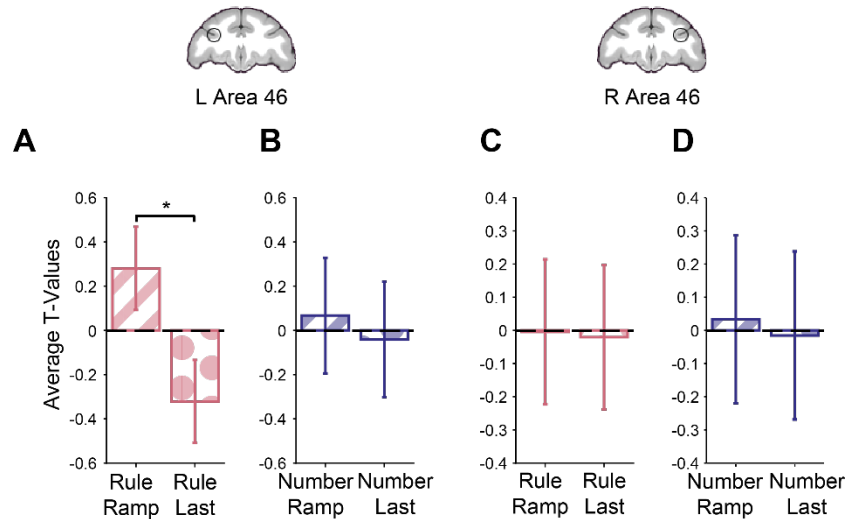


**Figure 8. Area 46 shows greater unique ramping than unique last item activity during abstract sequence deviants.** T-values for the condition of interest > baseline shown. **A.** Unique ramp compared to unique last item during rule deviants in L46 showed a reliable difference. **B.** Unique ramp compared to unique last item during number deviants in L46. **C.** Unique ramp compared to unique last item during rule deviants in R46. **D.** Unique ramp compared to unique last item during number deviants in R46. Comparisons that were not reliably different showed similar trends. Error bars are 95% confidence intervals (1.96 x standard error of the within-bin mean).

**Table 6.** Repeated measures ANOVAs comparing unique ramping activity to unique last item activity during rule and number deviants to NISR in L46 and R46.

Factor	dfs	L46			R 46		
		F	p	$\eta_p^2$	F	p	$\eta_p^2$
<i>Unique Ramp, Rule Deviants &gt; Unique Last Item, Rule Deviants</i>							
Regressor Type	1, 19	9.53	0.006	0.33	0.008	0.93	0.0004
Monkey	2, 19	1.02	0.38	0.97	0.72	0.5	0.07
Monkey x Regressor Type	2, 19	0.37	0.7	0.38	0.09	0.91	0.01
<i>Unique Ramp, Number Deviants &gt; Unique Last Item, Number Deviants</i>							
Regressor Type	1, 19	0.196	0.66	0.01	0.07	0.8	0.0036
Monkey	2, 19	2.08	0.15	0.18	1.47	0.25	0.13
Monkey x Regressor Type	2, 19	1.26	0.31	0.12	0.15	0.86	0.015

ROI results were supported by whole-brain contrasts that examined ramping and last item dynamics. Unique ramping was present in left area 46 during rule deviants compared to NISR (**Figure 9A, Table 7, Extended Data Figure 3-1C**). Other clusters of activation were present in the visual cortex and superior temporal gyrus that were similar to those observed for ramping activation in humans (Desrochers et al., 2015, 2019). As expected from the ROI analyses, the number deviant ramping contrast had significant whole brain clusters in areas such as visual cortex and putamen but no significant clusters in area 46 (**Figure 9B, Table 7**). The localization of significant unique last item clusters was different than ramping. Specifically, a more anterior region of ventral area 46 (46v), in contrast to more posterior and dorsal area 46 (46d) observed for unique ramping, showed significant activation for unique last item change in rule deviants compared to NISR (**Figure 10A, Table 8**). Other significant clusters of activation for last item change included the somatosensory cortex and central orbitofrontal cortex (area 13m). We also contrasted unique last item variance in number deviants compared to NISR, and observed activation in areas such as anterior cingulate gyrus, insula and visual cortices but no surviving clusters in area 46 (**Figure 10B, Table 8**). These results suggest that subregions of area 46 within the same hemisphere may reflect separable aspects of changes in sequential structure.

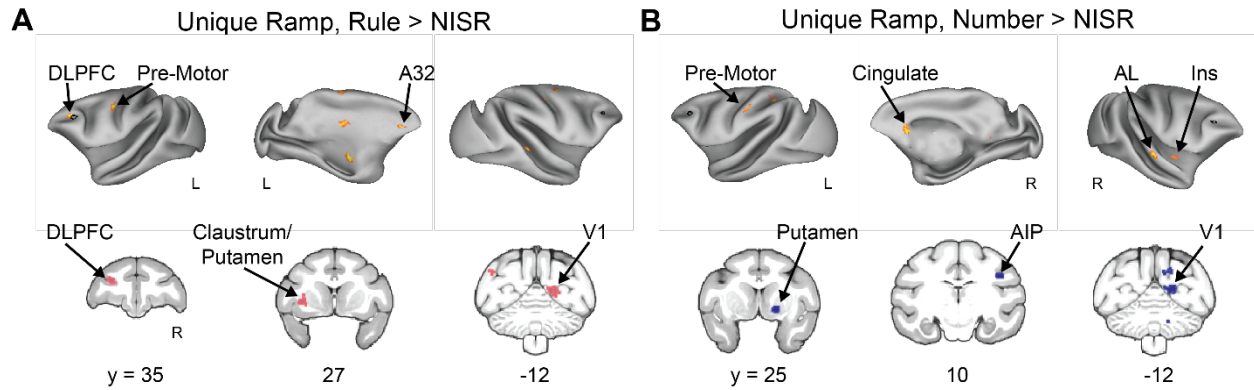


**Figure 9. Area 46 shows unique ramping during abstract sequence deviants. A. Unique Ramp, Rule Deviants > NISR (FDRc  $p < 0.05$ , height  $p < 0.005$  unc., ext. 82). Individual monkey data shown in **Extended Data Figure 3-1C**. B. Unique Ramp, Number Deviants > NISR (FDRc  $p < 0.05$ , height  $p < 0.005$  unc., ext. 89). Black outline on inflated brains indicates location of L46 or R46 (depending on the hemisphere shown) for reference. Medial Prefrontal Cortex (A32) Dorsal Lateral Pre-frontal Cortex (DLPFC), Primary Visual Cortex (V1), Insular Cortex (Ins), Anterior Lateral Belt Region of the Auditory Cortex (AL), Anterior Intraparietal Area (AIP).**

**Table 7.** Unique ramp rule and number deviants compared to NISR contrast activation coordinates.

Contrast Location	Extent (voxels)	x	y	z	Peak t-val
<b>Unique Ramp, Rule Deviants &gt; NISR</b>					
Primary Motor Cortex (F1)	153	11	13.5	29.5	6.48
Caudal Dorsal Pre-Motor Cortex (PMdc)	89	12	18	34.5	6.17
Dorsal Dorsal Lateral Prefrontal Cortex (46d)	130	-12.5	36	23	5.34
Intraparietal Area (IPa)	121	16	18.5	2	5.33
Rostral Area 12 (12r)	128	-15	29	14.5	5.19
Caudate Nucleus (Cd)	385	-10.5	19	23	5.15
Caudal Pre-Motor Cortex (PMdc)	113	-18.5	20	30	5
Secondary Visual Cortex (V2)	82	28	-7.5	14.5	4.67
Primary Visual Cortex (V1)	101	-20.5	-11	27	4.66
Body of the Fornix (bfx)	120	-1.5	12.5	22.5	4.49
Somatosensory Parietal Cortex (1,2)	120	-13	7.5	33.5	4.4
Primary Motor Cortex (M1)	97	-3.5	14.5	38	4.3
Medial Septum (ms)	82	-1	18.5	13	4.18
Secondary/Primary Visual Cortex (V2/V1)	129	9	-11	19	4.16

Intraparietal Area (IPa)	97	18.5	7.5	16	4.01
Globus Pallidus (MGPi)	250	-6.5	13	8	3.99
Pre-genual Cortex (24a)	101	-2	38.5	17	3.96
<b>Unique Ramp, Number Deviants &gt; NISR</b>					
Visual Area 3 (V3)	163	7.5	-12.5	26.5	6.42
Anterior Lateral Belt Region (AL)	130	28	17	12.5	6.35
Agranular and Dysgranular Insula (Ia/Id)	103	21	19	10.5	5.62
Putamen (Pu)	127	7	24.5	10.5	5.5
Caudate Nucleus (Cd)	772	-5.5	20	18	5.29
Primary Visual Cortex (V1)	132	9	-11.5	19	5.16
Cerebellum	250	7	-15.5	12	4.85
Somatosensory Parietal Cortex (1,2)	89	-4.5	4	35	4.72
Cerebellum	138	4	-18	5.5	4.67
Anterior Intraparietal Area (AIP)	123	18.5	10.5	25.5	4.65
Somatosensory Parietal Cortex (1,2)	115	-21	13	32.5	4.5
Caudal Dorsal Pre-Motor Cortex (PMdc)	324	-10.5	20	28	4.45
Ventral Tegmental Area (VTA)	282	-4	4	3	4.37
Posterior Cingulate Gyrus (23c)	100	-7.5	5.5	30.5	4.07
Somatosensory Parietal Cortex (1,2)	152	-12.5	6.5	35	4.01

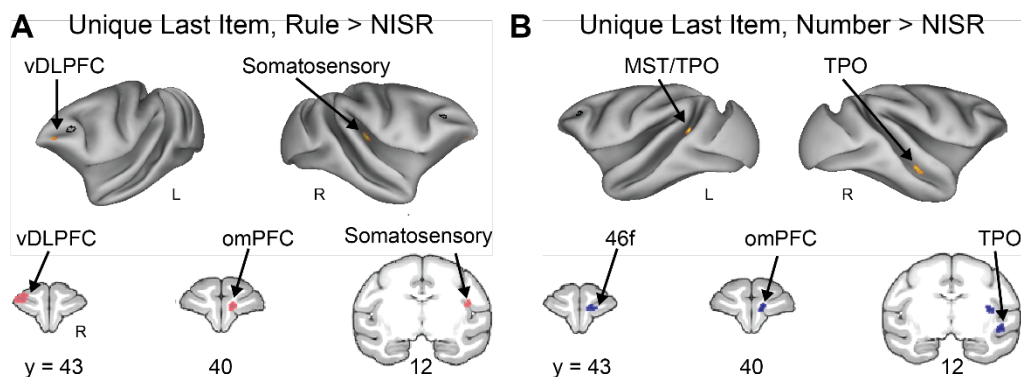


**Figure 10. DLPFC does not show significant responses to unique last items during abstract sequence deviants.**

**A.** Unique Last Item, Rule Deviants > NISR (FDRc < 0.05, height  $p < 0.005$  unc., extent = 148). **B.** Unique Last Item, Number Deviants > NISR (FDRc < 0.05, height  $p < 0.005$  unc., extent = 82). Black outline on inflated brains indicates location of L46 or R46 (depending on the hemisphere shown) for reference. Ventral Dorsal Lateral Prefrontal Cortex (vDLPFC), Medial Superior Temporal Cortex (MST), Superior Temporal Sulcus Dorsal Bank (TPO), Orbital Medial Prefrontal Cortex, Fundus of the Dorsal Lateral Prefrontal Cortex (46f).

**Table 8.** Unique last item rule and number deviants compared to NISR contrast activation coordinates.

Contrast Location	Extent (voxels)	x	y	z	Peak t-val
<b>Unique Last Item, Rule Deviants &gt; NISR</b>					
Ventral Dorsal Lateral Prefrontal Cortex (46v)	148	-12	43	22	5.23
Granular Insula (Ig)	170	19	11	20	5.06
Medial Area 11 (11m)	156	3.5	41	17.5	4.93
Ventral Intraparietal Area/White Matter (VIP/WM)	360	8.5	-1	22.5	4.1
<b>Unique Last Item, Number Deviants &gt; NISR</b>					
Area TFO (TFO)	121	-14	4	1.5	5.75
Caudate Nucleus	82	1	29.5	16.5	5.32
Primary Visual Cortex (V1)	247	-8.5	-18.5	12	5.13
Area 13 (13m)	184	4	38	18.5	4.92
Cerebellum	90	12.5	-12.5	5	4.89
Granular Insula (Ig)	117	17.5	16	15.5	4.36
Temporal Parietooccipital Associated Area (TPO)	88	21.5	14	7.5	4.32
Caudomedial Belt Region (CM)	116	-15	2.5	22	4.19
Anterior Cingulate Gyrus (24a)	85	-2	28.5	20.5	4.14
Posterior Cingulate Gyrus (29)	151	7	0.5	20.5	4.03

To determine if clusters of activation for unique ramping and unique last item were separable in the frontal cortex, we directly compared the amount of variance assigned to each cluster for both dynamics. One possibility is that, due to thresholding at the whole-brain level, there was similar activation for each dynamic across areas 46d and 46v, but that the peak, and thus the location of the thresholded cluster, differed slightly in location. To address this possibility, we created two ROIs from the clusters of significant activation in Unique Ramp, Rule Deviants > NISR contrast

(area 46d, center  $xyz = -12.2, 36, 23.8$  mm), and Unique Last Item, Rule Deviants > NISR contrast (area 46v, center  $xyz = -12.3, 42.9, 21.8$  mm). We found a significant interaction between ROI and model in rule deviants compared to NISR (**Figure 11**; regressor type:  $F(1, 40) = 0.13, p = 0.71, \eta_p^2 = 0.003$ ; monkey:  $F(2, 40) = 2.23, p = 0.12, \eta_p^2 = 0.1$ ; brain area:  $F(1, 40) = 0.09, p = 0.77, \eta_p^2 = 0.002$ ; monkey x regressor type:  $F(2, 40) = 0.33, p = 0.72, \eta_p^2 = 0.016$ ; brain area x sequence type:  $F(1, 40) = 29.3, p < 0.001, \eta_p^2 = 0.42$ ), indicating that responses in the ramping and last item clusters were reliably different. As expected from the whole-brain contrasts, there was no significant interaction for number deviants compared to NISR (not shown;  $F(1, 40) = 0.796, p = 0.38, \eta_p^2 = 0.02$ ). These results show that these nearby clusters in dorsal and ventral area 46 are separable in their dynamics.

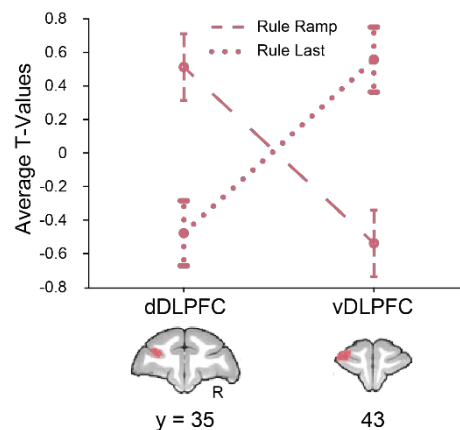


**Figure 11. Nearby regions of DLPFC show significantly different dynamics.** ROIs constructed from significant areas of activation in unique ramping (46d, dDLPFC) and unique last item (46v, vDLPFC) contrasts shown on coronal sections. T-values for the condition of interest > baseline shown. Models show a double dissociation in left area 46 during rule deviants. Error bars are 95% confidence intervals (1.96 x standard error of the within-bin mean).

## **2.7. Discussion**

In this study, we examined if and how monkey DLPFC (area 46) monitors abstract sequential information. We tested two main hypotheses: First, that evidence of abstract sequence monitoring would occur in the area of monkey DLPFC analogous to human RL PFC previously shown to be critical for abstract sequential tasks (Desrochers et al., 2015, 2019; McKim & Desrochers, 2022b); and, second, that ramping dynamics would be associated with abstract sequence monitoring and show changes when abstract sequential structure changed. These hypotheses were tested in a no-report sequence viewing task that allowed the isolation of dynamics associated with sequence monitoring from other potential confounds such as motor preparation. We found evidence to support both hypotheses. Right area 46 responded to abstract sequence changes in both rule and number. Interestingly, left area 46 also responded to changes in abstract sequential rules, but with ramping dynamics that were similar to those observed in humans and separable from an increase only at the last item. These results suggest that a specific subregion of monkey DLPFC is specialized for monitoring general visual abstract sequential information and is a point of critical potential functional homology between human and monkey PFC during higher-level cognitive function.

The activation patterns found, with ramping dynamics primarily on the left and onset-based on the right, are consistent with prior findings. Though not explicitly tested, in humans ramping was observed preferentially on the left during abstract sequential tasks (Desrochers et al., 2015, 2019), Experiment 1) in contrast to bilateral ramping activation observed in tasks where sequences were based on stimulus identity (i.e., ordered visual items; (Desrochers et al., 2019), Experiment 2; (McKim & Desrochers, 2022b). These human results are also consistent with the long-standing literature that emphasizes abstract cognitive functions in the left hemisphere of humans (e.g.,

(Badre & D'Esposito, 2007b; Bunge et al., 2009; Wendelken et al., 2012), with the most famous such example being language (Broca, 1861; Milner, 1971; Petrides, 2013). Ramping activity has been observed in human frontal cortex during sequential language information processing (i.e., sentence comprehension) with electrocorticography (ECoG) (Fedorenko et al., 2016). While generally consistent with prior work, future studies of the distinct left and right hemisphere activation dynamics will be needed to determine their underlying drivers and their potential cognitive import. In particular, the present findings suggest that neural dynamics underlying DLPFC sequence monitoring may be distinct to each hemisphere. The monkey fMRI findings described here can provide a guide for such recordings. In sum, our results raise the possibility that the representation in and contribution of DLPFC to abstract sequence monitoring is lateralized in monkeys, and provide a road map to future studies.

An advantage of fMRI is the whole brain view that is not afforded by typical electrophysiological techniques in macaques. This view leads to potential insights about functional organization of brain areas without the limitations of a recording chamber (Milham et al., 2022). For example, in recent literature, fMRI has enabled the mapping of projections to and from the PFC with a level of specificity and across distances not previously possible on this scale (R. Xu et al., 2022). This work found an overlap in topographically organized high-level visual maps from the dorsal and ventral streams in primate lateral prefrontal cortex. These results raise the possibility that the localization of abstract visual sequence monitoring in DLPFC results from its position near the apex of highly organized visuo-spatial maps. The overarching organization of more cognitive processes in monkey frontal cortex has remained more elusive (Hutchison & Everling, 2014; Neubert et al., 2014, 2014; Saleem et al., 2014), and the results presented here represent a critical step forward in understanding their topography.

We observed similarities and differences to a previous study using a similar auditory task (L. Wang et al., 2015) that may reflect the modality employed and the capacity for generalization. Areas of the brain that responded to deviant sequences in both the current visual and prior auditory studies may be modality general. These areas included premotor cortex, caudate nucleus, and the auditory cortex rostromedial belt. In contrast, brain areas that uniquely responded to deviants in the auditory or this visual task may be modality specific for abstract sequence changes. For example, deviant responses in ventral LPFC and superior temporal sulcus were unique to the auditory study. In this visual task, deviant responses in DLPFC, visual cortex, and mPFC were observed that were not observed in the auditory task. Though we cannot draw strong conclusions without direct comparison between the modalities, these results suggest that networks of brain areas that partially overlap may constitute abstract sequence tracking across modalities. One further important difference in the studies is that in the auditory study, there was a lack of overlap between areas that respond to rule and number deviants in the monkey (in contrast to the human). Here, we observed overlap in these responses in area 46, suggesting a higher level of visual integration in the monkey. The question of sensory domain generality and integration remains open to further investigation.

The results observed here in this no-report abstract sequence viewing task in monkeys are similar to those observed in humans during sequential tasks in important ways. First, ramping activation was observed in similar regions in the frontal cortex in the monkey (area 46) and human (RLPFC). Other similar areas included visual cortex, putamen, and pre-motor cortex (Desrochers et al., 2015, 2019; McKim & Desrochers, 2022b). Though the current experiment was only designed to detect the presence of ramping in relation to abstract sequences, by analogy, the function may be similar in the lateral prefrontal cortex across species. Ramping activity has been ascribed to many possible

functions across species, including accumulating evidence (Darriba & Waszak, 2018; de Lange et al., 2010; Krueger et al., 2017; Lin et al., 2020), keeping time (Berdyeva & Olson, 2011; Cueva et al., 2020; A. Nobre et al., 2007), reward anticipation (Chiew et al., 2016; Falcone et al., 2019; Horst & Laubach, 2013; McKim & Desrochers, 2022b; Roesch & Olson, 2007) and monitoring sequence position (Desrochers et al., 2015, 2019). These possibilities are not mutually exclusive, as recent evidence in humans suggests that reward anticipation and sequence information may be present simultaneously in this signal (McKim & Desrochers, 2022b). The current experiment identified ramping in the DLPFC as being sequence related, but did not examine other potential influences and therefore remains an open avenue of future inquiry. Similarly, other brain areas that display ramping activation remain open for investigation.

Though this study bears resemblance to a field of literature using statistical learning paradigms, the majority of those studies use tasks that rely on the identity of the stimuli themselves. Importantly, this study is distinct from most statistical learning studies because the identity of the stimulus alone cannot predict the following item (i.e., knowing the current fractal is the green one does not determine the next stimulus without also having sequential rule information). A subset of work in the infant learning literature examines statistical learning that is not dependent on stimulus identity (i.e., “artificial grammar”), but mostly auditory tasks were used (e.g., (J. R. Saffran et al., 1996)). To our knowledge, only one behavioral study examined violations to a visual (and auditory) artificial grammar where sequences of different lengths are constructed according to set transition probabilities (Milne et al., 2018). While the findings were important because violations were detected similarly in monkeys and humans, there were no neural data presented. Further, while transition probabilities created the sequences, there was not a set “rule” by which they were

constructed. Therefore, the present study is unique in examining neural responses to abstract visual sequences.

This study contained the following limitations. First, the timing of the stimuli in the current design did not allow examination of dynamics of individual sequence items, only across the sequence as a whole. In a single experiment, it was not feasible to separate each sequential item by the time required to model each separately in an event-related design. Therefore, future work will aim to examine the dynamics of individual sequential items in greater detail. Second, while the no-report task allowed the elimination of motor preparatory confounds, it did not allow for direct correlation with behavioral performance. Although the observed signals will potentially also underlie tasks that require responses, this assertion remains to be tested and the present study is an important foundation for further experiments. Third, we have focused here on the DLPFC because although its importance in cognitive processes in monkeys has been established, its response to visual abstract sequences and potential correspondence to dynamics in humans remained unknown. The DLPFC is part of a network of areas active in this task, and although they are outside the scope of the current experiment, they remain an important avenue of future research.

In summary, we provide evidence that a specific subregion of monkey DLPFC monitors abstract visual sequences and generalizes across different sequence violations (number and rule). Further, sequence related ramping dynamics were also observed in DLPFC. Importantly, this region is possibly analogous to human RL PFC, where necessary sequence-related ramping signals have been identified in the past. These results suggest functional homology across the species as to where and how more general abstract visual sequential information is represented in the brain. These findings, in turn, inform future models of how abstract sequential information is represented during more complex behaviors across species.

## 2.8. Extended Data

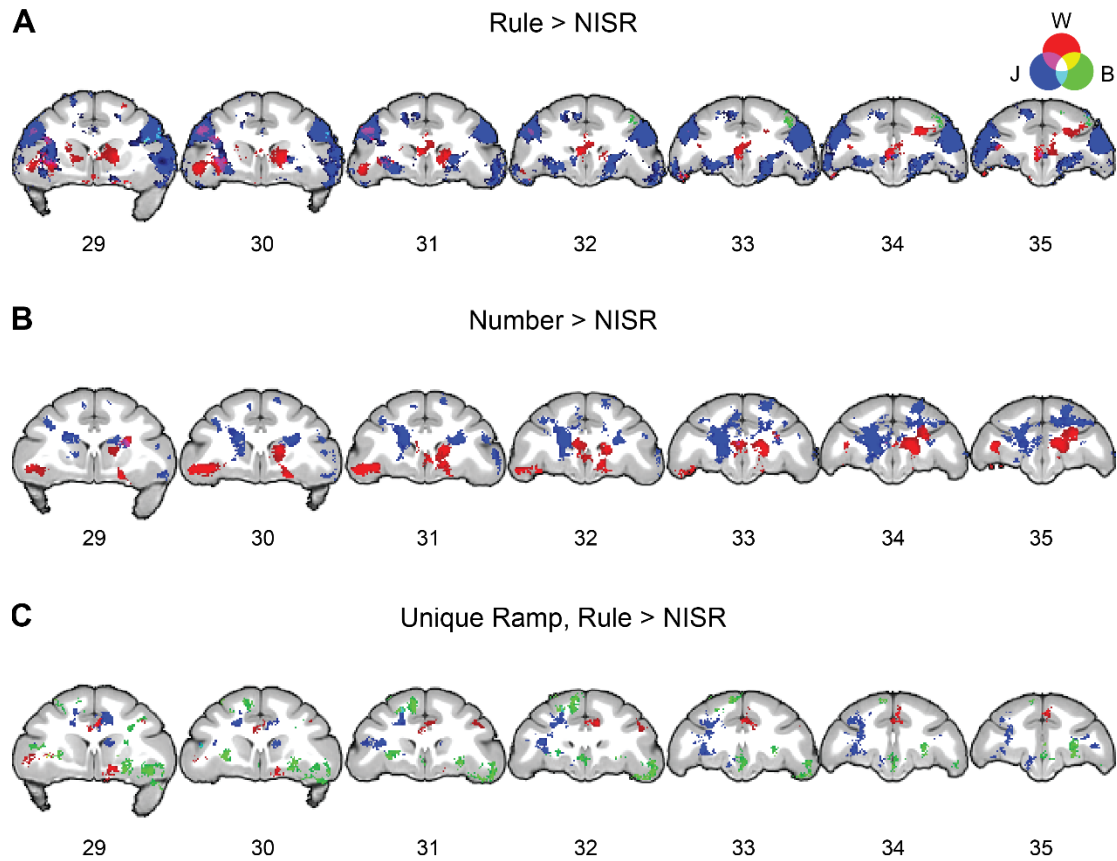


**Figure 3-1. Overlaid individual monkey contrasts for monkeys W, J, and B.** Three second level contrasts, one for each monkey, were created using only data bins that contained runs from each animal (W = 9, J = 6, B = 7 bins each). As described in Materials and Methods, each bin contained approximately 10 runs. A liberal height threshold of  $p < 0.05$  was chosen for illustrative purposes before applying and extent (extents listed for each monkey by contrast) and false discovery rate (FDR) error cluster corrected for multiple comparisons to  $p < 0.05$ . Slice number in the y direction is listed under each coronal section. **A.** Voxel wise contrast of Rule Deviants > New Items, Same Rule (NISR) (W extent = 560, J = 1296, B = 623 voxels). **B.** Voxel wise contrast of Number Deviants > NISR (W extent = 772, J = 750, B = 667 voxels). **C.** Voxel wise contrast of Unique Ramp, Rule Deviants > NISR (W extent = 560, J = 630, B = 581 voxels).

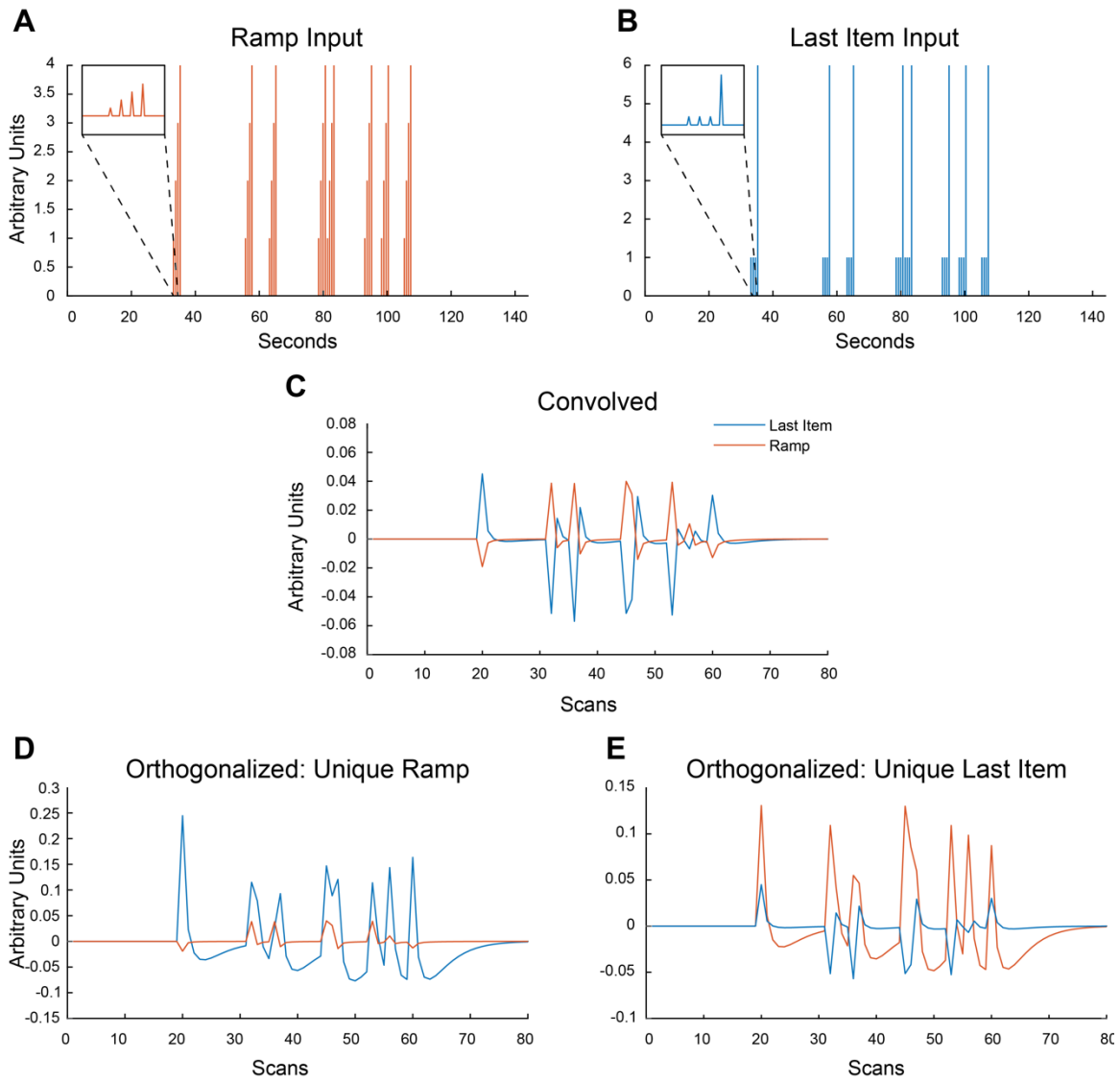


**Figure 4-1. Example Ramp and Last Item regressors through the orthogonalization process.** Note that SPM first creates regressors from onsets (in seconds, shown in A.) in samples using higher resolution to be convolved, and then they are down-sampled before being orthogonalized and entered in the GLM.

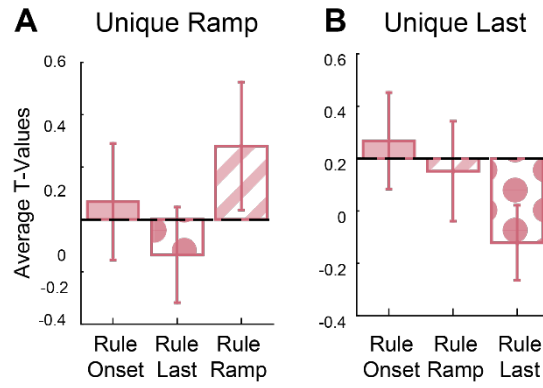


**Figure 4-2. Example Unique Ramp and Unique Last Item regressor T-values after orthogonalization for the Right Area 46 ROI. A.** Example T-values for the rule condition when Ramp is the last regressor in the model. **B.** Example T-values for the rule condition when Last Item is the last regressor in the model.

## **Chapter 3: Sequence rule modulates DLPFC activity within our established no-response abstract sequential paradigm**

### **3.1. Abstract**

In the previous chapter, we demonstrated that the monkey DLPFC sub-region Area 46 responds when viewing changes to an established sequence, with specific ramping dynamics present during sequential monitoring. These visual sequences can be described based on their abstract rule or structured timing, features which we have termed *sequential characteristics*. However, it is unknown whether either (or both) of these specific sequential characteristics modulate the observed neural responses in monkey Area 46. To determine which sequential characteristics modulate neural responses in DLPFC during no-response abstract sequence viewing we created task variants which isolated sequence rule, timing, and images. Monkeys underwent awake behaving functional magnetic resonance imaging (fMRI) while viewing these tasks variants. When monkeys performed the no-report sequence variants, we found that right area 46 shows increased activity for isolated abstract rule and isolated structured timing. These results suggest that both abstract rule and structured timing are involved in abstract sequence representations, with a neural activity that increases when both characteristics are present to define an abstract sequence in the DLPFC during abstract sequence viewing.

### 3.2. Introduction

Our previous experiments aimed to understand a very specific instantiation of visual abstract sequences. However, these sequences contained multiple features related to image presentation and timing. The co-occurrence of these features within sequential tasks can result in neural responses that are difficult to disambiguate from each other when studying abstract sequences. Therefore, to understand the underlying system that subserves these mechanisms, it is necessary to isolate these characteristics to identify how they may contribute to observed neural activity during abstract sequences.

For our study, we defined abstract sequences based on a specific set of sequential characteristics. These *sequential characteristics* are the features that can be used to describe the composition of an abstract sequence. One such characteristic, *abstract rule*, allows us to describe the higher order structure of the sequence independent of the individual images within the sequence. We constructed the simplest version of an abstract visual sequence as containing an abstract rule of either *three of the same, one different* or *all of the same* (AAAB or AAAA). An additional characteristic we selected was a specific application of timing which we termed *structured timing*. Structured timing refers to the uniformly spaced repetition of images which groups them temporally across sequence presentations. An example of such a timing structure would include equivalent 100 ms inter-image intervals for a four-image set grouping them proximally in time in a consistent manner. Both abstract rule and structured timing can be used to define an abstract sequence, and as such may contribute either independently or in combination to observed neural activity during sequential tasks.

Literature studying abstract sequence characteristics and their neural representations is notoriously sparse, limiting our understanding of their impact on neural responses. Previous work has studied

some of these sequential characteristics, albeit outside of the context of understanding abstract sequential tasks. Work studying rule has shown that specific brain areas process rule changes during no-response auditory tasks in both macaques and humans (Bekinschtein et al., 2009; Dehaene et al., 2015; Uhrig et al., 2014). On the other hand, there is an extensive literature on timing. These studies include anticipation time, rhythmic timing, and elapsed “wait” time (Coull & Nobre, 2008, 2008; A. Nobre et al., 2007; Schapiro, Rogers, et al., 2013). However, structured timing as it relates to abstract sequences and how it may modulate responses relevant to sequential monitoring has not been studied. These characteristics have been shown to modulate neural activity in the DLPFC both in sequential and non-sequential contexts. However, much of this work has studied these characteristics either 1) outside of a sequential context; 2) in tasks containing confounds with other features or 3) in scenarios where other cognitive processes could influence the observed neural responses. Therefore, there is a need to understand the influence of these sequential characteristics on neural activity in isolation of other task confounds.

The DLPFC has been implicated in the processing of sequential rule and ordinal position. As referenced in our general introduction the monkey DLPFC has been shown to process sequential rules and ordinal position during motor tasks (Averbeck et al., 2003, 2006; Shima et al., 2007). Work in both humans and monkeys has further supported the processing of sequential rules in the macaque PFC during auditory and visual tasks (Bellet et al., 2022; Uhrig et al., 2014; L. Wang et al., 2015, 2019). However, most of this work has not directly tested rule representations in isolation of additional tasks, or specifically for abstract visual sequences. This could result in neural dynamics relevant to rule and its related brain areas being confounded with other sequential characteristics or cognitive processes. It is possible that abstract rule in isolation is sufficient to define sequential boundaries and modulate DLPFC activity.

Another sequential characteristic thought to modulate DLPFC activity is timing. Timing can be described in a variety of ways including the passage of time or intervals in between the appearance of stimuli. Work studying timing has shown that prefrontal regions are involved in temporal processing (Gu et al., 2015; Lewis & Miall, 2003; Niki & Watanabe, 1979; Pouthas et al., 2005). Interval timing studies in rodents have shown that prefrontal regions have similar ramping dynamics as those seen during sequential tasks in humans (J. Kim et al., 2013; M. Xu et al., 2014). The monkey DLPFC shows neural activity for the temporal monitoring of timing (Chiba et al., 2021; Niki & Watanabe, 1979; Onoe et al., 2001). However, whether isolated structured timing on its own can modulate neural responses in the DLPFC associated to abstract sequential tasks has yet to be tested.

In our previous study, we showed that the DLPFC processes sequences containing the combined characteristics of abstract rule and structured timing during no-response abstract sequence viewing. Neural activity was present for changes to an established sequence, with the DLPFC showing *ramping* activity or an increasing pattern of activity as animals progressed through the items in the sequence (**Figure 12**) This ramping pattern of activity is thought to be related to the process of *sequential monitoring* or tracking one's place in a sequence. However, as we discussed in the previous paragraphs these ramping dynamics have been shown to be modulated by different characteristics present in sequential tasks, outside of the sequential context. Therefore, it is not known whether animals are engaging in monitoring, nor which of these sequential characteristics are implicated during abstract sequence monitoring. With the following set of experiments we will isolate the characteristics of timing and rule to test whether they modulate ramping dynamics related to sequential monitoring in the DLPFC.

We hypothesized that Area 46 of the monkey DLPFC is modulated by both *abstract rule* and *structured timing*. In our original experimental design these characteristics were present simultaneously for each sequential event. Therefore, to determine the influence of each characteristic on the observed neural dynamics in the monkey DLPFC, we tested abstract rule and structured timing in isolation. To test these hypotheses, we conducted event-related fMRI in awake nonhuman primates with a set of three tasks no-response tasks. The tasks were designed following a standard 2 x 2 design, with each task variant isolating either abstract rule (Rule Only) or structured timing (Time Only) characteristics present in the no-response abstract visual sequence paradigm (**Figure 12**, and no-response abstract visual sequence task as described in Yusif Rodriguez et al., 2022, **Figure 4**). A variant which contained neither structured timing nor abstract rule (Random) was used as a control. Results from these task variants identified that nonhuman primate DLPFC represents isolated abstract rule and isolated structured timing information, with similar ramping dynamics observed in humans and non-human primates during sequential tasks (Desrochers et al., 2015, 2019; McKim & Desrochers, 2022b; Yusif Rodriguez et al., 2022). These dynamics were not present when random fractal images are presented without abstract rule or structured timing. Comparisons across tasks suggest that the neural dynamics observed in the monkey DLPFC sub-region area 46 during abstract sequence viewing are a result of the combined characteristics of abstract rule and time. Overall, our findings suggest that individual sequential characteristics compound to larger neural response in area 46 for abstract sequence representations.

### **3.3. Materials and Methods**

#### **3.3.1. Subjects**

We tested three adult male rhesus macaques (ages spanning 6-12 years during data collection, 9-14 kg). All procedures followed the NIH Guide for Care and Use of Laboratory Animals and were approved by Institutional Animal Care and Use Committee (IACUC) at Brown University.

#### **3.3.2. No-Report Abstract Sequence Variants**

All visual stimuli used in this study were displayed using an OpenGL-based software system developed by Dr. David Sheinberg at Brown University. The experimental task was controlled by a QNX real-time operating system using a state machine. Eye position was monitored using video eye tracking (Eyelink 1000, SR Research). Stimuli were displayed at the scanner on a 24" BOLDscreen flat-panel display (Cambridge Systems). Task variants were designed following a 2x2 task design, including the no-report abstract visual sequence task (Yusif Rodriguez et al., 2022). Each task variant isolates one feature that was present in the original no-report task: abstract rule, structured timing, or image.

##### **3.3.2.1. Stimuli**

Each image presentation consisted of fractal stimulus (approximately 8° visual angle) with varying colors and features. Fractals were generated using MATLAB for each scanning session using custom scripts based on stimuli from (H. F. Kim & Hikosaka, 2013) following the instructions outlined in (Miyashita et al., 1991). For each scan session, new, luminance matched, fractal sets were generated. Therefore, the same fractal set was used for all task variants run in same scan session, and would match the stimuli presented in previous studies (Yusif Rodriguez et al., 2022). All stimuli were presented on a gray background, with a fixation spot that was always present on

the screen superimposed on the images. To provide behavioral feedback, the fixation spot was yellow when the monkey was successfully maintaining fixation and red if the monkey was not fixating.

Because each task draws fractal images from varying image pools, for clarity we will define each image pool as the following: images from the habituation image pool will be referred to as [A, B, C, D], images from the deviant image pool will be [E, F, G], and images from the novel image pool will be [H, I, J, K].

### **3.3.3. Sequence Rule Only Task**

#### **3.3.3.1. Sequence Types**

There are two possible sequence rules in this task (**Figure 13**). Sequences were composed of images drawn from the habituation image pool of four possible fractals. Sequences were composed from these images in one of two possible rules: three of the same, one different (e.g., AAAB, DDDC) and four of the same (e.g., AAAA, CCCC). All sequences contained four images with jittered inter-stimulus intervals to decorrelate between each sequential image presentation (mean 2 s, 0.25-8 s).

#### **3.3.3.2. Block Structure**

Each block contained a single stimulus presentation block containing 30 sequences (120 fractal image presentations) and lasted approximately 272 s on average. Sequences were presented in pseudo-random order such that a sequence could not begin with the same fractal as the final fractal of the previous sequence.

### 3.3.3.3. Run Structure

Each run was composed of a single block, starting, and ending with 14 s fixation blocks **Figure 13**. The same sequential rule was used for the entirety of a single run: three the same, one different (e.g., AAAB, DDDC) and four the same (e.g., AAAA, CCCC). Runs lasted approximately 5 min. The sequence rule (*three same, one different or four same*) used for each run was counterbalanced across each scanning session to have an equal number of runs for each rule. Monkeys typically completed 4-6 runs of this task (among other tasks not reported here) in a single scanning session (one day).

### 3.3.4. **Timing Only Task**

#### 3.3.4.1. Timing Types

There were fifteen possible condition combinations of timing and images that could occur in this task (**Figure 14**). This task intended to isolate the effects of familiar or habituated timings compared to rare, less frequent timings also referred to as “deviant” timings. Therefore, images were presented in a pseudorandom order, with no image repetitions following any given image presentation. To perceptually group the pseudo randomly presented images, sets of 2, 4 or 6 images were assigned particular timing templates. In the following section we will describe possible stimuli combinations in terms of possible timing template assignments (habituation timings or deviant timings), and possible fractal image category (habituation image, deviant image, or novel image pool) within a given timing assignment. The possible combinations are the following: habituation images with habituation timings, deviant and habituation images with habituation timings, habituation images with deviant timings, deviant and habituation images with deviant timings and novel images with habituation timings. Across these possible time and image combinations there a total of nine different timing templates used. These templates matched the

ones used in Yusif Rodriguez et al., 2022. The inter-image group interval was jittered to decorrelate across timing templates (mean 2 s, 0.25-8 s).

### Habituation Timings

Habituation timings were drawn from a pool of 6 possible templates. All templates contained four images and followed one of three possible general timings based on the total duration of the image presentations: short (1.1 s), medium (1.7 s), and long (2.3 s). Each template, in turn, had two possible timing variations within it, one with longer stimulus durations and one with shorter stimulus durations: short 0.1 s and 0.2 s, medium 0.1 s and 0.3 s, long 0.2 s and 0.3 s. Inter-stimulus intervals were arranged to evenly space the four stimulus presentations within the total sequence duration.

Fractal combinations to timings were categorized based on the total timing stimulus durations (short, medium or long). Additionally, within each combination images were pseudo randomly assigned such that there was no predictable pattern or subsequent image repetitions. Stimuli combinations for fractal images would then be the following:

*Habituation Image Combinations:* Short habituation timings with habituation images (HsH), medium habituation timings with habituation images (HmH), long habituation timings with habituation images (HIH). Therefore, an example image group could be ABAD assigned one of the aforementioned possible timing templates.

*Deviant Image Combinations:* Due to the rarity of deviant image presentations, images appearing within a habituation image and timing template combination would tend to occur mixed in with habituation images. These possible conditions were either short habituation timings with habituation and deviant images (HsHD), medium habituation timings with habituation and deviant

images (HmHD), or long habituation timings with habituation and deviant images (HIHD). An example image group could be EBAD, assigned one of the aforementioned total durations.

*Novel Image Combinations:* Short habituation timings with novel images (HsN), medium habituation timings with novel images (HmN), long habituation timings with novel images (HIN). An example image group could be IJHK, assigned one of the aforementioned total durations.

### Deviant Timings

Deviant timings were drawn from three possible timing templates. Across deviant timings, the total durations were matched to the short, medium, and long habituation timing templates. When images were assigned a deviant timing template, images are displayed for 0.2 s, regardless of deviant total timing type. There were three deviant timing templates, detailed as follows:

*Medium Deviant Combinations:* The timings within this template are assigned to four images and had a total duration of 1.7 s. Because deviant timings occurred in the same blocks where a deviant image occurrence was possible and with habituation images occurring, the image and timing combinations were as follows: Medium deviant timing with habituation images only (MDH); Medium deviant timing with habituation and deviant images (MDHD).

*Short and Long Timings:* The timings within this template are assigned to two (short timing template) or six (long timing template) images and had a total duration of either 1.1 s (short timing template) or 2.3 s (long timing template) respectively. Because deviant timings occurred in the same blocks where a deviant image occurrence was possible and with habituation images occurring, the image and timing combinations were as follows: Short deviant timing with habituation images only (SDH); Short deviant timing with habituation and deviant images

(SDHD); Long deviant timing with habituation images only (LDH); Long deviant timing with habituation and deviant images (LDHD).

#### **3.3.4.2. Block Structure**

Each block contained 30 sequences and lasted approximately 130 s on average. Habituation and Novel image blocks contained equal numbers of the six possible timing templates (two of each: short, medium, and long).

All fractal images were presented in pseudo-random order such that fractal presentations were counterbalanced, but the same fractal image could not follow the next. Deviant blocks were composed of 96 habituation images and 24 deviant images, each assigned a timing template for presentation. All deviant timing combinations within a block were of the same type. The six deviant timings were pseudo-randomly interspersed throughout the block such that deviant timings did not occur in the first 6 image timing assignments of the block (to avoid block initiation confounds), and deviant timings were not presented consecutively to each other. If deviant timings contained a variable number of items (i.e., short deviant timings and long deviant timings), then an equal number of two- and six-item timings were included within a single block. The 24 habituation timings within deviant blocks were presented in the same manner as in habituation blocks (i.e., evenly distributed timing templates and avoiding fractal image repeats).

#### **3.3.4.3. Run Structure**

Each run was composed of four blocks, interleaved with 14 s fixation blocks. The first block of each run contained only habituation timings with habituation images. The two subsequent blocks were either a medium deviant timing block or a short and long deviant timing block, with their order counterbalanced across runs. The last block was always a novel image with habituation timings block. The same habituation rule was used for the entirety of a single run. Runs lasted

approximately 10 min. Monkeys typically completed 2-4 runs of this task in a single scanning session (one day).

### **3.3.5. Image Only Task**

#### **3.3.5.1. Stimuli Types**

This task included stimuli from the habituation, deviant and novel images pool (**Figure 15**). The inter-stimulus interval was jittered to decorrelate across individual image presentations (mean 2 s, 0.25-8 s).

#### **3.3.5.2. Block Structure**

Each block contained 120 images and lasted approximately 112 s on average. Habituation blocks contained 120 images from the habituation image pool. Habituation images were presented in pseudo-random order such that a previous fractal presentation could not be followed by the same fractal. The deviant block was composed of 96 habituation images and 24 deviant images. The six deviant images were pseudo-randomly interspersed throughout the block such that deviant images did not occur in the first 24 image presentations of the block (to avoid block initiation confounds), and deviant images were not presented consecutively to each other. The 96 habituation images within the deviant block were presented in the same manner as in habituation blocks (i.e., pseudo-random order such that a previous fractal presentation could not be followed by the same fractal). The novel block contained images from the four possible novel image pool for that scan session. The novel image block presentation followed the same rules as the habituation image block.

#### **3.3.5.3. Run Structure**

Each run was composed of three blocks, interleaved with 14 s fixation blocks (**Figure 15**). The first block of each run contained only habituation sequences. The second block was always a deviant image block, and the third block was always a novel image block. Runs lasted

approximately 15 m. Monkeys typically completed 2-4 runs of this in a single scanning session (one day).

### **3.3.6. Pre-scan Fixation Period**

All runs were initiated according to the monkey's fixation behavior to ensure that the monkey was not moving and engaged in the task before acquiring functional images. During this pre-scan period, a fixation spot was presented. Once the monkey successfully acquired this fixation spot and received approximately four liquid rewards (12 – 16 s), functional image acquisition and the first habituation block were initiated.

### **3.3.7. Reward**

The timing of liquid rewards was not contingent upon task events, only on the monkey maintaining fixation. Rewards were delivered on a graduated schedule such that the longer the monkey maintained fixation, the more frequent rewards were administered (Leite et al., 2002). The first reward was given after 4 s of continuous fixation. After two consecutive rewards of the same fixation duration, the fixation duration required to obtain reward was decreased by 0.5 s. The minimum duration between rewards that the monkey could obtain was 0.5 s. Fixation had to be maintained within a small window (typically 3° of visual angle) around the fixation spot to not break fixation. The only exception was a brief time window (0.32 s) provided for blinks. If the monkey's eyes left the fixation window and returned within that time window, it would not trigger a fixation break. If fixation was broken, the reward schedule would restart at the maximum 4 s duration required to obtain reward.

### 3.3.8. FMRI Data Acquisition

Methods are as described in (Yusif Rodriguez et al., 2022). Monkeys were trained to sit in the “sphinx” position in a custom MR-safe primate chair (Applied Prototype, Franklin, MA or custom-made by Brown University). The monkey’s head was restrained from moving via a plastic “post” (PEEK, Applied Prototype, Franklin, MA) affixed to the monkeys’ head and the primate chair. Monkeys were habituated to contrast agent injection procedures, recorded MRI sounds, wearing earplugs (Mack's Soft Moldable Silicone Putty Ear Plugs, Kid’s size), and transportation to the scanner prior to MRI scanning sessions. Monkeys were trained on the behavioral task with different images that were not used during scanning.

Prior to each scanning session, monkeys were intravenously injected with a contrast agent: monocrystalline iron oxide nanoparticle (MION, Feraheme (ferumoxytol), AMAG Pharmaceuticals, Inc., Waltham, MA, 30 mg per mL or BioPal Molday ION, Biophysics Assay Lab Inc., Worcester, MA, 30 mg per mL). MION improves the contrast-to-noise ratio ~3-fold (Leite et al., 2002; Vanduffel et al., 2001) and enhances spatial selectivity of MR signal changes (Zhao et al., 2006). MION was injected, approximately 30-60 min before scanning, into the saphenous vein below the knee (7 mg/kg), then flushed with a volume of sterile saline approximately double the volume of the MION injected. No additional MION was added during scanning, as MION has a long blood half-life (15.3 +/- 3.5 hr) (Leite et al., 2002).

A Siemens 3T PRISMA MRI system with a custom six-channel surface coil (ScanMed, Omaha, NE) at the Brown University MRI Research Facility was used for whole-brain imaging. Anatomical scans consisted of a T1-MPRAGE (repetition time, TR, 2700 ms; echo time, TE, 3.16 ms; flip angle, 9°; 208 sagittal slices; 0.5 x 0.5 x 0.5 mm), a T2 anatomical (TR, 3200 ms; TE 410 ms; variable flip angle; 192 interleaved transversal slices; 0.4 x 0.4 x 0.4 mm), and an additional

high resolution T2 anatomical (TR, 8020 ms; TE 44 ms; flip angle, 122°; 30 interleaved transversal slices; 0.4 x 0.4 x 1.2 mm). Functional images were acquired using a fat-saturated gradient-echo planar sequence (TR, 1.8 s; TE, 15 ms; flip angle, 80°; 40 interleaved axial slices; 1.1 x 1.1 x 1.1 mm).

### 3.3.9. FMRI Data Analysis

The majority of the following analyses were performed in Matlab using SPM 12 (<http://www.fil.ion.ucl.ac.uk/spm>). Prior to analysis, data were preprocessed using the following steps: reorienting (to ensure proper assignment of the x,y,z planes), motion correction (realignment), normalization, and spatial smoothing (2 mm isotropic Gaussian kernel separately for gray matter and white matter). All steps were performed on individual runs separately. The T1-MPRAGE anatomical image was skull stripped using FSL BET brain extraction tool (<http://www.fmrib.ox.ac.uk/fsl/>) to facilitate normalization. All images were normalized to the 112-RM SL macaque atlas (McLaren et al., 2009).

Runs were included for analysis only if they met the following criteria: the monkey had to be performing well and a sufficient number of acquisition volumes within the run had to pass data quality checks. The monkey's performance was evaluated by calculating the percentage of time within a run that fixation was maintained. Runs were excluded if the monkey was fixating < 80% of the time (similar criteria as in Leite et al., 2002; Vanduffel et al., 2001; Wang et al., 2015). To evaluate data quality, we used the ART toolbox (Artifact Detection Tools, [https://www.nitrc.org/projects/artifact\\_detect](https://www.nitrc.org/projects/artifact_detect)) to detect outlier volumes. Any volumes that had motion greater than one voxel (1.1 mm) in any direction were excluded. Any run with greater than 12% of volumes excluded was excluded from analysis (see **Table 9** and total included data).

**Table 9.** Percentage of excluded data using fixation and motion criteria and total included data across tasks and animals.

% Excluded Fixation				
	Monkey B	Monkey J	Monkey W	
Rule Only	4.3%	8.24%	13.3%	
Time Only	5.06%	6.96%	10.13%	
Random	4.44%	7.78%	10.6%	
% Excluded Motion				
	Monkey B	Monkey J	Monkey W	
Rule Only	1.79%	16.1%	1.79%	
Time Only	1.89%	16.5%	0.63%	
Random	1.67%	13.3%	1.11%	
Total Included Runs				
	Monkey B	Monkey J	Monkey W	Total Runs
Rule Only	27	63	79	169
Time Only	17	38	43	98
Random	27	35	55	117

### 3.3.9.1. Models

Within-subject statistical models were constructed under the assumptions of the general linear model (GLM) in SPM 12 for each pseudo-subject bin. For all models, data were binned into approximately 10-run pseudo-subject bins. Each bin contained data from only one monkey. Runs were pseudo-randomly assigned to bins to balance the number of runs which followed each of the two sequential rules for the Rule Only task (three same, one different or four of the same) and the distribution of runs from earlier and later scanning sessions. Condition regressors were all convolved with a gamma function (shape parameter = 1.55, scale parameter = 0.022727) to model the MION hemodynamic response function (Vanduffel & Farivar, 2014). The first twenty four image presentations in a run and reward times were included as nuisance conditions. Additional nuisance regressors were included for the six motion estimate parameters (translation and rotation), outlier volumes, and image variability (standard deviation of within run image movement

variability, calculated using the ART toolbox). Outlier volumes were determined using the ART toolbox (standard global mean; global signal detection outlier detection threshold = 4.5; motion threshold = 1.1mm; scan to scan motion and global signal change for outlier detection) and one additional regressor with a “1” at only that volume was included for each volume to be “scrubbed”.

Regressors were estimated using a bin-specific fixed-effects model. Whole-brain estimates of bin-specific effects were entered into second-level analyses that treated bin as a random effect. One-sample t-tests (contrast value vs zero,  $p < 0.005$ ) were used to assess significance. These effects were corrected for multiple comparisons when examining whole-brain group voxelwise effects using extent thresholds at the cluster level to yield false discovery rate (FDR) error correction ( $p < 0.05$ ).

The following three GLMs were utilized for analyses as described:

*Onsets Model:* To assess the univariate effects of deviant sequences, we constructed a model using instantaneous stimulus onset regressors. For the Rule Only and Random tasks, onsets were modeled for each individual image presentation. For the Time Only task onsets were modeled for the first item in each timing “template” with the following twelve condition regressors for different timing types: short, medium, and long habituation timing templates; medium deviant timings; two- and six-item deviant timings; and habituation timings with novel items.

*Parametric Ramp Model:* To directly test whether variance could be better accounted for by ramping activation, we constructed a model that would allow a ramp regressor to compete for variance with onset activity. Onset regressors were constructed with an instantaneous stimulus onset regressor at each stimulus onset for the Image Only task, and at each image set onset for the Time Only task. Including an onset at each position effectively modeled sustained activation

throughout the sequence and enabled the inclusion of the following parametric regressors. The ramp parametric was entered as the structure position (1-4) for Time Only, or as “pseudo” position for the Image Only task. Parametric regressors were implemented hierarchically in the GLM. Therefore, variance explained by the last parametric regressor (in this case, ramping), is above and beyond what could be explained by the onsets regressor.

*Parametric Last Item versus Unique Ramp Model:* To directly test whether variance could be better accounted for by a phasic response at the last item in the sequence or ramping activation, we constructed a pair of models to allow last item and ramp regressors to compete for variance within the same model. Onset regressors were constructed with an instantaneous stimulus onset regressor at each image onset for all tasks.

The last item parametric was added as ones at the first sequence positions and an arbitrarily larger value (6) at the last item. The ramp parametric was entered as the sequence position (1-4, 1-2, or 1-6) for either each sequence (Rule Only) or timing template (Time Only). Because there was no sequence rule or timing structure to group images in the Random task, both the last item and ramp parametrics were entered as if items were grouped to test for the possibility of either dynamic existing. Parametric regressors were implemented hierarchically in the GLM. Therefore, variance explained by the last parametric regressor (in this case, ramping), is above and beyond what could be explained by the onsets or last item regressors.

*Parametric Ramp versus Unique Last Item Model:* This second model of the pair sought to identify variance uniquely explained by the last item regressor, above and beyond variance explained by the onsets or ramping regressors. All other aspects of the model were the same as the unique ramp model above.

### 3.3.9.2. ROI Analyses

The primary bilateral regions of interest were constructed using area 46 clusters that had shown significant activity in Yusif Rodriguez et al., 2022. We created the left ramp ROI utilizing the significant left DLPFC cluster of activation for Unique Ramp, Rule Deviants > NISR contrast in the unique ramp model (center  $xyz = -12.2, 36, 23$ ). The right conjunction ROI was created from the right DLPFC cluster from the conjunction map obtained from the contrasts Rule Deviants > NISR and Number Deviants > NISR in the sequence onset model (center  $xyz = 10.2, 33.7, 21.8$ ).

To compare activation within and across ROIs in a manner that controlled for variance, we extracted t-values from the condition of interest over baseline using the Marsbar toolbox (Jean-Baptiste Poline, 2002). T-values (one for each pseudo-subject bin: Rule Only,  $n = 16$  bins; Time Only,  $n = 10$ ; Random,  $n = 10$ ) were entered into RM-ANOVAs with the identity of the monkey entered as a covariate.

## 3.4. Results

Three monkeys (*macaca mulatta*) performed no-report viewing of sequential task variants while undergoing awake fMRI scanning. The monkeys were trained to fixate on a central spot while viewing a stream of fractal images that varied in presentation depending on the task variant (**Figure 12**). These task variants, like the one described in Yusif Rodriguez, et al., 2022, did not require responses, only fixation, and thus were also termed “no-report”. The tasks were performed in runs varying in total length between ~5-15 minutes. To encourage animals to maintain fixation throughout, rewards were administered on a graduated schedule not correlated with task image presentations: the longer they maintained fixation, the shorter the duration between rewards. Reward was thus decorrelated from the fractal visual stimuli (see **Methods** for more details).

Animals completed three possible tasks, with each one containing only the abstract rule (Rule Only), structured timing (Time Only), or neither (Random), as follows.

To maintain consistency in the naming scheme of the used image sets, we kept the names of the images based on their respective categories in our no-response abstract visual sequence task. Therefore, habituation images came from the habituation image set and were always the most familiar images across tasks and had the highest frequency of presentation across task variants. Deviant images were taken from the deviant image pool also used in the previous study and served a similar function of being infrequent events in the blocks in which they were presented. Novel images did not exist in the previous task and have been labeled as such to differentiate that they were not previously viewed by animals outside of their corresponding tasks.

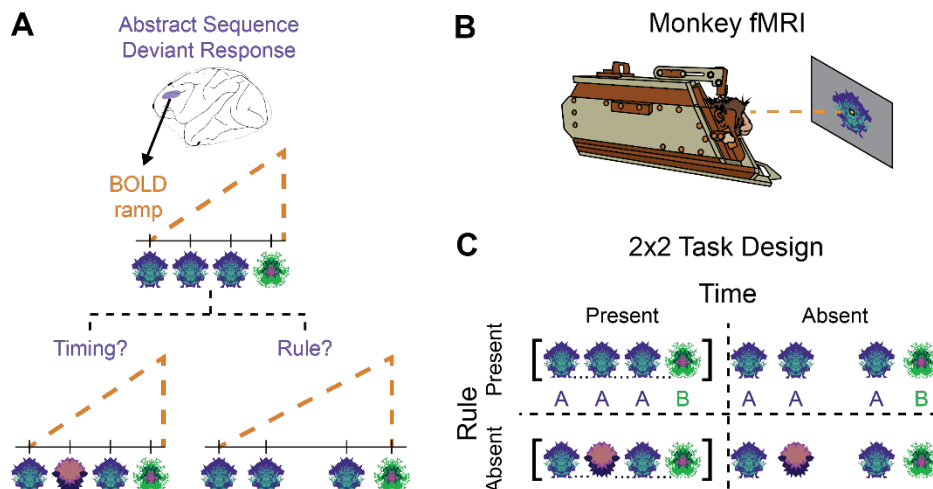


**Figure 12. Hypothesis summary and methodology.** **A.** Schematic representation of the monkey dorsolateral prefrontal cortex (DLPFC) depicting the main questions that were the focus of this study: Is ramping in the monkey DLPFC modulated by isolated timing (bottom left) or isolated rule (bottom right)? **B.** Monkeys only fixate throughout runs. Scanning is performed in the “sphinx” position. **C.** 2x2 task design to isolate sequential characteristics. Possible tasks could contain either abstract rule and structured timing (no-response abstract visual sequence task; top left), structured timing and no abstract rule (Time Only; bottom left), abstract rule and no structured timing (Rule Only; top right), or neither (Random; bottom right).

### 3.4.1. Rule Only Task

The sequence rule only task intends to isolate the abstract sequential rule. To isolate abstract sequential rule, we presented images where the only variable manipulated is whether animals view images following one of two possible sequential rules. In this task, timing between each image presentation has jittered inter-stimulus intervals (0.25s – 8s). Therefore, the timing is uninformative as it cannot be tracked nor predicted. This manipulation results in a task where no other information can be tracked other than the rule for the serial image presentation. For each run, animals viewed one of two possible sequential rules AAAB, or AAAA (A and B represent different images drawn from a pool of four possible images; 30 sequences in total per run, **Figure 13**). Each run began and ended with 14 s fixation blocks. A total of 169 (79 monkey W, 63 monkey J, 27 monkey B) runs were analyzed. Monkeys performed the task well and fixated for 95% of the time in included runs (see **Methods** for those excluded).

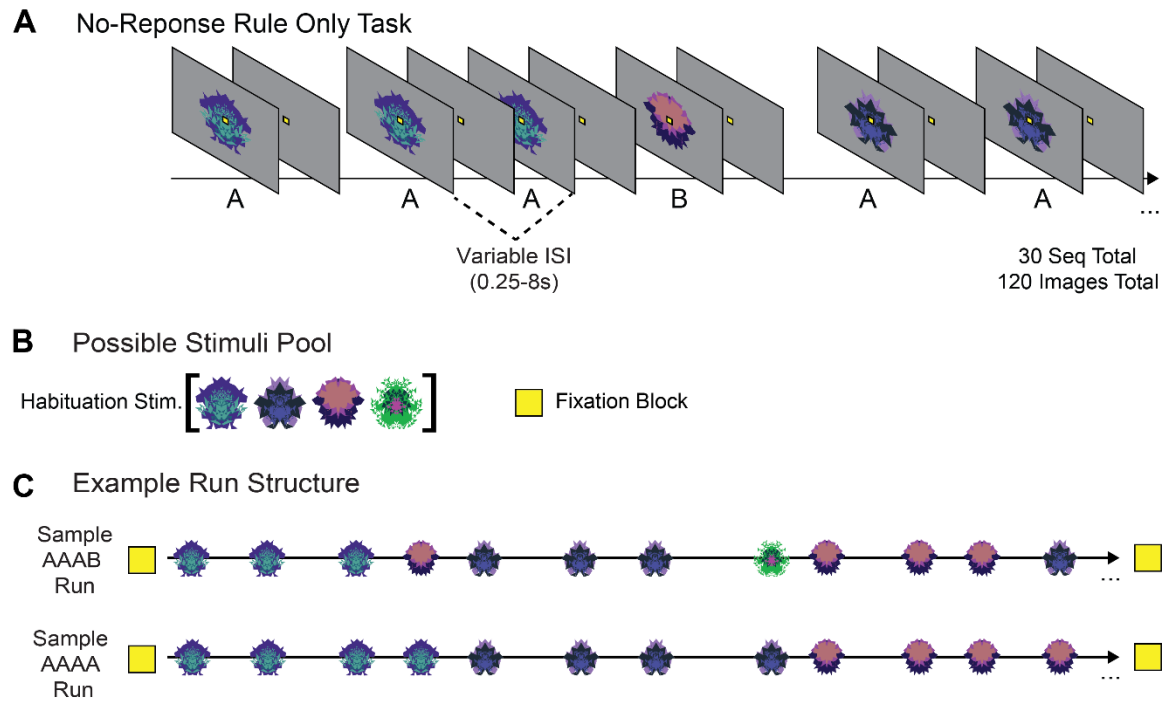


**Figure 13. No response rule-only task.** **A.** Example partial rule only block for sequence rule *three same, one different* (AAAB). Each run contained a single block with 30 sequences in total, each composed of four fractal images (120 images in total). **B.** Possible stimuli pool for rule only task. Stimuli come from the four possible images corresponding to the habituation stimuli fractal set. Yellow squares illustrate fixation blocks which occur at the beginning and end of the run. **C.** Segment of rule only runs with the two possible rule types: three of the same, one different (AAAB; top row), or four of the same (AAAA; bottom row). Blue water droplets schematize reward delivery, which is decoupled from sequence viewing and delivered on a graduated schedule based on the duration the monkey has maintained fixation.

### 3.4.2. Time Only Task

The time only task intends to isolate activity related to structured timing. To isolate structured timing, we presented fractal images in a pseudorandom order where the only variable manipulated is the assigned timing template. In this task, timing between each image presentation has jittered inter-structure intervals (0.25s – 8s) and timing templates have inter-stimulus intervals that are consistent within the template. This structured timing then allows images to appear perceptually

grouped based on time proximity. The images themselves are uninformative as there is no order to their presentation and cannot be tracked nor predicted. This task was performed in runs (~10 min each), that each contained four blocks (**Figure 14**). Each block contained specific timing template and image category pairings described in the following section (for more details on the task design see **Methods**).

*Habituation Images, Habituation Timings Block:* For each run, the first block was always a block containing fractals drawn from the habituation image pool paired with pseudo randomly assigned habituation timing templates. Image presentations were such that a presented image could not be followed by the same image. The same timing template could also not be immediately repeated if it had already been assigned to a set of images. All the timings corresponding to the habituation timing template were structured such that the same interstimulus interval and stimulus duration length was assigned to 4 images in a row.

*Deviant and Habituation Images, Deviant and Habituation Timings Blocks:* The two subsequent blocks contained both habituation image (96 of the 120 images, 80% of images in the block) presentations interspersed with rare deviant images which came from a separate image pool of three possible images (24 of the 120 images, 20% of images in the block). Image presentation frequency in this block was constructed to directly match the presentation frequency in the no-response abstract visual sequence task. We similarly matched the frequency of the structured timing templates used, with 80% corresponding to the habituation template and 20% to the deviant templates. Additionally, to mirror the organization of the no-response abstract visual sequence task each of the two possible deviant blocks could only contain either the medium deviant timing template or the short/long deviant timing template. Deviant timing templates were drawn from a timing pool separate from the possible habituation timings. The order of these deviant blocks

would be randomly selected between runs, such that each one did not always happen before the other and vice versa. Because we were isolating the effect of time, there were multiple possible image and timing template pairings illustrated in **Figure 14**.

*Novel Images, Novel Timings Block:* The last block of the run was always a block containing novel images that came from a separate pool of four possible novel fractals. Image presentations and timing assignments followed the same rules as described for the habituation images paired with habituation timings block.

The four total blocks were interleaved with 14 s fixation blocks. A total of 98 (43 monkey W, 38 monkey J, 17 monkey B) runs were analyzed. Monkeys performed the task well and fixated for 95% of the time in included runs (see **Methods** for those excluded).

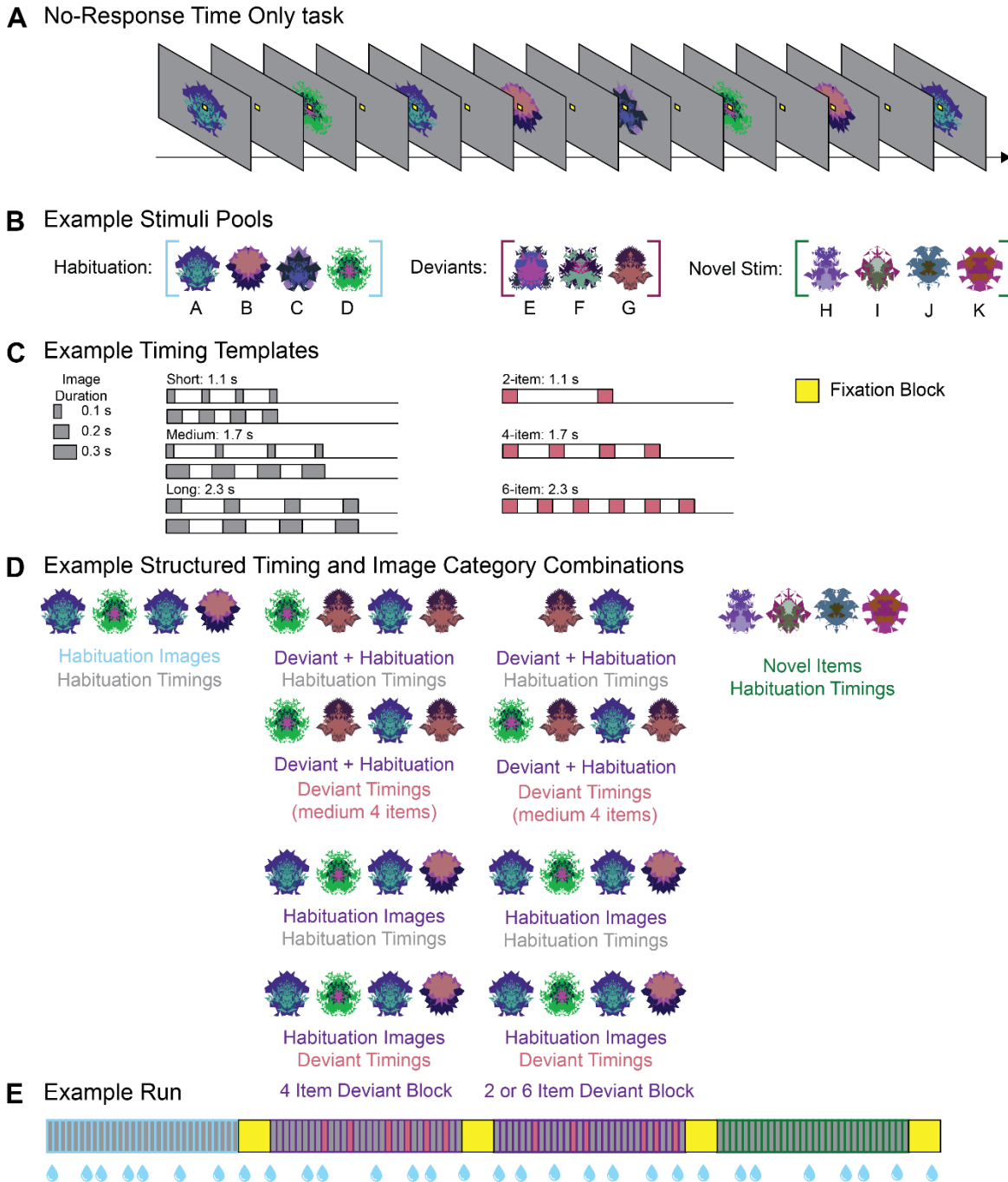


**Figure 14. No response time-only task.** **A.** Example partial habituation timing block with habituation images. **B.** Example stimulus pools show a set of images that would be used in a single scanning session. New images are used each session. **C.** Six possible habituation (frequent) timing templates (left) and deviant (infrequent) timings (right) illustrated with gray and colored rectangles indicating single images. Total sequence durations are listed for each template type. **D.** Examples of a sub-set of possible timing and image category combinations. **E.** Example run, with

each bar indicating one multi-image timing structure: Each gray bar corresponds to habituation timings, colored bars correspond to deviant timings. The first block contains only habituation images paired with habituation timings. The subsequent two blocks contain 80% habituation timing templates and 20% deviant timing templates that can be paired to either habituation images or a combination of habituation and deviant images. The final block is always a novel images block paired with habituation timings. Timing structure blocks alternate with fixation blocks. Blue water droplets schematize reward delivery, which is decoupled from time-image pairings and delivered on a graduated schedule based on the duration the monkey has maintained fixation.

### **3.4.3. Random Task**

The random task does not contain abstract rule nor structured timing, functioning as the control for our 2x2 task design. To make the task random, we presented images in a pseudorandom order with the only condition being that the previously presented image cannot be followed by the same one. In this task, timing between each image presentation had jittered intervals (0.25s – 8s). This task was performed in runs (~ 15 min each), that each contained three blocks. For each run, the first block contained only habituation images. The second block was always a deviant block containing both rare deviant image fractals (24 of the 120 image repetitions per block, 20% of image presentations) and habituation images (96 of the 120 images, 80% of images in the block) to match the image distribution of the no-response abstract visual sequence task with jittered stimulus presentation intervals. The last block of the run was always a block containing novel images with jittered stimulus presentation intervals. The three total blocks were interleaved with 14 s fixation blocks. A total of 117 (55 monkey W, 35 monkey J, 27 monkey B) runs were analyzed for this task.

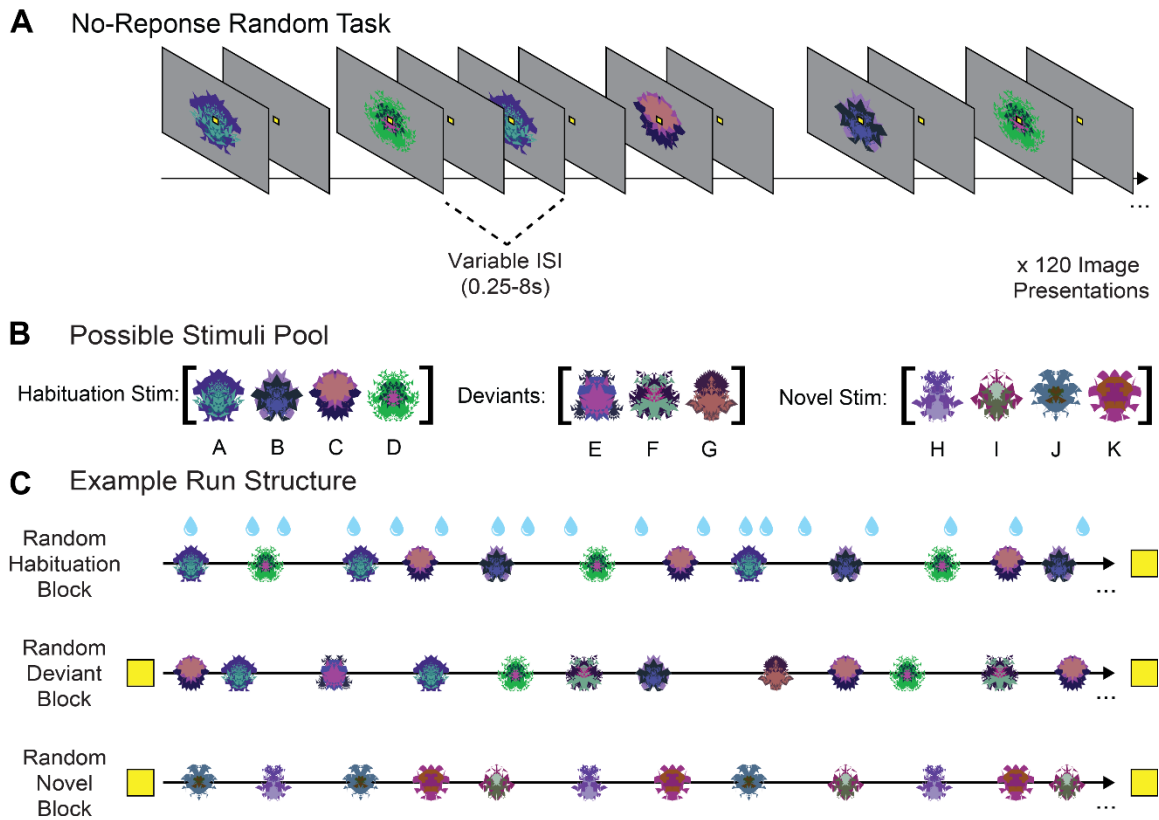


**Figure 15. No response random task.** **A.** Example partial random habituation image block. Each run contained three blocks with 120 presentations (360 image presentations in total). **B.** Possible stimuli pool for random task. Yellow squares illustrate fixation blocks which occur at the beginning and end of the run. **C.** Example block structure showing example segments of each block (in order of appearance within a run, top to bottom). Segment of random habituation images block (top row), stimuli come from the habituation stimuli pool. Segment of random deviant images block (middle row), stimuli come from the habituation stimuli pool (80% of images) or the deviant images pool (20% of images). Segment of random novel images block (bottom row), stimuli come from the novel stimuli pool. Blue water droplets schematize reward delivery, which is decoupled from image events and delivered on a graduated schedule based on the duration the monkey has maintained fixation.

#### **3.4.4. Isolated abstract sequential rule modulates DLPFC responses**

Our first goal for this set of experiments was to test the hypothesis that neural activity in the DLPFC sub-region Area 46 responds to abstract rule in the absence of structured timing. Because this and the following sets of tasks are no report, in this task variant we tested this hypothesis using neural (BOLD) responses to position activity during isolated abstract sequence rule. Previous work has shown that neural responses related to sequential structure and changes to it require attention (Bekinschtein et al., 2009). Additionally, the monitoring of these abstract sequences is thought to be associated with specific neural patterns of activity such as ramping dynamics (Desrochers et al., 2015, 2019; McKim & Desrochers, 2022a). Our previous study using a no-report abstract visual sequence task in non-human primates showed increased neural responses in Area 46, and these responses showed similar ramping dynamics observed during human sequential monitoring tasks (Yusif Rodriguez et al., 2022). These previous findings support the prediction that animals are processing the overall higher order structure of the abstract sequences since we observed responses to sequential rule deviants. Therefore, we predict that abstract rule in the absence of structured timing contributes to the observed neural dynamics during no-response abstract sequence viewing and should similarly elicit neural responses in the DLPFC.

Our 2x2 task design allowed us to test the combined influence of timing and rule on DLPFC activity, and now we can isolate these characteristics to test their individual influence. The no-response abstract visual sequence task allowed us to observe responses related to monitoring changes to an established sequence using rare sequential deviants. However, we also wanted to test for ramping activity that could indicate monitoring throughout each sequence step. Therefore, in this task variant which we have named “Rule Only”, we have isolated one specific characteristic present in our previous no-response abstract visual sequence task, abstract sequence rule. Using

the rule only task we could identify position by position neural activity in Area 46 to determine whether abstract rule is monitored throughout and with similar ramping dynamics. Here, animals viewed a single block containing images from the habituation pool of images. These images were presented as sequences that followed a rule of either three of the same and one different (AAAB) or four of the same images.

To test the prediction that isolated abstract visual sequence rule elicits ramping activity, we first constructed an unbiased region of interest (ROI) located in monkey area 46 in each hemisphere to compare activity across sequence positions. Our previous work identified specific sub-regions of activation within area 46 related to the processing of deviations to an established abstract sequence (Yusif Rodriguez et al., 2022). Therefore, we defined two ROIs from Yusif Rodriguez et al., (2022) during the no-report abstract visual sequence task on which this task is based on. One ROI was defined from the parametric ramping cluster in left area 46 (center  $xyz = -12.2, 36, 22.8$ ; size = 16.25 mm), and another from the conjunction map showing overlapping activity between rule and number changes in right area 46 (center  $xyz = 10.2, 33.7, 21.8$ ; size = 5.2 mm). In all following sections we will refer to these ROIs as *Left Ramp ROI* and *Right Conjunction ROI* respectively. The resulting ROIs spanned a small region of area 46 that mainly contained area 46d (NIMH Macaque Template, NMT v2.0 Macaque Atlas, Jung et al., 2021; Seidlitz et al., 2018).

To test for a ramping increase in activity we created a model that included separate regressors for each position in the four-item sequence, modeled as zero-duration onsets. Statistical testing was performed on ~10 run bins ( $n = 16$ ), each consisting of data from a single monkey (see **Methods**). We compared t-values from the contrast of each condition over baseline (e.g., Position 1 > Baseline vs. Position 2 > Baseline, etc.) to account for potential differences in variance across conditions. This type of comparison was used to examine ROI activity throughout, and we refer to

comparisons by the conditions of interest (without listing the contrast over baseline, e.g., Position 4 > Position 1, etc.). All statistical tests on ROIs were performed on binned data and included a covariate for monkey identity ( $n = 3$ ). While we report the effect of monkey in the following analyses, the focus of the study was not on individual differences, and our discussion centers on condition effects.

### **3.4.5. Activity in area 46 increases as a result of progression through sequence position**

We found that activity in the left ramp ROI represented abstract sequence changes, with the lowest activation in position 1, and highest activation occurring in position 4 (**Figure 16, Table 10**; position:  $F(3, 39) = 3.397$ ,  $p = 0.027$ ,  $\eta_p^2 = 0.207$ ). Responses matched a significant pattern of ramping activity across sequence positions (ramp:  $F(1, 13) = 11.78$ ,  $p = 0.0045$ ,  $\eta_p^2 = 0.475$ ). Position and ramping responses did not reach statistical significance in the right conjunction ROI (position:  $F(3, 39) = 0.316$ ,  $p = 0.814$ ,  $\eta_p^2 = 0.024$ ; ramp:  $F(1,13) = 0.940$ ,  $p = 0.350$ ,  $\eta_p^2 = 0.067$ ). Despite the lack of significant ramping in the right conjunction ROI, there were no significant differences between the left ramp ROI and the right conjunction ROI (position x brain area:  $F(3,84) = 2.347$ ,  $p = 0.08$ ,  $\eta_p^2 = 0.055$ ).

As a control for the possibility that increasing ramping activity was occurring due to progression through the block, we created a model with regressors for positions one through eight. When comparing activity at position eight to activity at position four there was no significant difference (position:  $F(3, 39) = 3.397$ ,  $p = 0.027$ ,  $\eta_p^2 = 0.207$ ; **Figure 16**). Altogether these results suggest that area 46 responses are modulated by isolated abstract sequential rule.

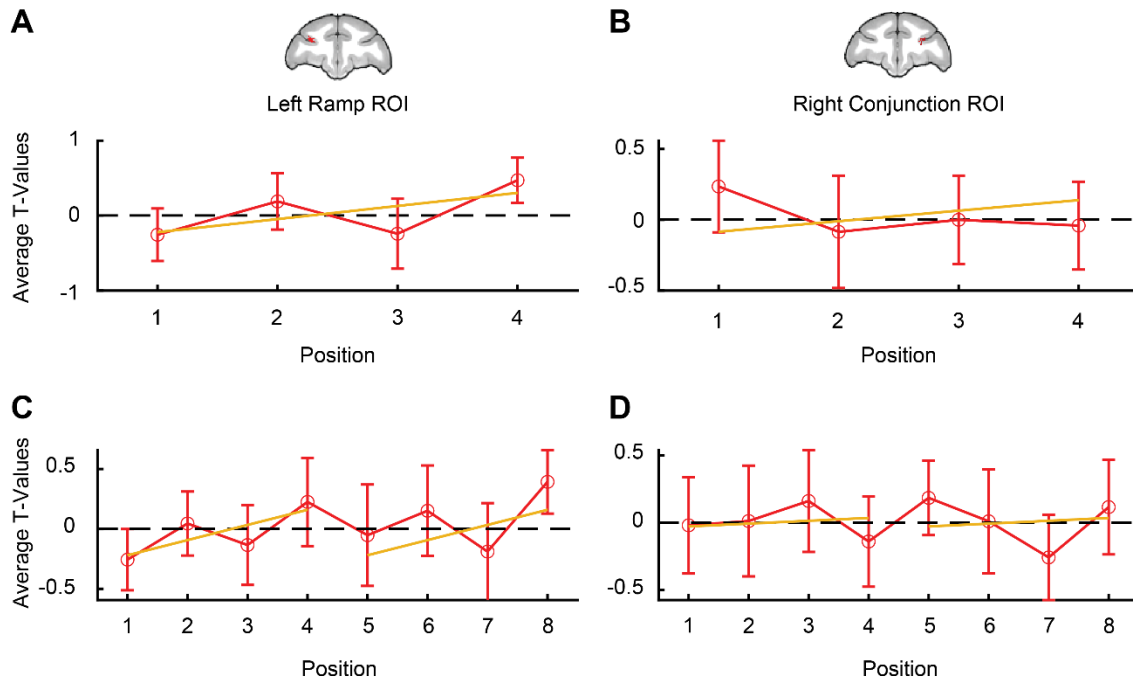


**Figure 16. Isolated abstract rule modulates ramping activity in area 46.** T-values for the position of interest > baseline are shown. The locations of area 46 regions of interest (ROIs), left ramp ROI and right conjunction ROI, are illustrated in red on coronal sections ( $y = 35$ ). **A.** Positions 1-4 compared to each other in left ramp ROI showed a reliable difference and a significant positive linear trend. **B.** Positions 1-4 compared to each other in right conjunction ROI. **C.** Positions 1-8 compared to each other in left ramp ROI show significant ramping activity. **D.** Positions 1-8 compared to each other in right conjunction ROI. Error bars are 95% confidence intervals (1.96 x standard error of the within-bin mean).

**Table 10. Repeated measures ANOVAs comparing position activity in L46 and R46**

Factor	dfs	Left Ramp ROI			Right Conjunction ROI		
		F	p	$\eta_p^2$	F	p	$\eta_p^2$
<i>Positions 1-4</i>							
Position	3, 39	3.397	0.027	0.207	0.316	0.814	0.024
Ramp	1, 13	11.78	0.0045	0.475	0.940	0.350	0.067
Monkey	2, 13	2.297	0.140	0.261	3.295	0.070	0.336
Monkey x Position	6, 39	0.683	0.664	0.261	1.376	0.249	0.336
Monkey x Ramp	2, 13	1.304	0.304	0.095	0.376	0.694	0.175
<i>Positions 1-8</i>							
Position	7, 91	1.905	0.078	0.128	0.854	0.546	0.062
Ramp	1, 13	5.111	0.042	0.282	0.013	0.911	0.001
Monkey	2, 13	2.065	0.166	0.241	2.602	0.112	0.286

Monkey x Position	14, 91	0.783	0.685	0.241	0.685	0.783	0.286
Monkey x Ramp	2, 13	1.610	0.237	0.108	0.293	0.751	0.095
<i>Positions 4 Vs 8</i>							
Position	1, 13	0.053	0.821	0.0041	1.738	0.210	0.118
Monkey	2, 13	0.970	0.405	0.130	0.281	0.759	0.041
Monkey x Position	2, 13	0.378	0.692	0.055	0.593	0.567	0.084

We next aimed to confirm whether a parametric ramp model could explain the observed ramping pattern of activity in this neural data, as was demonstrated in the previous study (Yusif Rodriguez et al., 2022). We hypothesized that isolated abstract rule would similarly produce changes in ramping activation in area 46 if abstract sequence monitoring underlies this dynamic. To confirm if a linear model of BOLD dynamics would capture also capture variance due to ramping in area 46 during this task, we used the same model designed to isolate these dynamics as described in (**Methods**, Yusif Rodriguez et al., 2022). Because variance due to changes at the last item of the sequence could be misattributed to ramping regressors, we directly compared activity in both ROIs that could be accounted for by ramping and last item change regressors. In this control analysis, we found that activity was not significantly different between unique ramping and unique last item change across all positions in either the left ramp ROI (unique ramp:  $F(1,13) = 0.700$ ,  $p = 0.418$ ,  $\eta_p^2 = 0.051$ ; monkey x ramp:  $F(2,13) = 0.015$ ,  $p = 0.985$ ,  $\eta_p^2 = 0.054$ ) nor the right conjunction ROI (unique ramp:  $F(1,13) = 0.136$ ,  $p = 0.718$ ,  $\eta_p^2 = 0.0104$ ; monkey x ramp:  $F(2,13) = 0.843$ ,  $p = 0.453$ ,  $\eta_p^2 = 0.0215$ ; **Figure 17**).

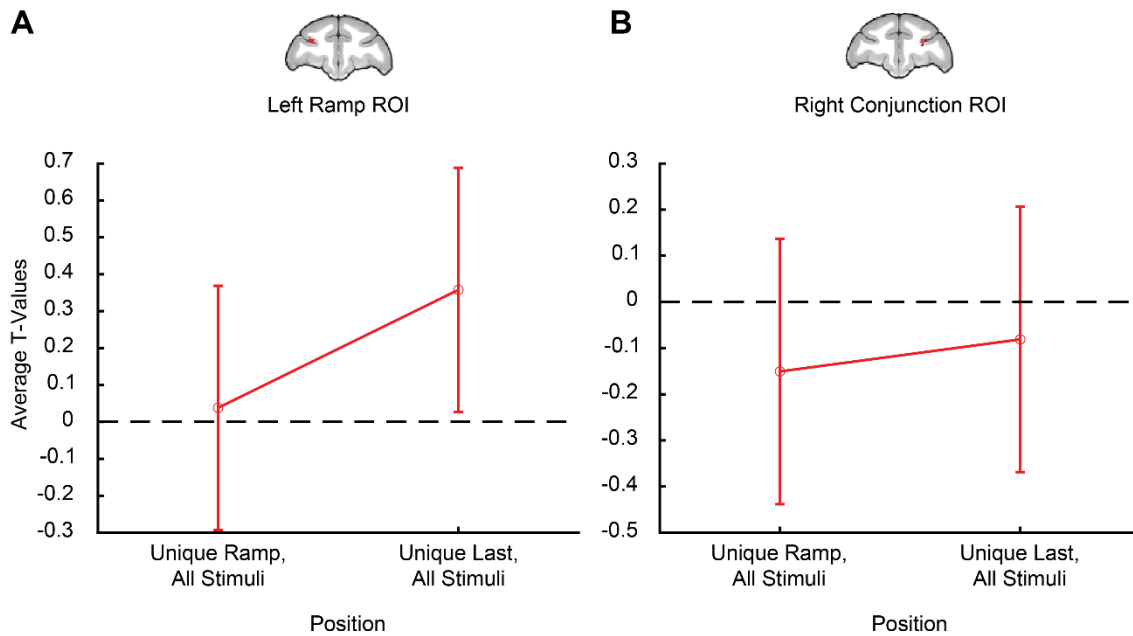


**Figure 17. No significant difference between unique ramping and unique last item activity for abstract rule in area 46 during Rule Only.** T-values for the condition of interest > baseline shown. **A.** Unique ramp compared to unique last item in left ramp ROI showed no significant difference. **B.** Unique ramp compared to unique last item in right conjunction ROI showed no significant difference. Error bars are 95% confidence intervals (1.96 x standard error of the within-bin mean).

Whole-brain contrasts further demonstrated the presence of significant activity in various brain areas for unique ramp activity and unique last item activity, but any significant activity was absent in either left or right area 46 (**Figure 18**). These comparisons supported the results of the ROIs in which there was no significant activity in area 46 for either unique ramp or unique last item. These results suggest that the dynamics in area 46 are potentially non-linear in nature, or capture more variance explained by last item responses with the jittered timing of this task. Further analysis and experiments will be necessary to tease these options apart.

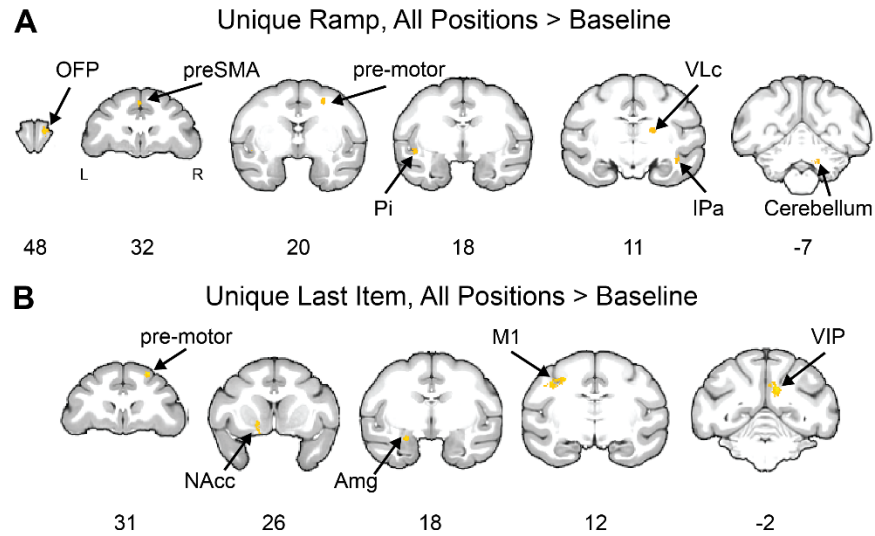


**Figure 18. Whole brain activity does not show significant unique ramping activity in Area 46 for Rule Only. A.** Unique Ramp, All Positions > Baseline (FDRc  $p < 0.05$ , height  $p < 0.005$  unc., ext. 94). **B.** Unique Last Item, All Positions > Baseline (FDRc  $p < 0.05$ , height  $p < 0.005$  unc., ext. 115). Orbital Frontal Pole (OFP), Pre-Supplementary Motor Area (Pre-SMA), Pre-Motor Cortex (Pre-Motor), Parainsular Area (Pi), Intraparietal Area (IPa), Nucleus Accumbens (NAcc), Amygdala (Amg), Primary Motor Cortex (M1), Ventral Intraparietal Area.

Because a parametric ramp model did not capture variance in area 46, yet we did observe a significant linear increase in the left ramp ROI (**Figure 16**), we next examined whole-brain contrasts for areas that showed an increase across the sequence, regardless of the dynamics. To make this comparison, we compared activity at the last (fourth) and first positions in the sequence. Contrasts of All Positions > Baseline and Position 4 > Position 1 both showed significant clusters of activation in left area 46 (**Figure 19**). Other significant clusters of activation were located in areas such as the visual cortex, the hippocampus and caudate nucleus, which are some areas that were also observed in a similar auditory sequence task (L. Wang et al., 2015) as well as our previous work (Yusif Rodriguez et al., 2022). Therefore, while a parametric ramp model may not best explain the observed ramping dynamics, there is evidence for an increase in activity at the last position of the sequence when compared to the first.

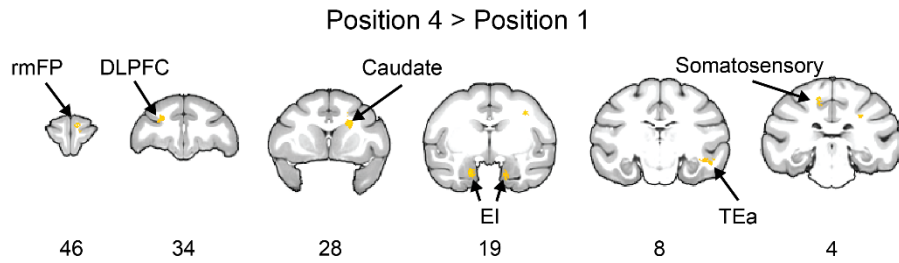


**Figure 19. Whole brain activity for last position compared to first suggests that isolated rule modulates DLPFC activity for Rule Only. A.** Position 4 > Position 1 (FDRc  $p < 0.05$ , height  $p < 0.005$  unc., ext. 80). Rostro Medial Frontal Pole (rmFP), Dorsolateral Prefrontal Cortex (DLPFC), Caudate, Entorhinal Cortex (EI), Superior Temporal Sulcus Ventral Bank (TEa), Somatosensory Area.

**Table 11. Last position compared to first position contrast activation coordinates.**

Contrast Location	Extent (voxels)	x	y	z	Peak t-val
<b>Rule Only Position 4 &gt; Position 1</b>					
Amygdala	464	-8.5	20	0	6.05
Somatosensory Areas I-II	111	-6.0	4.5	32.5	5.66
Entorhinal Cortex	200	5.5	16.5	1.0	5.27
Caudate	280	8.5	28.0	22.5	5.19
Rostro Medial PFC	153	4.0	48.0	17.5	4.94
Dorsal Lateral PFC (Area 46)	140	-10.0	33.5	24.0	4.92
Caudal Dorsal Pre-Motor Cortex	93	17.0	21.5	27.5	4.64
Superior Temporal Area	80	12.0	3.0	25.0	4.63
Area PGa	118	22.0	8.0	5.5	4.54
Area TEa	123	16.5	13.5	0.5	4.17

Overall, activity related to position onset activity suggests ramping dynamics are present for isolated rule in areas 46. This activity is similar to what was seen in our previous work seen in a task containing both abstract sequence rule and structured timing. Unlike what was seen in these previous results, a model for unique parametric ramping activity does not explain activity observed in area 46. However, unique last activity is not significant in area 46 either. Despite these findings it is possible then that the main “driver” of activity in area 46 of the DLPFC activity is abstract

rule. Isolated sequence rule is sufficient to define an abstract sequence and elicit DLPFC activity and could be sufficient sequential information to engage in sequential monitoring.

#### **3.4.6. Isolated structured timing does not modulate monkey DLPFC activity**

Our previous section suggested that rule in isolation could be sufficient to elicit ramping activity in the monkey DLPFC. However, given that our previous work showed ramping activity occurring when sequences contained both rule and timing information, it was necessary to test whether timing in isolation could also modulate DLPFC activity. Previous work has suggested that timing on its own can drive ramping activity in the frontal cortex (Bekolay et al., 2014; Narayanan, 2016; Narayanan & Laubach, 2009; Niki & Watanabe, 1979). It is possible then that the resulting ramping activity previously observed in our work resulted from a combination of timing and rule tracking. Because the utilized timing templates had set frequencies of appearance, it is also possible that animals were engaging in monitoring the timings as well, and not necessarily only monitoring the abstract sequences.

In this experiment we aim to test the hypothesis that isolated structured timing, in the absence of an abstract rule, elicits neural activity in the DLPFC sub-region Area 46. Previous work has shown that the DLPFC responds to different types of timing structures including interval timing (Gu et al., 2015; J. Kim et al., 2013; M. Xu et al., 2014), temporal expectation (Coull & Nobre, 2008; Roesch & Olson, 2007) and structured timing (Cueva et al., 2020; Meirhaeghe et al., 2021; reviewed in A. C. Nobre & van Ede, 2018; J. Wang et al., 2018). Additionally, studies in both humans and other animals have shown that ramping dynamics can also occur in this region as a result of the influence of timing information (Desrochers et al., 2019; Ding, 2015). Our previous study using a no-report abstract visual sequence task in non-human primates suggests that timing information could be modulating increased neural responses and ramping dynamics in Area 46

(Yusif Rodriguez et al., 2022). To determine the influence of timing of the DLPFC activity and ramping dynamics, we created a 2 x 2 task design which includes a paradigm that queries structured timing as a variable.

In this task variant which we have named “Time Only”, we have isolated one specific characteristic present in our previous no-response abstract visual sequence task, structured timing. Here, animals viewed a single block containing stimulus and timing pairings composed of habituation images with habituation timings, deviant and habituation images with deviant and habituation timings, and novel images with habituation timings (**Figure 14**). Two models were utilized to test the neural activity in the DLPFC related to structured timing. First, to generally test if isolated structured timing elicits a response in the DLPFC we used an instantaneous event onset model, where each timing structure is an individual event. Conditions were modelled according to all possible image and timing combinations (see **Methods** for more details). Because there were multiple possible image combinations, and these were often grouped in the following sets of analyses we identified each category with the names as follows: Habituation timings paired with habituation images (HH), deviant timings paired with deviant and habituation images (DHD), habituation timings paired with novel images (NH). Afterwards, to test whether structured timing in isolation results in a ramping DLPFC activity we constructed a parametric ramp model with the same regressor categories as described for the instantaneous onsets model.

#### **3.4.7. Animals attend to task stimuli**

First, to determine whether animals were generally attending to visual stimuli, we tested activity from novel images compared to habituation images. Work in both humans and monkeys has implicated the PFC for the processing of novel stimuli information (Daffner et al., 2003; Ghazizadeh et al., 2020; Matsumoto et al., 2007). In the study by Ghazizadeh et al., 2020, a set of

fronto-cortical networks which included regions such as the ventral PFC and lateral PFC were identified as processing relationships between novel and familiar fractal stimuli during no-response awake behaving monkey fMRI. These novelty responses are also thought to require attention to drive neural activity, suggesting that we would only observe them when animals are engaged with the task and attending to the different stimuli categories present.

We predicted that if animals were attending the varying stimuli presented in the task, that we should be able to observe novelty responses in relevant brain areas including prefrontal regions. ROI comparisons were completed using the same right ramp ROI and left conjunction ROI as described in the beginning of this chapter. Because the timings assigned to both novel and habituation images in this task corresponded to the same timing templates (**Methods**), any observed contrast activity should be specific to differences in image, and not timing. Results from ROI comparisons in the DLPFC show no significant differences between novel images and habituation images assigned the same timing templates (**Figure 20**; left ramp ROI; timings:  $F(1,7) = 0.084$ ,  $p = 0.78$ ,  $\eta_p^2 = 0.012$ ; monkey =  $F(2,7) = 5.8$ ,  $p = 0.033$ ,  $\eta_p^2 = 0.624$ ; monkey x timing:  $F(1,7) = 0.4$ ,  $p = 0.685$ ,  $\eta_p^2 = 0.103$ ; right conjunction ROI; timings:  $F(1,7) = 1.54$ ,  $p = 0.25$ ,  $\eta_p^2 = 0.18$ ; monkey =  $F(2,7) = 2.02$ ,  $p = 0.203$ ,  $\eta_p^2 = 0.365$ ; monkey x timing:  $F(1,7) = 1.38$ ,  $p = 0.313$ ,  $\eta_p^2 = 0.282$ ).

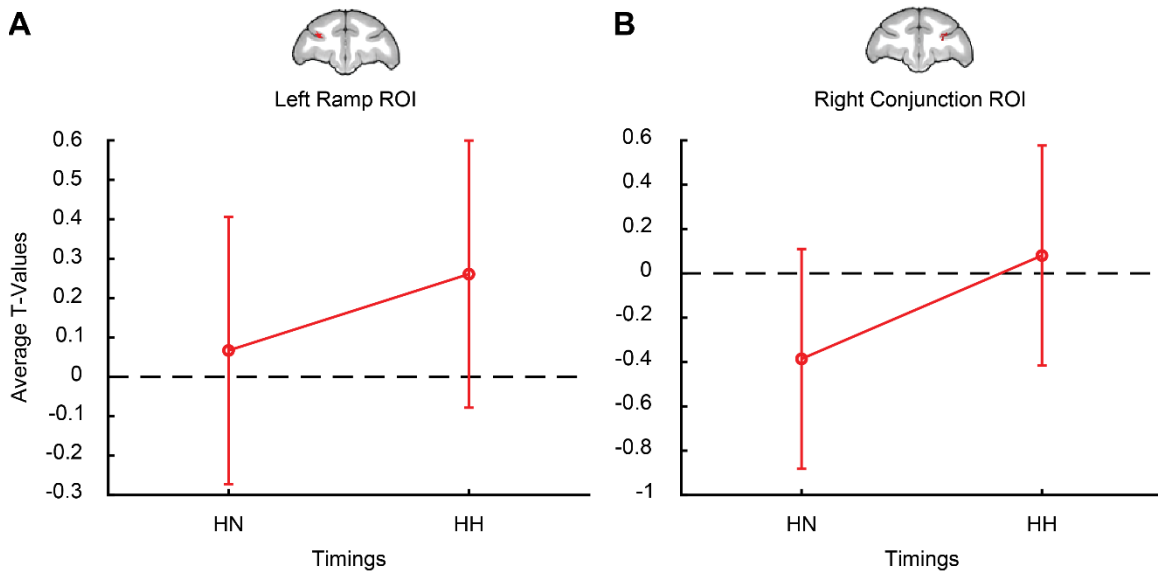


**Figure 20. DLPFC does not show significant activity for novel images when compared to habituation images in Time Only.** T-values for the condition of interest > baseline shown. **A.** Onset activity for structured habituation timings with novel images (HN), compared to habituation timings with habituation images (HH) in left ramp ROI showed no significant difference. **B.** Onset activity for structured habituation timings with novel images (HN), compared to habituation timings with habituation images (HH) right conjunction ROI showed no significant difference. Error bars are 95% confidence intervals (1.96 x standard error of the within-bin mean).

We additionally investigated whole brain activity to determine if novelty responses were present in other brain regions. As mentioned previously, a variety of brain regions have been implicated in the processing of novelty responses in the brain. Therefore, a simple ROI analysis in a specific sub-region may not accurately capture task relevant novelty responses. To identify whole brain neural activity related to novelty, we contrasted novel images to habituation images with the same timing templates (Timing HN > Timing HH) and combined habituation with deviant images to habituation images with the same timing templates (Timing HDH > Timing HH; **Figure 21**).

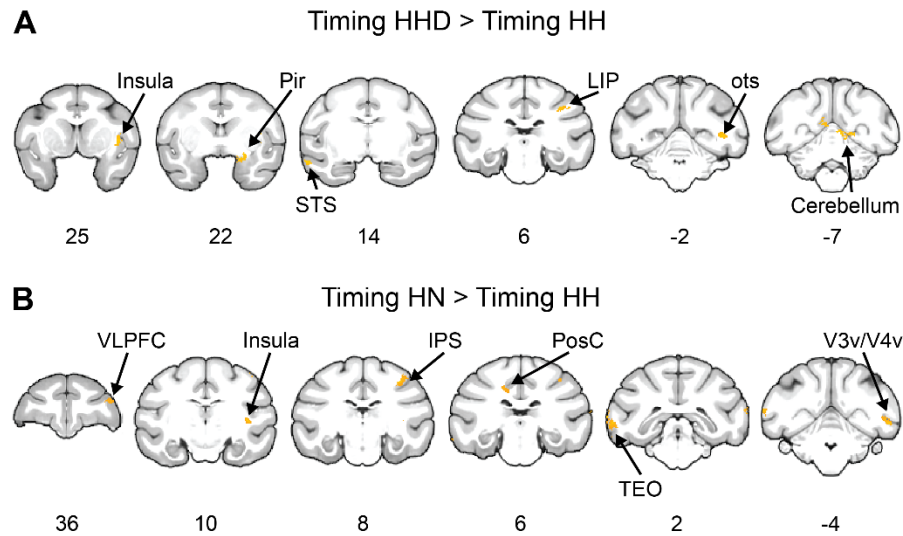


**Figure 21. Novelty responses in different brain areas suggest that animals are attending to visual stimuli during Time Only task. A.** Timing HHD > Timing HH (FDRc  $p < 0.05$ , height  $p < 0.005$  unc., ext. 82). **B.** Timing HN > Timing HH (FDRc  $p < 0.05$ , height  $p < 0.005$  unc., ext. 82). Insula, Piriform Cortex (Pir), Superior Temporal Sulcus (STS), Lateral Intraparietal Area (LIP), Occipitotemporal sulcus (ots), Cerebellum, Ventral Lateral Prefrontal Cortex (VLPFC), Intraparietal Sulcus (IPS).

Results from these contrasts show activity we see activity in brain areas that have been identified as being related to novelty detection when compared to highly familiar stimuli during passive viewing. Some of the relevant brain areas include the VLPFC for novelty responses and LIP for deviant responses, both areas implicated in the processing of novel stimuli. Therefore, the current contrast results indicate that animals are attending to the changing visual stimuli. These findings suggest that animals are engaged with the task, which is essential to know given otherwise it would not be possible to determine whether results are related to engagement (or lack thereof) with the task stimuli.

### 3.4.8. Timing deviations in absence of abstract rule does not modulate activity in the DLPFC during Time Only task

After determining that animals are attending to the presented image categories, we tested whether structured timing in isolation elicits responses in area 46. We utilized the same ROIs described in the previous section to first test whether there were significant differences in timing activity across possible conditions. T maps used to look at this activity were obtained by modelling the instantaneous onset of the beginning of each timing template (as described in **Methods**).

To determine if isolate timing structure modulates DLPFC responses, we first tested if deviant timing templates would elicit greater DLPFC activity when compared to habituation timing templates. Previous work in timing literature has suggested that temporal expectation can modulate neural responses (Coull & Nobre, 2008). It is then possible that while completing this task, animals can create distinct expectations of frequent and less frequent time structures that could result in increased DLPFC responses. To test this prediction, we compared ROI activity in both the left ramp ROI and right conjunction ROI for deviant timings assigned to habituation and deviant images (DHD) to habituation timings assigned to habituation images (HH). Results from this ROI analysis were not significant (**Figure 22**; left ramp ROI; timings:  $F(1, 7) = 0.573$ ,  $p = 0.474$ ,  $\eta_p^2 = 0.08$ ; monkey:  $F(2, 7) = 5.22$ ,  $p = 0.04$ ,  $\eta_p^2 = 0.599$ ; monkey x timing:  $F(1, 7) = 4.67$ ,  $p = 0.05$ ,  $\eta_p^2 = 0.572$ ; right conjunction ROI; timings:  $F(1, 7) = 0.171$ ,  $p = 0.692$ ,  $\eta_p^2 = 0.024$ ; monkey:  $F(2, 7) = 2.23$ ,  $p = 0.178$ ,  $\eta_p^2 = 0.39$ ; monkey x timing:  $F(1, 7) = 0.243$ ,  $p = 0.79$ ,  $\eta_p^2 = 0.065$ ). This suggests that animals may not be actively tracking timing structure.

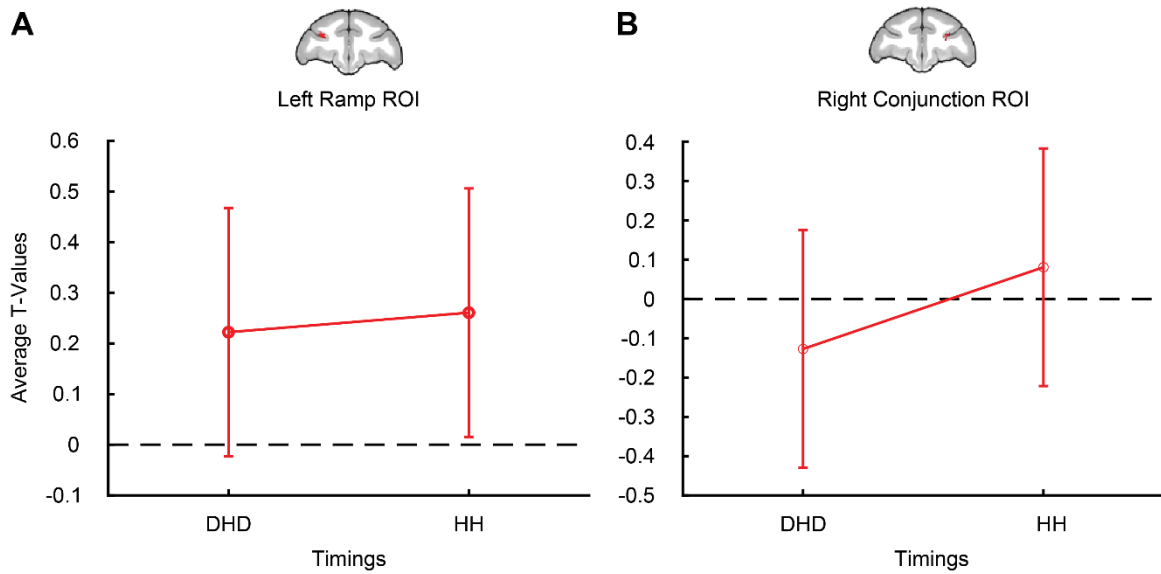


**Figure 22. Deviant timing structure does not affect DLPFC activity in Time Only.** T-values for the condition of interest > baseline shown. **A.** Onset activity for structured deviant timings with habituation and deviant images (DHD), compared to habituation timings with habituation images (HH) in left ramp ROI showed no significant difference. **B.** Onset activity for structured deviant timings with habituation and deviant images (DHD), compared to habituation timings with habituation images (HH) in right conjunction ROI showed no significant difference. Error bars are 95% confidence intervals (1.96 x standard error of the within-bin mean).

We next aimed to determine whether image identity paired with timing modulated DLPFC responses. It is possible that while timing structure on its own may not modulate DLPFC activity, that the combined timing and associated images can affect neural responses, in absence of an abstract rule. To test this prediction, we compared activity in the DLPFC across matched timing structure. These comparisons were carried out for habituation timing templates exclusively containing habituation images to templates containing deviant images (Figure 23, **A and B**; left ramp ROI; timings:  $F(2, 32) = 0.242$ ,  $p = 0.786$ ,  $\eta_p^2 = 0.015$ ; timings x monkey:  $F(4, 32) = 0.89$ ,  $p = 0.481$ ,  $\eta_p^2 = 0.435$ ; right conjunction ROI; timings:  $F(2, 32) = 1.038$ ,  $p = 0.37$ ,  $\eta_p^2 = 0.0609$ ; timings x monkey:  $F(4, 32) = 1.138$ ,  $p = 0.36$ ,  $\eta_p^2 = 0.2622$ ) and habituation timing templates with novel images (**Figure 23, C and D**; left ramp ROI; timings:  $F(2, 32) = 0.46$ ,  $p = 0.63$ ,  $\eta_p^2 = 0.03$ ;

timings x monkey:  $F(4, 32) = 0.65$ ,  $p = 0.63$ ,  $\eta_p^2 = 0.44$ ; right conjunction ROI; timings:  $F(2, 32) = 1.02$ ,  $p = 0.37$ ,  $\eta_p^2 = 0.06$ ; timings x monkey:  $F(4, 32) = 0.77$ ,  $p = 0.55$ ,  $\eta_p^2 = 0.14$ ). Results from this analysis did not show significant differences in DLPFC activity for structured timing and image identity pairings.

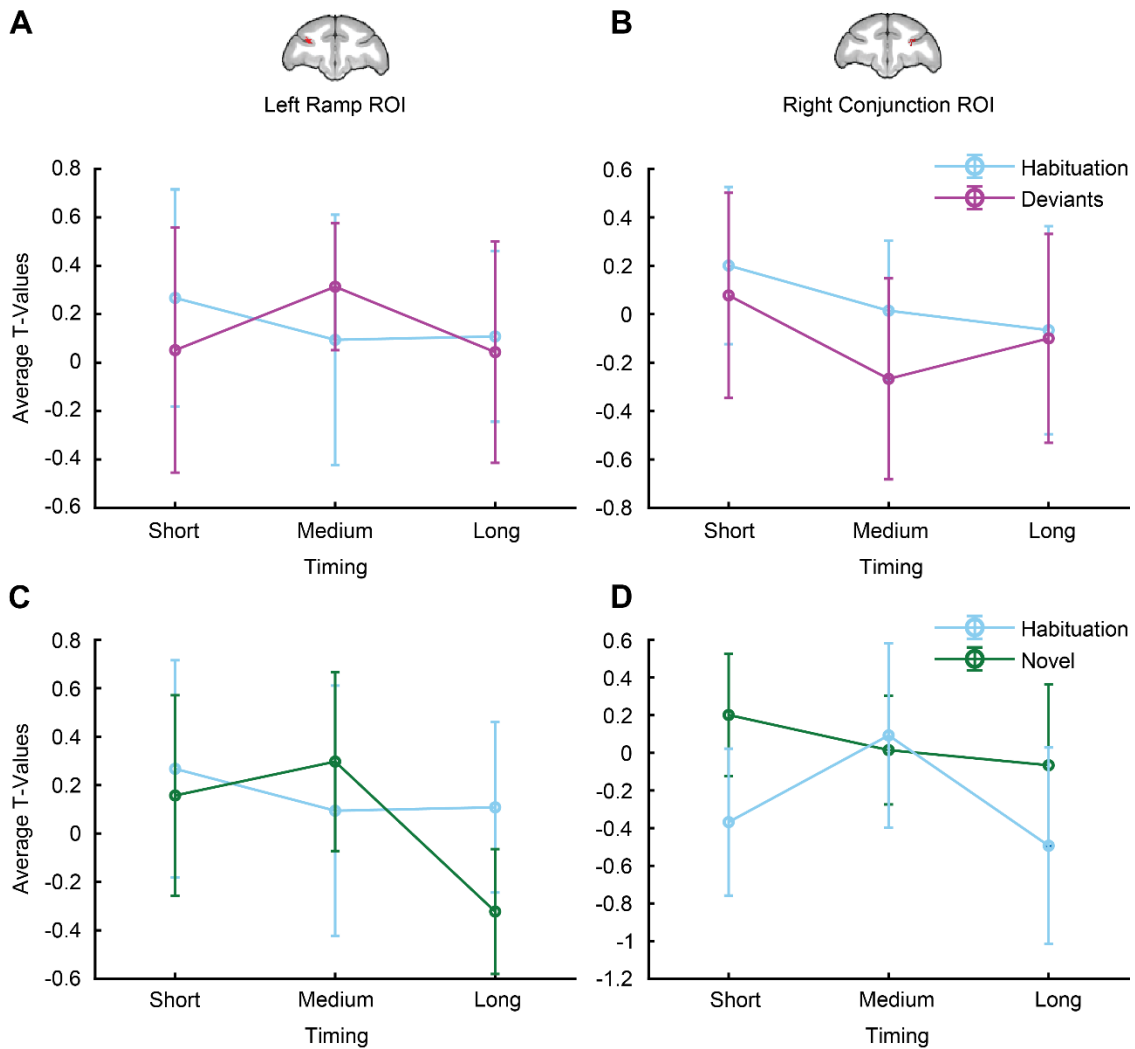


**Figure 23. There is no significant effect of image identity on area 46 activity in Time Only.** T-values for the condition of interest > baseline shown. **A.** Onset activity for all short, medium, and long habituation timings assigned to deviants combined with habituation stimuli (purple line), compared to short, medium, and long habituation timings assigned to habituation images (light blue line) in left ramp ROI showed no significant difference (top left). **B.** Onset activity for all short, medium, and long habituation timings assigned to deviants combined with habituation stimuli

(purple line), compared to short, medium, and long habituation timings assigned to habituation images (light blue line) in right conjunction ROI showed no significant difference (top right). **C.** Onset activity for all short, medium, and long habituation timings assigned to novel stimuli (green line), compared to short, medium, and long habituation timings assigned to habituation images (light blue line) in left ramp ROI showed no significant difference (bottom left). **D.** Onset activity for all short, medium, and long habituation timings assigned to novel stimuli (green line), compared to short, medium, and long habituation timings assigned to habituation images (light blue line) in right conjunction ROI showed no significant difference (bottom right). Error bars are 95% confidence intervals (1.96 x standard error of the within-bin mean).

Results in this section suggest that while animals are attending to stimuli, structured timing in absence of abstract sequence does not seem to be modulating DLPFC activity. Overall, responses related to novelty were seen in a variety of areas suggested to process novel image information such as VLPFC and LIP. These findings support that animals are attending to the image set, however they may not specifically be attending to the timing structures that perceptually group the images. Additionally, the deviant timing structures themselves may not be distinct enough to elicit a deviant response that would result in increased DLPFC activity.

#### **3.4.9. Isolated structured timing does not elicit ramping activity in the monkey DLPFC**

We demonstrated in the previous section that the DLPFC regions involved in our previous sequential task that had structured timing did not respond to isolated structured timing. However, in our previous work images presented in an abstract sequence paired with specific timing templates elicited ramping responses in the DLPFC. It is possible that these ramping responses were the result of combined monitoring of both abstract rule and timing structure. Therefore, we predicted that while these ramping responses may not be as large as those observed when both sequential characteristics are combined, that ramping activity would still be present in the DLPFC

due to processing of the timing templates. For these next set of analyses conditions were modeled to test using a parametric ramp (**Methods**). Unlike the unique ramp model used for the rule only task, given that there wasn't a concern for activity related to a last item effect in this task design, regressors accounted for timing template onset, and then unique ramping activity.

First, we tested whether there was a significant difference in ramping across the different possible image sets that are assigned the same timings. We mainly wanted to determine if any difference existed across timing types that could be a result of the influence of the images that were used. There were no significant differences in either the left ramp ROI or the right conjunction ROI when comparing across all task conditions with equivalent length structured timings (**Figure 24**; left ramp ROI; timings:  $F(2, 50) = 0.31$ ,  $p = 0.74$ ,  $\eta_p^2 = 0.012$ ; timings x monkey:  $F(4, 50) = 3.5$ ,  $p = 0.014$ ,  $\eta_p^2 = 0.05$ ; right conjunction ROI; timings:  $F(2, 50) = 0.06$ ,  $p = 0.94$ ,  $\eta_p^2 = 0.002$ ; timings x monkey:  $F(4, 50) = 1.06$ ,  $p = 0.39$ ,  $\eta_p^2 = 0.03$ ).

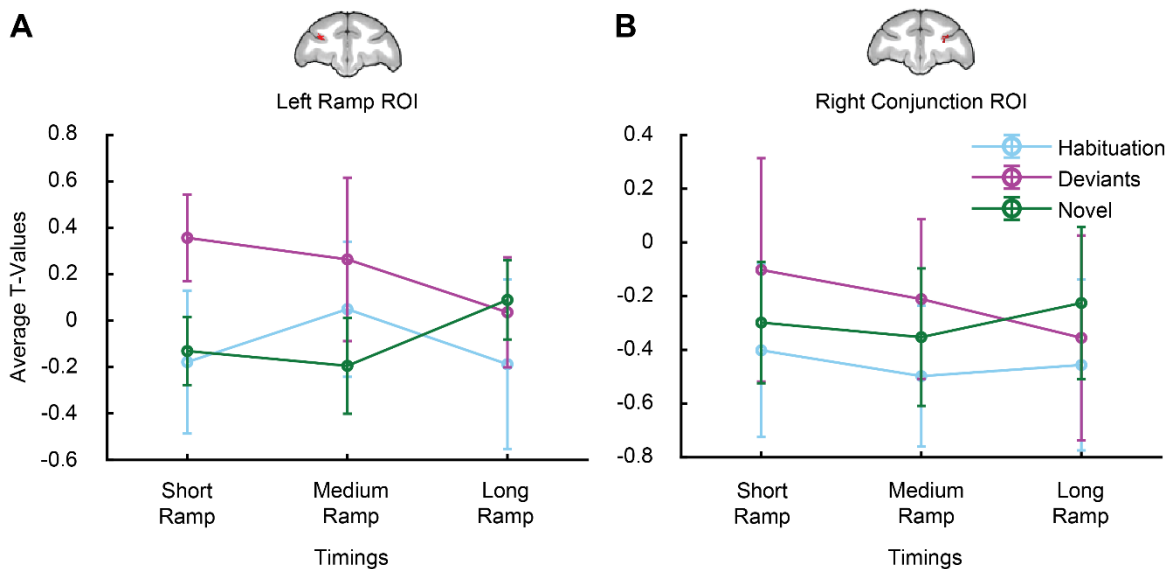


**Figure 24. Structured timing does not drive ramping activity in the DLPFC in Time Only.** T-values for the condition of interest > baseline shown. **A.** Onset activity for all short, medium, and long habituation timings assigned to novel stimuli (green line), compared to short, medium, and long habituation timings assigned to habituation images

(light blue line) and short, medium, and long habituation timings assigned to deviants combined with habituation stimuli (purple line) in left ramp ROI showed no significant difference. **B.** Onset activity for all short, medium, and long habituation timings assigned to novel stimuli (green line), compared to short, medium, and long habituation timings assigned to habituation images (light blue line) and short, medium, and long habituation timings assigned to deviants combined with habituation stimuli (purple line) in right conjunction ROI showed no significant difference. Error bars are 95% confidence intervals (1.96 x standard error of the within-bin mean).

In our previous study, deviant images elicited activity in the DLPFC when they were components of an abstract visual sequence. Therefore, we aimed to determine whether animals were similarly tracking for deviant fractal appearance in a way that would elicit ramping activity, potentially indicating monitoring in the absence of an abstract rule. To test for ramping related to a deviant response in DLPFC outside of the sequential context, we compared deviant images that had habituation timing templates to habituation images assigned to habituation timing ramping activity. This would allow us to test for effects that are specific for the image type, and not the structured timing.

Results from this comparison show areas including the insula, VLPFC, and dorsal Pre-motor are significantly more active for groups containing deviant fractals. This brain areas have also been shown to respond to deviant responses in tasks containing auditory sequences (L. Wang et al., 2015). It is possible that there is a deviant response simply from the infrequent images that results in higher ramping activity. Overall, while there is interesting timing related activity in other related brain structures, there is no evidence that structured timing modulates ramping dynamics in the DLPFC.

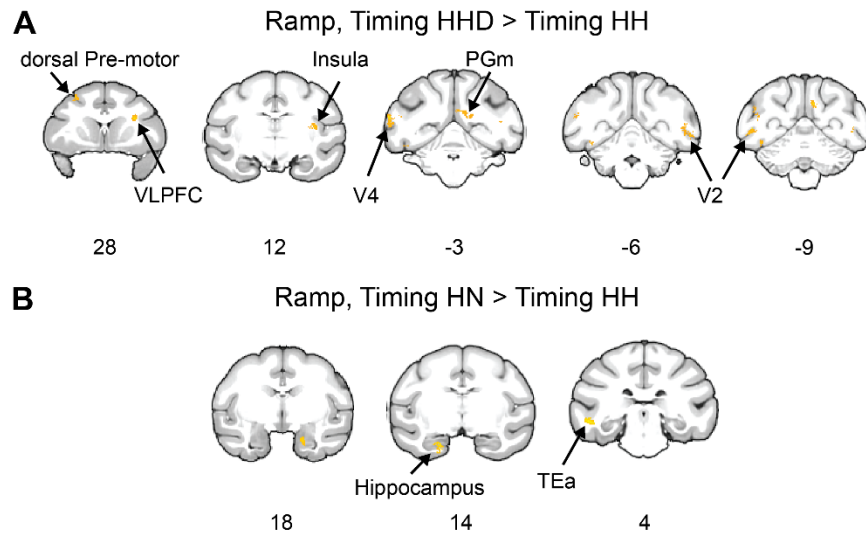


**Figure 25. No effect of deviant or novel image ramping activity when compared to habituation images with the same timing templates in Time Only. A.** Ramp, Habituation Timings assigned to Habituation and Deviant Images (HHD) > Habituation Timings assigned to Habituation Images (HH) (FDRc  $p < 0.05$ , height  $p < 0.005$  unc., ext. 90). **B.** Ramp, Habituation Timings assigned to Novel Images > Habituation Timings assigned to Habituation Images (HH) (FDRc  $p < 0.05$ , height  $p < 0.005$  unc., ext. 106).

### 3.4.10. Simply viewing random fractal images is not enough to elicit DLPFC activity

As part of our 2x2 study design, we included a task variant which isolated individual fractal images (as described in **Figure 12**). In the Random task (**Figure 15**) the fractal images used in all previous task variants are serially presented with no rule or timing. This task is meant to function as a control, such that we could test the following predictions. First, we aimed to test whether animals were attending to the task overall. Given that this is a no response task, we have limited ways in testing for task engagement. Therefore, while animals could be fixating, there is a possibility that they are not attending to the image contents. The random task variant is structured similarly to the time only variant, in that the final block contains novel fractal images. Other awake monkey fMRI studies have demonstrated that novelty responses in the brain only occur when animals are attending (Monosov et al., 2015; Zhang et al., 2019). Therefore, observing novelty responses in

this task would allow us to determine task engagement in absence of a response. Second, we aimed to test whether the DLPFC exclusively shows ramping responses due to sequential monitoring, and not due to other processes such as anticipating the end of a block, or simply viewing images. Previous work has suggested that ramping dynamics in the PFC can arise simply due to anticipation of a particular event (Berdyeva & Olson, 2011; Coull & Nobre, 2008; Roesch & Olson, 2007). Therefore, while this task does not contain structured timing as we have presented previously, it is possible that neural responses tested in other task variants could be misinterpreted for a goal progression response.

#### **3.4.11. Animals attend to task stimuli**

Similar to the analysis carried out in the timing only section, we conducted a control comparison to determine whether animals were generally attending to visual stimuli. For this comparison we contrasted activity from novel images compared to habituation images. Findings from the contrasted Random Deviant > Habituation Images (**Figure 26 A**) and Random Novel > Habituation Images (**Figure 26, B**) show activity in brain areas that have been identified as being related to novelty detection when compared to highly familiar stimuli during passive viewing, including VLPFC (Ghazizadeh et al., 2020). These results mirror the findings from the timing only task, further supporting that animals are attending to the changing stimuli, but not necessarily processing them as sequential information in the absence of an abstract rule.

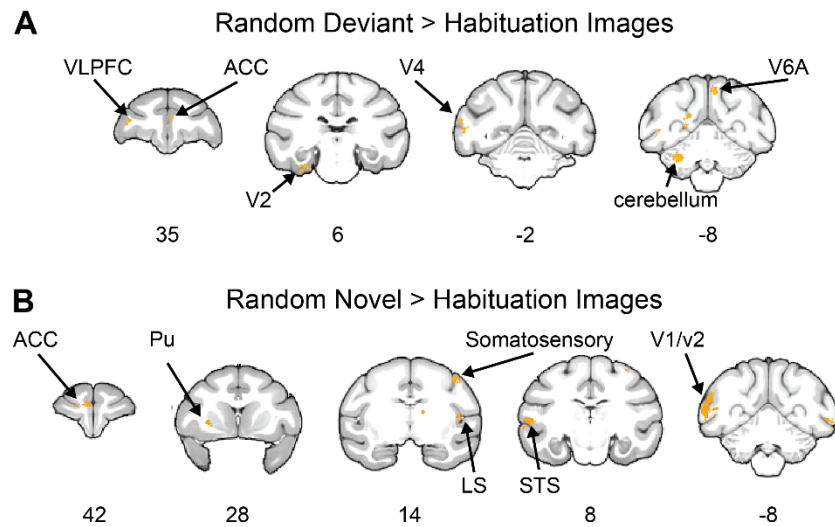


**Figure 26. Responses related to detecting deviants and novel images indicate animals attend to task stimuli during Random task. A.** Random Deviant > Habituation Images (FDRc  $p < 0.05$ , height  $p < 0.005$  unc., ext. 89). **B.** Random Novel > Habituation Images (FDRc  $p < 0.05$ , height  $p < 0.005$  unc., ext. 91).

### 3.4.12. Task progression in the absence of abstract rule and structured time does not elicit increasing activity in area 46

In another control analysis we tested our main hypothesis that simply viewing fractal images would not elicit ramping responses related to progression through the block. We specifically tested for increasing ramp-like dynamics that would indicate monitoring in the absence of an abstract rule and structured timing. To do this, we created a model in which position onsets were pseudo assigned in a similar manner to onsets from the Rule Only task. ROI analysis for position activity showed a significant effect of position for novel images on the left ramp ROI, other comparisons did not show a significant effect of position in area 46 (**Figure 27, Table 12**).

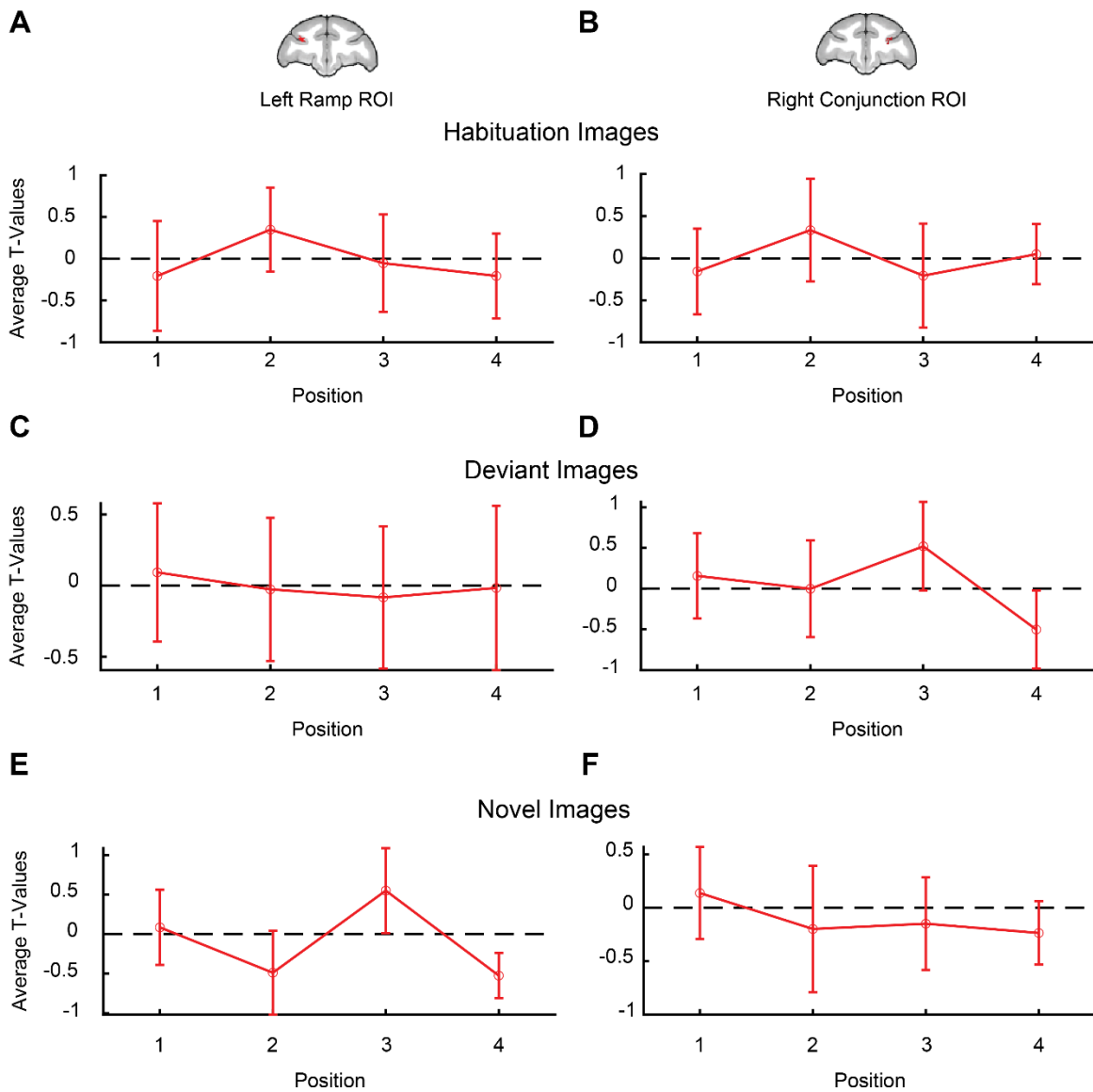


**Figure 27. Ramping pattern of activity is not present in the DLPFC in the absence of abstract rule or structured timing in Random task.** T-values for the condition of interest > baseline shown. **A, B.** Position onset activity for random habituation images in left ramp ROI and right conjunction ROI showed no significant difference. **C, D.** Position onset activity for random deviant images in left ramp ROI and right conjunction ROI showed no significant difference. **E, F.** Position onset activity for random novel images in left ramp ROI and right conjunction ROI showed no significant difference. Error bars are 95% confidence intervals (1.96 x standard error of the within-bin mean).

**Table 12. Repeated measures ANOVAs comparing position activity in left ramp ROI and right ramp ROI**

Factor	dfs	left ramp ROI			right ramp ROI		
		F	p	$\eta_p^2$	F	p	$\eta_p^2$
<i>Random Habituation Positions 1-4</i>							
Position	3, 21	2.5	0.088	0.263	0.35	0.8	0.05
Monkey	2, 7	1.03	0.40	0.223	0.5	0.64	0.12
Ramp	1, 7	0.065	0.81	0.009	0	0.99	< 0.001
<i>Random Deviant Positions 1-4</i>							
Position	3, 21	0.13	0.94	0.02	1.87	0.17	0.21
Monkey	2, 7	1.02	0.41	0.23	2.4	0.16	0.41
Ramp	1, 7	0.28	0.62	0.04	3.05	0.12	0.30
<i>Random Novel Positions 1-4</i>							
Position	3, 21	5.63	0.005	0.45	0.33	0.81	0.45
Monkey	2, 7	0.16	0.86	0.04	0.11	0.9	0.029
Ramp	1, 7	2.09	0.19	0.23	1.03	0.34	0.13

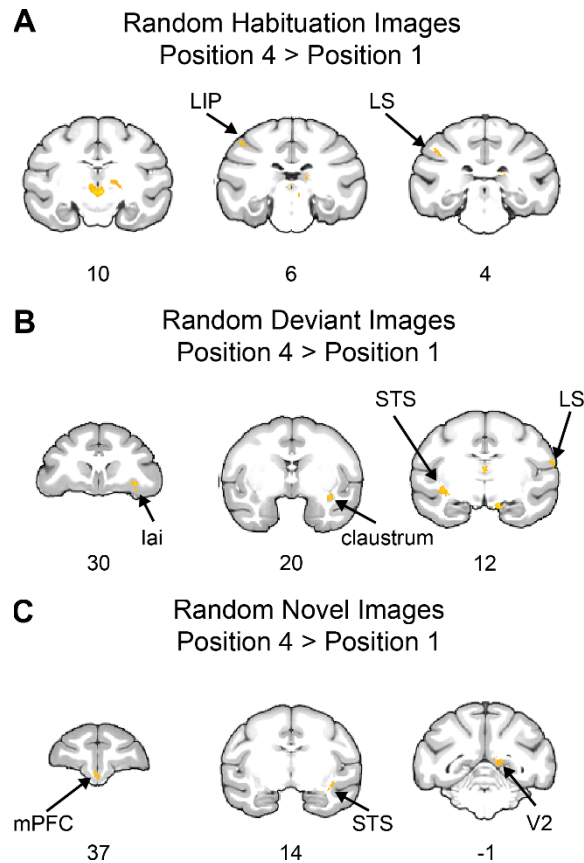


**Figure 28. No increase in activity at last position compared to first in area 46 for isolated image during Random task. A. Random Habituation Images Position 4 > Position 1 (FDRc  $p < 0.05$ , height  $p < 0.005$  unc., ext. 93). B.**

Random Deviant Images Position 4 > Position 1 (FDRc  $p < 0.05$ , height  $p < 0.005$  unc., ext. 106). C. Random Deviant Images Position 4 > Position 1 (FDRc  $p < 0.05$ , height  $p < 0.005$  unc., ext. 91). Lateral Intraparietal Area (LIP), Lateral Sulcus (LS), Intermediate Agranular Insular Area (Iai), Medial Prefrontal Cortex (mPFC).

We additionally contrasted the last position activity to first position activity to test for the possibility of increasing activity in other brain areas (**Figure 28**). Contrasts of Position 4 > Position 1 across all image categories did not show significant activity in left area 46. However, we did observe activity in the lateral intraparietal area, superior temporal sulcus, and medial PFC.

As an additional test for ramping dynamics in area 46 during this task, we utilized the same model designed to isolate these dynamics as described in (**Methods**, Yusif Rodriguez et al., 2022). In this control analysis, we found that activity was not significantly different for ramping across different image categories (**Figure 29**; left ramp ROI; image:  $F(2, 14) = 2.6$ ,  $p = 0.1$ ,  $\eta_p^2 = 0.27$ ; image x monkey:  $F(4, 14) = 0.965$ ,  $p = 0.46$ ,  $\eta_p^2 = 0.5$ ; right conjunction ROI; image:  $F(2, 14) = 0.107$ ,  $p = 0.9$ ,  $\eta_p^2 = 0.0151$ ; image x monkey:  $F(4, 14) = 0.79$ ,  $p = 0.55$ ,  $\eta_p^2 = 0.086$ ).

Overall, results from our random task confirmed our control predictions. First, we were able to determine that animals are attending to the image set that is being presented, as evidence by neural activity in brain areas known to process novelty. Additionally, we do not observe ramping dynamics in the DLPFC for progression through the images. Overall, animals are attending to the stimuli, and ramping does not occur for random image presentations in the absence of an abstract rule or timing structure.

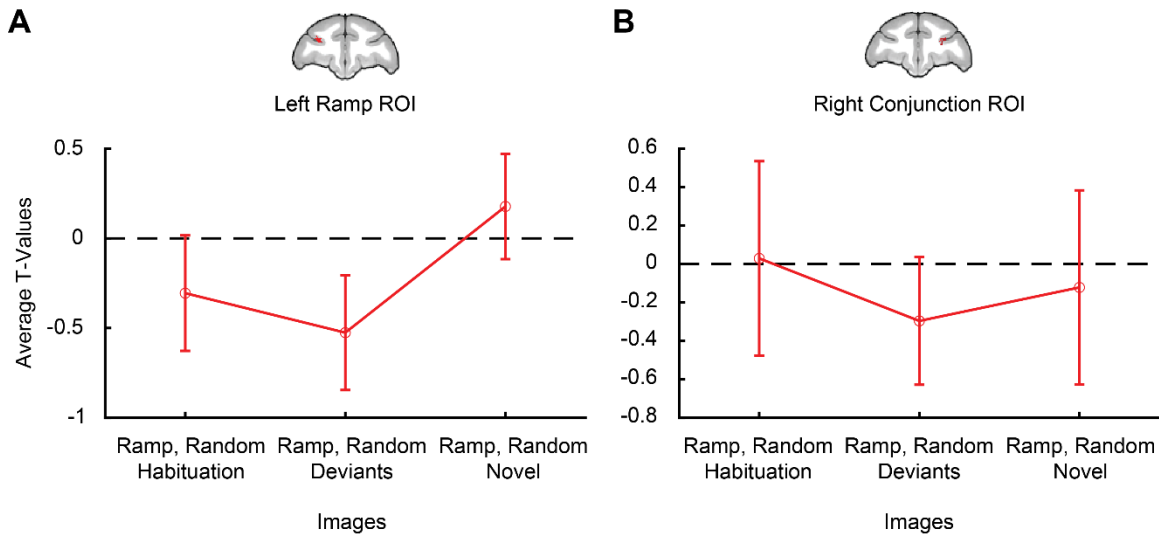


**Figure 29. A parametric ramping novel supports the prediction that the DLPFC does not show ramping activity in different stimulus categories in the absence of abstract rule and structured timing during Random task.** T-values for the condition of interest > baseline shown. **A.** Ramping activity across image categories in the random task in left ramp ROI showed no significant difference. **B.** Ramping activity across image categories in the random task in right conjunction ROI showed no significant difference. Error bars are 95% confidence intervals (1.96 x standard error of the within-bin mean).

### 3.4.13. Cross task comparisons show significant differences in area 46 activity when abstract rule and structured timing are present

For our final set of analyses, we first compared activity between the Rule Only and Random task for position. Our tasks were designed such that we would be able to compare activity across position for the first pair of tasks, to determine whether there were any significant differences between observed neural activity in progression across positions. Comparisons between the Rule only and Random tasks for ramping activity across position was not significantly different (left ramp ROI; position:  $F(3, 66) = 1.3$ ,  $p = 0.3$ ,  $\eta_p^2 = 0.12$ ; right conjunction ROI; position:  $F(3, 66) = 0.95$ ,  $p = 0.42$ ,  $\eta_p^2 = 0.02$ )

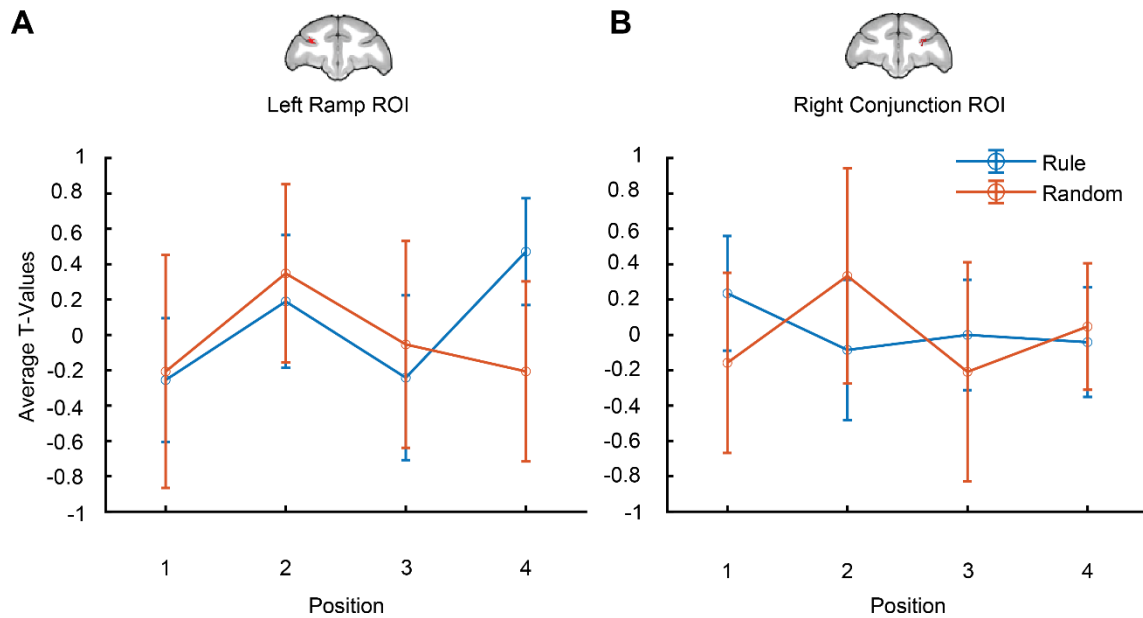


**Figure 30. Comparison across position activity for Rule Only compared to Random is not significant.** T-values for the condition of interest > baseline shown. **A.** Position activity across habituation in left ramp ROI showed no significant difference. **B.** Position activity across habituation in right conjunction ROI showed no significant difference. Error bars are 95% confidence intervals (1.96 x standard error of the within-bin mean).

Due to the design of our tasks, it was not possible to similarly compare activity across all tasks at each individual fractal onset. Therefore, to determine differences between ramping activity across tasks we compared activity modelled as a parametric ramp. An ANOVA comparison showed significant differences between tasks. Tukey’s post-hoc test showed a significant difference between ramping in the no-response abstract visual sequence task (original task described in Yusif Rodriguez et al., 2022) and the random task (ANOVA;  $F(3, 52) = 5.0298$   $p = 0.0039$ ). As illustrated in **Figure 31**, the combined activity from the no-response sequence task containing both time and rule show the highest t-values, while the Random task show the lowest. Data from the Rule Only and Time Only tasks show intermediate t-values when compared to the no-response sequence task and Random task. Findings from these comparisons suggest that abstract rule and structured timing

in isolation individually contribute to the neural activity observed for when these are combined for an abstract visual sequence representation.

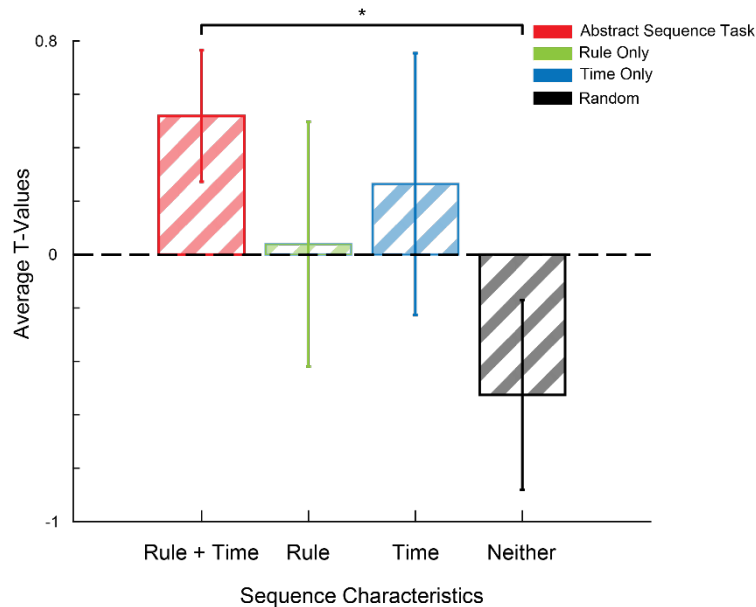


**Figure 31. Left area 46 ramping activity across tasks suggests additive effect of abstract rule and structured timing.** T-values in left Ramp ROI for parametric ramping in habituation image categories across all tasks. Activity in this region for the no-response abstract visual sequence task (Structured Time + Abstract Rule, red) is significantly different than activity in the same region during habituation image viewing during the Random task (No Structured Time + No Abstract Rule, black). There are no significant differences between the Rule Only task (isolated Abstract Rule, green) or the Time Only task (isolated Structured Time, blue) when compared against all other tasks.

### 3.5. Discussion

In this study we examined how monkey DLPFC (Area 46) represents distinct abstract sequential features in isolation. We tested two main hypotheses: First, that abstract rule in the absence of a timing structure elicits DLPFC activity suggesting sequential monitoring, and that structured timing in isolation without an abstract rule elicits DLPFC. We constructed these hypotheses predicting that both characteristics contribute to a combined response in the DLPFC sub-region area 46 (Yusif Rodriguez et al., 2022). These hypotheses were tested in a 2x2 study design of no-

report viewing tasks that isolated the different features we identified as composing abstract visual sequences: abstract rule and structured timing, as well as including a control that we named random. We found evidence to support the hypothesis that both isolated abstract rule and isolated structured timing drive DLPFC activity related to abstract sequential representations in area 46 during our abstract sequential task.

Results from our rule only task variant support our previously observed findings that animals are engaging in abstract sequence monitoring. Specifically, we saw ramping activity occurring in area 46 for abstract rule. This finding suggests that isolated rule is sufficient to elicit increased area 46 ramping activity, potentially indicating that animals are monitoring the abstract sequential structure. Our data from whole brain activity further supports these findings. We identified a significant cluster of activity when contrasting Position 4 > Position 1 in other additional brain areas. Some of these areas have been identified as being involved in tasks with similar features as sequential tasks, including the hippocampus during visual statistical learning (Cerreta et al., 2018; Schapiro et al., 2016; Schlichting et al., 2013), suggesting that working memory could be playing a role and animals are engaged in remembering their place in the sequence. It is then possible that abstract rule on its own is a characteristic that determines “what is a sequence” in the context of our task. Overall, these findings are consistent with our expected results based on previous work in humans, where ramping activity mainly depended on the monitoring of sequential images following a specific abstract rule (Desrochers et al., 2015, 2019).

Another characteristic present in abstract sequences that has been known to influence neural dynamics in DLPFC is timing. Tasks in humans and animals have shown that different types of timing processing, such as prediction of intervals or progression towards a goal elicits ramping activity in the DLPFC (M. Xu et al., 2014). Other brain areas have also been identified as being

involved during time processing including the basal ganglia (Monosov et al., 2015), the cerebellum, and motor cortical regions (Merchant & Averbach, 2017). However, given the potential influence of timing in the previously observed DLPFC activity during abstract sequential tasks we tested the dynamics of structured timing in isolation.

We predicted that isolated timing would modulate DLPFC activity based on prior literature. Our initial findings from the Time Only task did not provide evidence that structured timing in isolation influences DLPFC activity. There are a few speculations as to why we didn't observe any ramping responses related to isolated structured timing. First, many of the experiments studying timing often have a task directed at making a choice related to the timing itself. Studies showing ramping dynamics in the brain related to elapsed time, often demand that a decision is made (Blanchard et al., 2015; de Lange et al., 2010), or occur during task engagement towards a goal (even if that goal is timing related) (J. Kim et al., 2013; M. Xu et al., 2014). In these instances, it is possible there are multiple variables that can explain these neural dynamics. First, animals are completing additional cognitive computations, such as decisions, which can contribute to the observed ramping signal. Additionally, because animals have to provide a specific response, it means that their attention is oriented towards the event which is directly being anticipated in time. Previous literature has shown that attending to time events and stimuli results in a signal gain (reviewed in A. C. Nobre & van Ede, 2018). It can be argued that, in our task design the most consistent and salient stimulus throughout all task variants are the fractal visual stimuli. This would in turn mean that, animals were not attending to the timing structure in such a way that it could elicit ramping dynamics in the way that previous studies in timing have shown. Additionally, this would support our findings that ramping occurs during all events that have abstract sequential image presentations since these are being actively attended to. Another possibility is that this type of structured timing

does not drive ramping dynamics. However, in order to determine this it would be necessary to construct a task that would better allow us to account for the influence of different timing structures in sequential tasks.

Comparisons between task variants suggest a potentially intermediate effect of abstract rule and structured timing when presented in isolated, compared to when they are combined in a sequential structure. When comparing for position effects between the Rule Only and Random tasks, we did not see a significant increase in ramping across sequence position. While this was not necessarily unexpected, we did predict that there would be a significant difference for position increase ramping activity between Rule Only and the Random task variants. It is possible that the statistical test used was not appropriate to determine the difference in activity between both variants. However, findings from the Rule Only task show a significant response for ramping throughout position, while this type of dynamic is non-existent in the Random task. When comparing across tasks using a parametric model, we instead are able to see significant differences in activity in area 46 when there is abstract rule when combined with structured timing (no-response abstract visual sequence task) as opposed to when neither of these characteristics are present (Random task). While there is not a significant difference between the Rule Only and Time only task when compared to other task variants, it is worth noting that their values lie in between the values for task variants containing either a combination of these characteristics or none. The data trends suggest a potential intermediate modulation of area 46 neural activity when only some sequential characteristics are present, and a compounded effect when they are both used to define a sequential structure, positively modulating DLPFC dynamics.

Ramping dynamics are present for a variety of cognitive processes, one of which is anticipation. It is worth noting that there is a variety of information that can drive anticipatory responses.

Anticipation, and its related neural dynamics have been studied in the context of anticipating a reward (Falcone et al., 2019; McKim & Desrochers, 2022b; Monosov et al., 2015), decision-making (de Lange et al., 2010; Lin et al., 2020), and goal related anticipation (Borra et al., 2011; Ma et al., 2014; Peters et al., 2005). While many of these are not of concern in our particular set of no-response tasks (reward is specifically decorrelated from task events; there is no decision or explicit goal), it was possible that anticipating the end of a block or run could elicit DLPFC ramping. However, when testing for ramping related to continuing through fractal images, it is evident that there was no neural activity in the DLPFC that indicated block end anticipation.

Because our tasks were no-response, there was a possibility that animals could be viewing stimuli, but not necessarily attending to the different task contents and organization. Previous work has shown that without attention, task relevant dynamics do not occur (Bekinschtein et al., 2009; Chennu et al., 2013). Additionally, it has been demonstrated using no-response awake monkey fMRI, that both novel and familiar task images elicit neural responses in specific brain areas including the VLPFC, but only if animals are attending and engaged (Ghazizadeh et al., 2020). When testing for responses related to image deviants, we did not see neural activity indicating that deviants were being processed as changes in the same way as when they are placed in an abstract sequence. However, when identifying if novelty responses existed in our task, as an indicator of attention, we see similar brain areas active in both our Time Only and Random task variants. In either variant, both deviants and novel image contrasts showed activity in brain areas relevant to novelty processing such as the VLPFC, striatum and parietal cortex (**Figure 21, Figure 26**). Overall these findings suggest that animals are attending the stimuli, and not processing task relevant stimuli the same way as when they are organized according to abstract rule.

Some limitations on the present study were as follows. First, we are limited in the assertions that can be made regarding more active aspects of cognitive engagement given that all tasks were no-response. While the tasks were designed this way intentionally, to avoid unwanted task confounds such as decision planning or motor task engagement, the task design also limits our evaluation of behavior related to sequential task processing. However, findings from this study have allowed us to identify specific task features that can be further studied in the future work using tasks with more behavioral engagement. Therefore, findings from this set of experiments provide an important foundation for future studies that will allow us to study sequential behaviors. Another limitation we encountered was more related to the specific scope of the analysis. An awake behaving fMRI study results in a wealth of data. Given our specific hypotheses about the role of the DLPFC in abstract sequence, we have not yet determined the involvement and potential influence of other brain areas in this set of experiments. Future work can then expand on these findings through the identification of regions that contribute to the observed DLPFC neural dynamics, and the relevant networks necessary for abstract sequential monitoring.

In summary, the present study provides evidence that both abstract rule and structure timing are characteristics that in combination modulate DLPFC activity in the sub-region area 46. Additionally, this sub-region shows a ramping pattern of activity, similar to what has been shown in previous human studies during sequential task monitoring. There is a limited amount of work in non-human primates elaborating on the role of the DLPFC in abstract visual sequences. Furthermore, even fewer have identified the functional relevance of different sequential characteristics in abstract sequential monitoring and its related neural dynamics. These findings provide important information for our understanding of the functional organization of the monkey

pre-frontal cortex regarding sequential information, and the task relevant characteristics that may represent abstract sequential structures in the brain.

## Chapter 4: General Discussion and Final Remarks

### 4.1. Overall Summary and Final Remarks

In this thesis, we discuss several experiments used to determine the neural representation of abstract visual sequences in the monkey brain. While we had the benefit of having whole brain neural data using fMRI as the methods through which the experiments were conducted, we focused our hypotheses on the monkey DLPFC. Specifically, we developed distinct hypotheses for a sub-region within DLPFC known as area 46. Throughout the introduction and other chapters in this work we have highlighted that other brain areas show neural activity during abstract sequence viewing. However, we focused our attention on the monkey DLPFC due to its identified homologies in connectivity to the human RLPFC (Neubert et al., 2014; Sallet et al., 2013). This was particularly motivated by previous work completed in humans where the human RLPFC was shown to be necessary for abstract sequential monitoring (Desrochers et al., 2015, 2019; McKim & Desrochers, 2022b)

In our first experiment we identified that the DLPFC sub-region area 46 is involved in the processing of abstract visual sequences. One key finding from this study was the overlapping activity for both abstract rule and number processing in this sub-region. This is particularly interesting because we could consider a change in number itself to be construed as a different type of sequence, and similarly be processed as a deviation to an established rule. We thought that similarly to the way that a rule change is processed as an overall change in the sequential structure, requiring monitoring, that a number change would also result in an overall larger change in neural activity due to increased monitoring. Therefore, we had initially predicted that ramping dynamics would be similarly present in the DLPFC for the number deviants. This prediction was informed

by previous findings related to number processing in the brain (Dehaene et al., 2015; L. Wang et al., 2015). As shown in our no-response abstract visual sequence task, this was not the case. However, we believe this might be due to experimental design issues which limited our capacity to make any claims about the effect of number and whether it is overall processed as a higher order sequential change.

Our second key finding was determining the influence of abstract rule and structured timing in the ramping dynamics we had observed in the first experiment. Abstract sequential information, and its representation in the primate and non-human primate brain has not been extensively studied. Much of the work done in this field has focused on sequences with fixed image identities, motor sequences or active task sequences. This work is novel in that we sought to tease apart the representation of the characteristics of abstract sequences in the brain with the simplest possible set of tasks that separated each of these sequential features. This work identified that in our specific definition of a simple abstract sequence, in a no-response task, the DLPFC shows a ramping pattern of activity for abstract rule. We additionally identify that a combination of abstract rule and structured timing could modulate neural responses in the DLPFC. This suggests the engagement of animals in monitoring sequential structures given sufficient sequential characteristics present, even in the absence of an instruction to do so. We consider these findings to provide a significant contribution to the field, in helping us understand what information in our environment helps us create boundaries between sequential events.

#### **4.2. Future Directions**

As any question in science, while we gained much understanding about the neural representation of sequences in the brain, there are still many more questions left to answer for our understanding of sequential processing. One of these possible future directions consists in further parsing out how

abstract sequences are represented in the monkey PFC. In the discussed set of experiments, we studied a very specific instance of abstract sequence. Even more specifically, we studied abstract visual sequences containing two very simple possible rules and a specific timing structure. Therefore, it is unknown whether the observed dynamics would generalize across different types of sequences with different rules, length, or number of items. Future experiments could be constructed to test whether DLPFC forms generalizable abstract sequential representations. Finally, fMRI has many benefits, but it is unable to answer all questions related to specific cell level activity that could influence the observed BOLD dynamics. Future work is already developing towards using monkey electrophysiology guided by these findings to better understand the cell level dynamics in the DLPFC during sequential tasks.

## References

- Allen, T. A., Morris, A. M., Mattfeld, A. T., Stark, C. E. L., & Fortin, N. J. (2014). A sequence of events model of episodic memory shows parallels in rats and humans. *Hippocampus*, *24*(10), 1178–1188. <https://doi.org/10.1002/hipo.22301>
- Averbeck, B. B., Crowe, D. A., Chafee, M. V., & Georgopoulos, A. P. (2003). Neural activity in prefrontal cortex during copying geometrical shapes. *Experimental Brain Research*, *150*(2), 142–153. <https://doi.org/10.1007/s00221-003-1417-5>
- Averbeck, B. B., & Lee, D. (2007). Prefrontal Neural Correlates of Memory for Sequences. *Journal of Neuroscience*, *27*(9), 2204–2211. <https://doi.org/10.1523/JNEUROSCI.4483-06.2007>
- Averbeck, B. B., Sohn, J.-W., & Lee, D. (2006). Activity in prefrontal cortex during dynamic selection of action sequences. *Nature Neuroscience*, *9*(2), 276–282. <https://doi.org/10.1038/nn1634>
- Badre, D., & D'Esposito, M. (2007a). Functional magnetic resonance imaging evidence for a hierarchical organization of the prefrontal cortex. *Journal of Cognitive Neuroscience*, *19*, 2082–2099. <https://doi.org/10.1162/jocn.2007.19.12.2082>
- Badre, D., & D'Esposito, M. (2007b). Functional magnetic resonance imaging evidence for a hierarchical organization of the prefrontal cortex. *Journal of Cognitive Neuroscience*, *19*, 2082–2099. <https://doi.org/10.1162/jocn.2007.19.12.2082>
- Badre, D., Hoffman, J., Cooney, J. W., & D'Esposito, M. (2009). Hierarchical cognitive control deficits following damage to the human frontal lobe. *Nature Neuroscience*, *12*(4), 515–522. <https://doi.org/10.1038/nn.2277>
- Badre, D., & Nee, D. E. (2018). Frontal Cortex and the Hierarchical Control of Behavior. *Trends in Cognitive Sciences*, *22*(2), 170–188. <https://doi.org/10.1016/j.tics.2017.11.005>
- Barone, P., & Joseph, J.-P. (1989). Prefrontal cortex and spatial sequencing in macaque monkey. *Experimental Brain Research*, *78*(3). <https://doi.org/10.1007/BF00230234>
- Bekinschtein, T. A., Dehaene, S., Rohaut, B., Tadel, F., Cohen, L., & Naccache, L. (2009). Neural signature of the conscious processing of auditory regularities. *Proceedings of the National Academy of Sciences of the United States of America*, *106*(5), 1672–1677. <https://doi.org/10.1073/pnas.0809667106>
- Bekolay, T., Laubach, M., & Eliasmith, C. (2014). A Spiking Neural Integrator Model of the Adaptive Control of Action by the Medial Prefrontal Cortex. *Journal of Neuroscience*, *34*(5), 1892–1902. <https://doi.org/10.1523/JNEUROSCI.2421-13.2014>

- Bellet, J., Gay, M., Dwarakanath, A., Jarraya, B., van Kerkoerle, T., Dehaene, S., & Panagiotaropoulos, T. I. (2022). Decoding rapidly presented visual stimuli from prefrontal ensembles without report nor post-perceptual processing. *Neuroscience of Consciousness*, 2022(1), niac005. <https://doi.org/10.1093/nc/niac005>
- Berdyeva, T. K., & Olson, C. R. (2010). Rank Signals in Four Areas of Macaque Frontal Cortex During Selection of Actions and Objects in Serial Order. *Journal of Neurophysiology*, 104(1), 141–159. <https://doi.org/10.1152/jn.00639.2009>
- Berdyeva, T. K., & Olson, C. R. (2011). Relation of ordinal position signals to the expectation of reward and passage of time in four areas of the macaque frontal cortex. *Journal of Neurophysiology*, 105(5), 2547–2559. <https://doi.org/10.1152/jn.00903.2010>
- Bernardi, S., Benna, M. K., Rigotti, M., Munuera, J., Fusi, S., & Salzman, C. D. (2020). The Geometry of Abstraction in the Hippocampus and Prefrontal Cortex. *Cell*, 0(0). <https://doi.org/10.1016/j.cell.2020.09.031>
- Blanchard, T. C., Strait, C. E., & Hayden, B. Y. (2015). Ramping ensemble activity in dorsal anterior cingulate neurons during persistent commitment to a decision. *Journal of Neurophysiology*, 114(4), 2439–2449. <https://doi.org/10.1152/jn.00711.2015>
- Bodnar et al. (n.d.). *Automatic change detection in vision: Adaptation, memory mismatch, or both? II: Oddball and adaptation effects on event-related potentials.*
- Boehnke, S. E., Berg, D. J., Marino, R. A., Baldi, P. F., Itti, L., & Munoz, D. P. (2011). Visual adaptation and novelty responses in the superior colliculus. *The European Journal of Neuroscience*, 34(5), 766–779. <https://doi.org/10.1111/j.1460-9568.2011.07805.x>
- Borra, E., Ferroni, C. G., Gerbella, M., Giorgetti, V., Mangiaracina, C., Rozzi, S., & Luppino, G. (2019). Rostro-caudal Connectional Heterogeneity of the Dorsal Part of the Macaque Prefrontal Area 46. *Cerebral Cortex*, 29(2), 485–504. <https://doi.org/10.1093/cercor/bhx332>
- Borra, E., Gerbella, M., Rozzi, S., & Luppino, G. (2011). Anatomical Evidence for the Involvement of the Macaque Ventrolateral Prefrontal Area 12r in Controlling Goal-Directed Actions. *Journal of Neuroscience*, 31(34), 12351–12363. <https://doi.org/10.1523/JNEUROSCI.1745-11.2011>
- Broca, P. (1861). Remarques sur le siège de la faculté du langage articulé, suivies d'une observation d'aphémie (perte de la parole). *Bulletin et Memoires de La Societe Anatomique de Paris*, 6, 330–357.
- Bunge, S. A., Helskog, E. H., & Wendelken, C. (2009). Left, but not right, rostrolateral prefrontal cortex meets a stringent test of the relational integration hypothesis. *NeuroImage*, 46(1), 338–342. <https://doi.org/10.1016/j.neuroimage.2009.01.064>

- Burgess, P. W., Scott, S. K., & Frith, C. D. (2003). The role of the rostral frontal cortex (area 10) in prospective memory: A lateral versus medial dissociation. *Neuropsychologia*, *41*(8), 906–918. [https://doi.org/10.1016/S0028-3932\(02\)00327-5](https://doi.org/10.1016/S0028-3932(02)00327-5)
- Carpenter, A. F., Baud-Bovy, G., Georgopoulos, A. P., & Pellizzer, G. (2018). Encoding of Serial Order in Working Memory: Neuronal Activity in Motor, Premotor, and Prefrontal Cortex during a Memory Scanning Task. *Journal of Neuroscience*, *38*(21), 4912–4933. <https://doi.org/10.1523/JNEUROSCI.3294-17.2018>
- Cerreta, A. G. B., Vickery, T. J., & Berryhill, M. E. (2018). Visual statistical learning deficits in memory-impaired individuals. *Neurocase*, *24*(5–6), 259–265. <https://doi.org/10.1080/13554794.2019.1579843>
- Chennu, S., Noreika, V., Gueorguiev, D., Blenkmann, A., Kochen, S., Ibanez, A., Owen, A. M., & Bekinschtein, T. A. (2013). Expectation and Attention in Hierarchical Auditory Prediction. *Journal of Neuroscience*, *33*(27), 11194–11205. <https://doi.org/10.1523/JNEUROSCI.0114-13.2013>
- Chiba, A., Morita, K., Oshio, K., & Inase, M. (2021). Neuronal activity in the monkey prefrontal cortex during a duration discrimination task with visual and auditory cues. *Scientific Reports*, *11*(1), Article 1. <https://doi.org/10.1038/s41598-021-97094-w>
- Chiew, K. S., Stanek, J. K., & Adcock, R. A. (2016). Reward Anticipation Dynamics during Cognitive Control and Episodic Encoding: Implications for Dopamine. *Frontiers in Human Neuroscience*, *10*. <https://doi.org/10.3389/fnhum.2016.00555>
- Clower, W. T., & Alexander, G. E. (1998). Movement sequence-related activity reflecting numerical order of components in supplementary and presupplementary motor areas. *Journal of Neurophysiology*, *80*(3), 1562–1566.
- Conway, C. M., & Christiansen, M. H. (2005). Modality-Constrained Statistical Learning of Tactile, Visual, and Auditory Sequences. *Journal of Experimental Psychology: Learning, Memory, and Cognition*, *31*(1), 24–39. <https://doi.org/10.1037/0278-7393.31.1.24>
- Coull, J. T., & Nobre, A. C. (2008). Dissociating explicit timing from temporal expectation with fMRI. *Current Opinion in Neurobiology*, *18*(2), 137–144. <https://doi.org/10.1016/j.conb.2008.07.011>
- Cueva, C. J., Saez, A., Marcos, E., Genovesio, A., Jazayeri, M., Romo, R., Salzman, C. D., Shadlen, M. N., & Fusi, S. (2020). Low-dimensional dynamics for working memory and time encoding. *Proceedings of the National Academy of Sciences*, *117*(37), 23021–23032. <https://doi.org/10.1073/pnas.1915984117>
- Daffner, K. R., Scinto, L. F. M., Weitzman, A. M., Faust, R., Rentz, D. M., Budson, A. E., & Holcomb, P. J. (2003). Frontal and Parietal Components of a Cerebral Network Mediating

- Voluntary Attention to Novel Events. *Journal of Cognitive Neuroscience*, 15(2), 294–313. <https://doi.org/10.1162/089892903321208213>
- Dahms, C., Brodoehl, S., Witte, O. W., & Klingner, C. M. (2020). The importance of different learning stages for motor sequence learning after stroke. *Human Brain Mapping*, 41(1), 270–286. <https://doi.org/10.1002/hbm.24793>
- Darriba, Á., & Waszak, F. (2018). Predictions through evidence accumulation over time. *Scientific Reports*, 8(1), 1–15. <https://doi.org/10.1038/s41598-017-18802-z>
- de Lange, F. P., Jensen, O., & Dehaene, S. (2010). Accumulation of evidence during sequential decision making: The importance of top-down factors. *The Journal of Neuroscience*, 30(2), 731–738. <https://doi.org/10.1523/JNEUROSCI.4080-09.2010>
- Dehaene, S., Meyniel, F., Wacongne, C., Wang, L., & Pallier, C. (2015). The Neural Representation of Sequences: From Transition Probabilities to Algebraic Patterns and Linguistic Trees. *Neuron*, 88(1), 2–19. <https://doi.org/10.1016/j.neuron.2015.09.019>
- Desrochers, T. M., Ahuja, A., Maechler, M. R., Shires, J., Yusif Rodriguez, N., & Berryhill, M. E. (2022). Caught in the ACTS: Defining Abstract Cognitive Task Sequences as an Independent Process. *Journal of Cognitive Neuroscience*, 34(7), 1103–1113. [https://doi.org/10.1162/jocn\\_a\\_01850](https://doi.org/10.1162/jocn_a_01850)
- Desrochers, T. M., Burk, D. C., Badre, D., & Sheinberg, D. L. (2016). The Monitoring and Control of Task Sequences in Human and Non-Human Primates. *Frontiers in Systems Neuroscience*, 9(January), 1–18. <https://doi.org/10.3389/fnsys.2015.00185>
- Desrochers, T. M., Chatham, C. H., & Badre, D. (2015). The necessity of rostralateral prefrontal cortex for higher-level sequential behavior. *Neuron*, 87(6), 1357–1368. <https://doi.org/10.1016/j.neuron.2015.08.026>
- Desrochers, T. M., Collins, A. G. E., & Badre, D. (2019). Sequential Control Underlies Robust Ramping Dynamics in the Rostrolateral Prefrontal Cortex. *The Journal of Neuroscience*, 39(8), 1471–1483. <https://doi.org/10.1523/JNEUROSCI.1060-18.2018>
- Ding, L. (2015). Distinct dynamics of ramping activity in the frontal cortex and caudate nucleus in monkeys. *Journal of Neurophysiology*, 114(3), 1850–1861. <https://doi.org/10.1152/jn.00395.2015>
- Du, J., Rolls, E. T., Cheng, W., Li, Y., Gong, W., Qiu, J., & Feng, J. (2020). Functional connectivity of the orbitofrontal cortex, anterior cingulate cortex, and inferior frontal gyrus in humans. *Cortex*, 123, 185–199. <https://doi.org/10.1016/j.cortex.2019.10.012>
- Eiselt, A.-K., & Nieder, A. (2013). Representation of Abstract Quantitative Rules Applied to Spatial and Numerical Magnitudes in Primate Prefrontal Cortex. *Journal of Neuroscience*, 33(17), 7526–7534. <https://doi.org/10.1523/JNEUROSCI.5827-12.2013>

- Ekman, M., Kok, P., & de Lange, F. P. (2017). Time-compressed preplay of anticipated events in human primary visual cortex. *Nature Communications*, 8(1), 15276. <https://doi.org/10.1038/ncomms15276>
- Emmons, E. B., De Corte, B. J., Kim, Y., Parker, K. L., Matell, M. S., & Narayanan, N. S. (2017). Rodent Medial Frontal Control of Temporal Processing in the Dorsomedial Striatum. *The Journal of Neuroscience: The Official Journal of the Society for Neuroscience*, 37(36), 8718–8733. <https://doi.org/10.1523/JNEUROSCI.1376-17.2017>
- Endress, A. D., Nespors, M., & Mehler, J. (2009). Perceptual and memory constraints on language acquisition. *Trends in Cognitive Sciences*, 13(8), 348–353. <https://doi.org/10.1016/j.tics.2009.05.005>
- Falcone, R., Weintraub, D. B., Setogawa, T., Wittig, J. H., Chen, G., & Richmond, B. J. (2019). Temporal Coding of Reward Value in Monkey Ventral Striatal Tonicly Active Neurons. *Journal of Neuroscience*, 39(38), 7539–7550. <https://doi.org/10.1523/JNEUROSCI.0869-19.2019>
- Farooqui, A. A., Mitchell, D., Thompson, R., & Duncan, J. (2012). Hierarchical Organization of Cognition Reflected in Distributed Frontoparietal Activity. *Journal of Neuroscience*, 32(48), 17373–17381. <https://doi.org/10.1523/JNEUROSCI.0598-12.2012>
- Fedorenko, E., Scott, T. L., Brunner, P., Coon, W. G., Pritchett, B., Schalk, G., & Kanwisher, N. (2016). Neural correlate of the construction of sentence meaning. *Proceedings of the National Academy of Sciences of the United States of America*, 113(41), E6256–E6262. <https://doi.org/10.1073/pnas.1612132113>
- Fiser, J., & Aslin, R. N. (2002). Statistical Learning of Higher-Order Temporal Structure from Visual Shape Sequences. *Journal of Experimental Psychology: Learning Memory and Cognition*, 28(3), 458–467. <https://doi.org/10.1037//0278-7393.28.3.458>
- Fujii, N., & Graybiel, A. M. (2003). Representation of Action Sequence Boundaries by Macaque Prefrontal Cortical Neurons. *Science*, 301(5637), 1246–1249. <https://doi.org/10.1126/science.1086872>
- Garrido, M. I., Kilner, J. M., Stephan, K. E., & Friston, K. J. (2009). The mismatch negativity: A review of underlying mechanisms. *Clinical Neurophysiology*, 120(3), 453–463. <https://doi.org/10.1016/j.clinph.2008.11.029>
- Gerbella, M., Belmalih, A., Borra, E., Rozzi, S., & Luppino, G. (2010). Cortical Connections of the Macaque Caudal Ventrolateral Prefrontal Areas 45A and 45B. *Cerebral Cortex*, 20(1), 141–168. <https://doi.org/10.1093/cercor/bhp087>
- Gerbella, M., Borra, E., Tonelli, S., Rozzi, S., & Luppino, G. (2013). Connectional Heterogeneity of the Ventral Part of the Macaque Area 46. *Cerebral Cortex*, 23(4), 967–987. <https://doi.org/10.1093/cercor/bhs096>

- Ghazizadeh, A., Fakharian, M. A., Amini, A., Griggs, W., Leopold, D. A., & Hikosaka, O. (2020). Brain Networks Sensitive to Object Novelty, Value, and Their Combination. *Cerebral Cortex Communications*, *1*(1), tgaa034. <https://doi.org/10.1093/texcom/tgaa034>
- Gilbert, S. J., Gonen-Yaacovi, G., Benoit, R. G., Volle, E., & Burgess, P. W. (2010). Distinct functional connectivity associated with lateral versus medial rostral prefrontal cortex: A meta-analysis. *NeuroImage*, *53*(4), 1359–1367. <https://doi.org/10.1016/j.neuroimage.2010.07.032>
- Gu, B.-M., van Rijn, H., & Meek, W. H. (2015). Oscillatory multiplexing of neural population codes for interval timing and working memory. *Neuroscience & Biobehavioral Reviews*, *48*, 160–185. <https://doi.org/10.1016/j.neubiorev.2014.10.008>
- Henin, S., Turk-Browne, N. B., Friedman, D., Liu, A., Dugan, P., Flinker, A., Doyle, W., Devinsky, O., & Melloni, L. (2021). Learning hierarchical sequence representations across human cortex and hippocampus. *Science Advances*, *7*(8), eabc4530. <https://doi.org/10.1126/sciadv.abc4530>
- Henssen, A., Zilles, K., Palomero-Gallagher, N., Schleicher, A., Mohlberg, H., Gerboga, F., Eickhoff, S. B., Bludau, S., & Amunts, K. (2016). Cytoarchitecture and probability maps of the human medial orbitofrontal cortex. *Cortex*, *75*, 87–112. <https://doi.org/10.1016/j.cortex.2015.11.006>
- Horst, N. K., & Laubach, M. (2013). Reward-related activity in the medial prefrontal cortex is driven by consumption. *Frontiers in Neuroscience*, *7*. <https://doi.org/10.3389/fnins.2013.00056>
- Hoshi, E., Shima, K., & Tanji, J. (1998). Task-Dependent Selectivity of Movement-Related Neuronal Activity in the Primate Prefrontal Cortex. *Journal of Neurophysiology*, *80*(6), 3392–3397. <https://doi.org/10.1152/jn.1998.80.6.3392>
- Hutchison, R. M., & Everling, S. (2014). Broad intrinsic functional connectivity boundaries of the macaque prefrontal cortex. *NeuroImage*, *88*, 202–211. <https://doi.org/10.1016/j.neuroimage.2013.11.024>
- Jean-Baptiste Poline, M. B. (2002). *Region of interest analysis using an SPM toolbox*. 8th international conference on functional mapping of the human brain.
- Jung, B., Taylor, P. A., Seidlitz, J., Sponheim, C., Perkins, P., Ungerleider, L. G., Glen, D., & Messinger, A. (2021). A comprehensive macaque fMRI pipeline and hierarchical atlas. *NeuroImage*, *235*, 117997. <https://doi.org/10.1016/j.neuroimage.2021.117997>
- Kim, H. F., & Hikosaka, O. (2013). Distinct Basal Ganglia Circuits Controlling Behaviors Guided by Flexible and Stable Values. *Neuron*, *79*(5), 1001–1010. <https://doi.org/10.1016/j.neuron.2013.06.044>

- Kim, J., Ghim, J.-W., Lee, J. H., & Jung, M. W. (2013). Neural correlates of interval timing in rodent prefrontal cortex. *The Journal of Neuroscience*, *33*(34), 13834–13847. <https://doi.org/10.1523/JNEUROSCI.1443-13.2013>
- Kim, Y.-C., Han, S.-W., Alberico, S. L., Ruggiero, R. N., De Corte, B., Chen, K.-H., & Narayanan, N. S. (2017). Optogenetic Stimulation of Frontal D1 Neurons Compensates for Impaired Temporal Control of Action in Dopamine-Depleted Mice. *Current Biology*, *27*(1), 39–47. <https://doi.org/10.1016/j.cub.2016.11.029>
- Koechlin, E., Corrado, G., Pietrini, P., & Grafman, J. (2000). Dissociating the role of the medial and lateral anterior prefrontal cortex in human planning. *Proceedings of the National Academy of Sciences*, *97*(13), 7651–7656. <https://doi.org/10.1073/pnas.130177397>
- Krueger, P. M., van Vugt, M. K., Simen, P., Nystrom, L., Holmes, P., & Cohen, J. D. (2017). Evidence accumulation detected in BOLD signal using slow perceptual decision making. *Journal of Neuroscience Methods*, *281*, 21–32. <https://doi.org/10.1016/j.jneumeth.2017.01.012>
- Lashley, K. (1951). The problem of serial order in behavior. *1951*, *7*, 112–147. <https://doi.org/10.1093/rfs/hhq153>
- Leite, F. P., Tsao, D., Vanduffel, W., Fize, D., Sasaki, Y., Wald, L. L., Dale, A. M., Kwong, K. K., Orban, G. a, Rosen, B. R., Tootell, R. B. H., & Mandeville, J. B. (2002). Repeated fMRI using iron oxide contrast agent in awake, behaving macaques at 3 Tesla. *NeuroImage*, *16*(2), 283–294. <https://doi.org/10.1006/nimg.2002.1110>
- Lewis, P. A., & Miall, R. C. (2003). Brain activation patterns during measurement of sub- and supra-second intervals. *Neuropsychologia*, *41*(12), 1583–1592. [https://doi.org/10.1016/S0028-3932\(03\)00118-0](https://doi.org/10.1016/S0028-3932(03)00118-0)
- Lin, Z., Nie, C., Zhang, Y., Chen, Y., & Yang, T. (2020). Evidence accumulation for value computation in the prefrontal cortex during decision making. *Proceedings of the National Academy of Sciences*, *117*(48), 30728–30737. <https://doi.org/10.1073/pnas.2019077117>
- Ma, L., Hyman, J. M., Phillips, A. G., & Seamans, J. K. (2014). Tracking Progress toward a Goal in Corticostriatal Ensembles. *Journal of Neuroscience*, *34*(6), 2244–2253. <https://doi.org/10.1523/JNEUROSCI.3834-13.2014>
- Marcus, G. F., Fernandes, K. J., & Johnson, S. P. (2007). Infant Rule Learning Facilitated by Speech. *Psychological Science*, *18*(5), 387–391. <https://doi.org/10.1111/j.1467-9280.2007.01910.x>
- Marcus, G. F., Vijayan, S., Bandi Rao, S., & Vishton, P. M. (1999). Rule Learning by Seven-Month-Old Infants. *Science*, *283*(5398), 77. <https://doi.org/10.1126/science.283.5398.77>

- Matsumoto, M., Matsumoto, K., & Tanaka, K. (2007). Effects of novelty on activity of lateral and medial prefrontal neurons. *Neuroscience Research*, 57(2), 268–276. <https://doi.org/10.1016/j.neures.2006.10.017>
- May, P. J. C., & Tiitinen, H. (2010). Mismatch negativity (MMN), the deviance-elicited auditory deflection, explained. *Psychophysiology*, 47(1), 66–122. <https://doi.org/10.1111/j.1469-8986.2009.00856.x>
- McKim, T. H., & Desrochers, T. M. (2022a). Reward Value Enhances Sequence Monitoring Ramping Dynamics as Ending Rewards Approach in the Rostrolateral Prefrontal Cortex. *ENeuro*, 9(2), ENEURO.0003-22.2022. <https://doi.org/10.1523/ENeuro.0003-22.2022>
- McKim, T. H., & Desrochers, T. M. (2022b). Reward Value Enhances Sequence Monitoring Ramping Dynamics as Ending Rewards Approach in the Rostrolateral Prefrontal Cortex. *ENeuro*, 9(2), ENEURO.0003-22.2022. <https://doi.org/10.1523/ENeuro.0003-22.2022>
- McLaren, D. G., Kosmatka, K. J., Oakes, T. R., Kroenke, C. D., Kohama, S. G., Matochik, J. A., Ingram, D. K., & Johnson, S. C. (2009). A Population-Average MRI-Based Atlas Collection of the Rhesus Macaque. *NeuroImage*, 2(March 2009), 52–59. <https://doi.org/10.1016/j.neuroimage.2008.10.058>
- Meirhaeghe, N., Sohn, H., & Jazayeri, M. (2021). A precise and adaptive neural mechanism for predictive temporal processing in the frontal cortex. *Neuron*, 109(18), 2995–3011.e5. <https://doi.org/10.1016/j.neuron.2021.08.025>
- Merchant, H., & Averbeck, B. B. (2017). The Computational and Neural Basis of Rhythmic Timing in Medial Premotor Cortex. *The Journal of Neuroscience*, 37(17), 4552–4564. <https://doi.org/10.1523/JNEUROSCI.0367-17.2017>
- Meyer, T., Ramachandran, S., & Olson, C. R. (2014). Statistical Learning of Serial Visual Transitions by Neurons in Monkey Inferotemporal Cortex. *Journal of Neuroscience*, 34(28), 9332–9337. <https://doi.org/10.1523/JNEUROSCI.1215-14.2014>
- Meyer, T., Walker, C., Cho, R. Y., & Olson, C. R. (2014). Image familiarization sharpens response dynamics of neurons in inferotemporal cortex. *Nature Neuroscience*, 17(10), Article 10. <https://doi.org/10.1038/nn.3794>
- Milham, M., Petkov, C., Belin, P., Ben Hamed, S., Evrard, H., Fair, D., Fox, A., Froudust-Walsh, S., Hayashi, T., Kastner, S., Klink, C., Majka, P., Mars, R., Messinger, A., Poirier, C., Schroeder, C., Shmuel, A., Silva, A. C., Vanduffel, W., ... Zuo, Z. (2022). Toward next-generation primate neuroscience: A collaboration-based strategic plan for integrative neuroimaging. *Neuron*, 110(1), 16–20. <https://doi.org/10.1016/j.neuron.2021.10.015>
- Miller, E. K., & Cohen, J. D. (2001). *An Integrative Theory of Prefrontal Cortex Function*. 167–202.

- Milne, A. E., Petkov, C. I., & Wilson, B. (2018). Auditory and Visual Sequence Learning in Humans and Monkeys using an Artificial Grammar Learning Paradigm. *Neuroscience*, 389, 104–117. <https://doi.org/10.1016/j.neuroscience.2017.06.059>
- Milner, B. (1971). Interhemispheric differences in the localization of psychological processes in man. *British Medical Bulletin*.
- Miyashita, Y., Higuchi, S.-I., Sakai, K., & Masui, N. (1991). Generation of fractal patterns for probing the visual memory. *Neuroscience Research*, 12(1), 307–311. [https://doi.org/10.1016/0168-0102\(91\)90121-E](https://doi.org/10.1016/0168-0102(91)90121-E)
- Moayed, M., Salomons, T. V., Dunlop, K. A. M., Downar, J., & Davis, K. D. (2015). Connectivity-based parcellation of the human frontal polar cortex. *Brain Structure and Function*, 220(5), 2603–2616. <https://doi.org/10.1007/s00429-014-0809-6>
- Monosov, I. E., Leopold, D. A., & Hikosaka, O. (2015). Neurons in the Primate Medial Basal Forebrain Signal Combined Information about Reward Uncertainty, Value, and Punishment Anticipation. *Journal of Neuroscience*, 35(19), 7443–7459. <https://doi.org/10.1523/JNEUROSCI.0051-15.2015>
- Musz, E., Weber, M. J., & Thompson-Schill, S. L. (2015). Visual statistical learning is not reliably modulated by selective attention to isolated events. *Attention, Perception, & Psychophysics*, 77(1), 78–96. <https://doi.org/10.3758/s13414-014-0757-5>
- Narayanan, N. S. (2016). Ramping activity is a cortical mechanism of temporal control of action. *Current Opinion in Behavioral Sciences*, 8, 226–230. <https://doi.org/10.1016/j.cobeha.2016.02.017>
- Narayanan, N. S., & Laubach, M. (2009). Delay Activity in Rodent Frontal Cortex During a Simple Reaction Time Task. *Journal of Neurophysiology*, 101(6), 2859–2871. <https://doi.org/10.1152/jn.90615.2008>
- Naya, Y., Chen, H., Yang, C., & Suzuki, W. A. (2017). Contributions of primate prefrontal cortex and medial temporal lobe to temporal-order memory. *Proceedings of the National Academy of Sciences*, 114(51), 13555–13560. <https://doi.org/10.1073/pnas.1712711114>
- Neubert, F.-X., Mars, R. B., Thomas, A. G., Sallet, J., & Rushworth, M. F. S. (2014). Comparison of Human Ventral Frontal Cortex Areas for Cognitive Control and Language with Areas in Monkey Frontal Cortex. *Neuron*, 81(3), 700–713. <https://doi.org/10.1016/j.neuron.2013.11.012>
- Niki, H., & Watanabe, M. (1979). Prefrontal and cingulate unit activity during timing behavior in the monkey. *Brain Research*, 171(2), 213–224. [https://doi.org/10.1016/0006-8993\(79\)90328-7](https://doi.org/10.1016/0006-8993(79)90328-7)

- Ninokura, Y., Mushiake, H., & Tanji, J. (2004). Integration of temporal order and object information in the monkey lateral prefrontal cortex. *Journal of Neurophysiology*, *91*(1), 555–560. <https://doi.org/10.1152/jn.00694.2003>
- Nobre, A. C., & van Ede, F. (2018). Anticipated moments: Temporal structure in attention. *Nature Reviews Neuroscience*, *19*(1), 34–48. <https://doi.org/10.1038/nrn.2017.141>
- Nobre, A., Correa, A., & Coull, J. (2007). The hazards of time. *Current Opinion in Neurobiology*, *17*(4), 465–470. <https://doi.org/10.1016/j.conb.2007.07.006>
- Onoe, H., Komori, M., Onoe, K., Takechi, H., Tsukada, H., & Watanabe, Y. (2001). Cortical Networks Recruited for Time Perception: A Monkey Positron Emission Tomography (PET) Study. *NeuroImage*, *13*(1), 37–45. <https://doi.org/10.1006/ning.2000.0670>
- Paton, J. J., & Buonomano, D. V. (2018). The Neural Basis of Timing: Distributed Mechanisms for Diverse Functions. *Neuron*, *98*(4), 687–705. <https://doi.org/10.1016/j.neuron.2018.03.045>
- Pazo-Alvarez, P., Cadaveira, F., & Amenedo, E. (2003). MMN in the visual modality: A review. *Biological Psychology*, *63*(3), 199–236. [https://doi.org/10.1016/s0301-0511\(03\)00049-8](https://doi.org/10.1016/s0301-0511(03)00049-8)
- Peters, Y. M., O'Donnell, P., & Carelli, R. M. (2005). Prefrontal cortical cell firing during maintenance, extinction, and reinstatement of goal-directed behavior for natural reward. *Synapse*, *56*(2), 74–83. <https://doi.org/10.1002/syn.20129>
- Petrides, M. (2013). *Neuroanatomy of language regions of the human brain*. Academic Press.
- Pouthas, V., George, N., Poline, J., Pfeuty, M., VandeMoorteele, P., Hugueville, L., Ferrandez, A., Lehericy, S., LeBihan, D., & Renault, B. (2005). Neural network involved in time perception: An fMRI study comparing long and short interval estimation. *Human Brain Mapping*, *25*(4), 433–441. <https://doi.org/10.1002/hbm.20126>
- Roesch, M. R., & Olson, C. R. (2007). Neuronal activity related to anticipated reward in frontal cortex: Does it represent value or reflect motivation? *Annals of the New York Academy of Sciences*, *1121*, 431–446. <https://doi.org/10.1196/annals.1401.004>
- Saffran, J., Hauser, M., Seibel, R., Kapfhamer, J., Tsao, F., & Cushman, F. (2008). Grammatical pattern learning by human infants and cotton-top tamarin monkeys. *Cognition*, *107*(2), 479–500. <https://doi.org/10.1016/j.cognition.2007.10.010>
- Saffran, J. R., Aslin, R. N., & Newport, E. L. (1996). Statistical Learning by 8-Month-Old Infants. *Science*, *274*(5294), 1926–1928. <https://doi.org/10.1126/science.274.5294.1926>
- Saleem, K. S., Miller, B., & Price, J. L. (2014). Subdivisions and connectional networks of the lateral prefrontal cortex in the macaque monkey. *Journal of Comparative Neurology*, *522*(7), 1641–1690. <https://doi.org/10.1002/cne.23498>

- Sallet, J., Mars, R. B., Noonan, M. P., Neubert, F.-X., Jbabdi, S., O'Reilly, J. X., Filippini, N., Thomas, A. G., & Rushworth, M. F. (2013). The Organization of Dorsal Frontal Cortex in Humans and Macaques. *Journal of Neuroscience*, *33*(30), 12255–12274. <https://doi.org/10.1523/JNEUROSCI.5108-12.2013>
- Schall, J. D. (2019). Accumulators, Neurons, and Response Time. *Trends in Neurosciences*, *42*(12), 848–860. <https://doi.org/10.1016/j.tins.2019.10.001>
- Schapiro, A. C., Greogry, E., Landau, B., McCloskey, M., & Turk-Browne, N. B. (2013). The necessity of the medial temporal lobe for statistical learning. *Journal of Cognitive Neuroscience*, *26*(3), 194–198. <https://doi.org/10.1162/jocn>
- Schapiro, A. C., Rogers, T. T., Cordova, N. I., Turk-Browne, N. B., & Botvinick, M. M. (2013). Neural representations of events arise from temporal community structure. *Nature Neuroscience*, *16*(4), 486–492. <https://doi.org/10.1038/nn.3331>
- Schapiro, A. C., Turk-Browne, N. B., Norman, K. A., & Botvinick, M. M. (2016). Statistical learning of temporal community structure in the hippocampus. *Hippocampus*, *26*(1), 3–8. <https://doi.org/10.1002/hipo.22523>
- Schlichting, M. L., Guarino, K. F., Schapiro, A. C., Turk-Browne, N. B., & Preston, A. R. (2013). Hippocampal structure predicts statistical learning and associative inference abilities during development. *Journal of Cognitive Neuroscience*, *26*(3), 194–198. <https://doi.org/10.1162/jocn>
- Schultz, W. (2000). Multiple reward signals in the brain. *Nature Reviews. Neuroscience*, *1*(3), 199–207. <https://doi.org/10.1038/35044563>
- Seidlitz, J., Sponheim, C., Glen, D., Ye, F. Q., Saleem, K. S., Leopold, D. A., Ungerleider, L., & Messinger, A. (2018). A population MRI brain template and analysis tools for the macaque. *NeuroImage*, *170*, 121–131. <https://doi.org/10.1016/j.neuroimage.2017.04.063>
- Shima, K., Isoda, M., Mushiake, H., & Tanji, J. (2007). Categorization of behavioural sequences in the prefrontal cortex. *Nature*, *445*(7125), Article 7125. <https://doi.org/10.1038/nature05470>
- Shin, J. C., & Ivry, R. B. (2002). Concurrent learning of temporal and spatial sequences. *Journal of Experimental Psychology: Learning, Memory, and Cognition*, *28*(3), 445–457. <https://doi.org/10.1037/0278-7393.28.3.445>
- Sirmpilatze, N., & Klink, P. C. (2020). *RheMAP: Non-linear warps between common rhesus macaque brain templates* [Data set]. Zenodo. <https://doi.org/10.5281/zenodo.3668510>
- Soch, J., & Allefeld, C. (2018). MACS – a new SPM toolbox for model assessment, comparison and selection. *Journal of Neuroscience Methods*, *306*, 19–31. <https://doi.org/10.1016/j.jneumeth.2018.05.017>

- Strauss, M., Sitt, J. D., King, J.-R., Elbaz, M., Azizi, L., Buiatti, M., Naccache, L., Wassenhove, V. van, & Dehaene, S. (2015). Disruption of hierarchical predictive coding during sleep. *Proceedings of the National Academy of Sciences*, *112*(11), E1353–E1362. <https://doi.org/10.1073/pnas.1501026112>
- Tanji, J., & Shima, K. (1994). Role for supplementary motor area cells in planning several movements ahead. *Nature*, *371*(6496), Article 6496. <https://doi.org/10.1038/371413a0>
- Tiganj, Z., Cromer, J. A., Roy, J. E., Miller, E. K., & Howard, M. W. (2018). Compressed Timeline of Recent Experience in Monkey Lateral Prefrontal Cortex. *Journal of Cognitive Neuroscience*, *30*(7), 935–950. [https://doi.org/10.1162/jocn\\_a\\_01273](https://doi.org/10.1162/jocn_a_01273)
- Trach, J. E., McKim, T. H., & Desrochers, T. M. (2021). Abstract sequential task control is facilitated by practice and embedded motor sequences. *Journal of Experimental Psychology: Learning, Memory, and Cognition*, *47*(10), 1638–1659. <https://doi.org/10.1037/xlm0001004>
- Turk-Browne, N. B., Scholl, B. J., Chun, M. M., & Johnson, M. K. (2009). Neural Evidence of Statistical Learning: Efficient Detection of Visual Regularities Without Awareness. *Journal of Cognitive Neuroscience*, *21*(10), 1934–1945. <https://doi.org/10.1162/jocn.2009.21131>
- Uhrig, L., Dehaene, S., & Jarraya, B. (2014). A Hierarchy of Responses to Auditory Regularities in the Macaque Brain. *Journal of Neuroscience*, *34*(4), 1127–1132. <https://doi.org/10.1523/JNEUROSCI.3165-13.2014>
- Van Essen, D. C., Drury, H. A., Dickson, J., Harwell, J., Hanlon, D., & Anderson, C. H. (2001). An Integrated Software Suite for Surface-based Analyses of Cerebral Cortex. *Journal of the American Medical Informatics Association*, *8*(5), 443–459. <https://doi.org/10.1136/jamia.2001.0080443>
- Vanduffel, W., & Farivar, R. (2014). Functional MRI of Awake Behaving Macaques Using Standard Equipment. In *Advanced Brain Neuroimaging Topics in Health and Disease—Methods and Applications*. IntechOpen. <https://doi.org/10.5772/58281>
- Vanduffel, W., Fize, D., Mandeville, J. B., Nelissen, K., Van Hecke, P., Rosen, B. R., Tootell, R. B. H., & Orban, G. A. (2001). Visual motion processing investigated using contrast agent-enhanced fMRI in awake behaving monkeys. *Neuron*, *32*(4), 565–577. [https://doi.org/10.1016/S0896-6273\(01\)00502-5](https://doi.org/10.1016/S0896-6273(01)00502-5)
- Vergnienx, V., & Vogels, R. (2020). Statistical Learning Signals for Complex Visual Images in Macaque Early Visual Cortex. *Frontiers in Neuroscience*, *14*. <https://www.frontiersin.org/article/10.3389/fnins.2020.00789>
- Wallis, J. D., Anderson, K. C., & Miller, E. K. (2001). Single neurons in prefrontal cortex encode abstract rules. *Nature*, *411*(6840), Article 6840. <https://doi.org/10.1038/35082081>

- Wang, J., Narain, D., Hosseini, E. A., & Jazayeri, M. (2018). Flexible timing by temporal scaling of cortical responses. *Nature Neuroscience*, *21*(1), 102–110. <https://doi.org/10.1038/s41593-017-0028-6>
- Wang, L., Amalric, M., Fang, W., Jiang, X., Pallier, C., Figueira, S., Sigman, M., & Dehaene, S. (2019). Representation of spatial sequences using nested rules in human prefrontal cortex. *NeuroImage*, *186*, 245–255. <https://doi.org/10.1016/j.neuroimage.2018.10.061>
- Wang, L., Uhrig, L., Jarraya, B., & Dehaene, S. (2015). Representation of numerical and sequential patterns in macaque and human brains. *Current Biology: CB*, *25*(15), 1966–1974. <https://doi.org/10.1016/j.cub.2015.06.035>
- Warden, M. R., & Miller, E. K. (2010). Task-Dependent Changes in Short-Term Memory in the Prefrontal Cortex. *Journal of Neuroscience*, *30*(47), 15801–15810. <https://doi.org/10.1523/JNEUROSCI.1569-10.2010>
- Wen, T., Duncan, J., & Mitchell, D. J. (2020). Hierarchical Representation of Multistep Tasks in Multiple-Demand and Default Mode Networks. *Journal of Neuroscience*, *40*(40), 7724–7738. <https://doi.org/10.1523/JNEUROSCI.0594-20.2020>
- Wendelken, C., Chung, D., & Bunge, S. A. (2012). Rostrolateral prefrontal cortex: Domain-general or domain-sensitive? *Human Brain Mapping*, *33*(8), 1952–1963. <https://doi.org/10.1002/hbm.21336>
- White, I. M., & Wise, S. P. (1999). Rule-dependent neuronal activity in the prefrontal cortex. *Experimental Brain Research*, *126*(3), 315–335. <https://doi.org/10.1007/s002210050740>
- Xie, Y., Hu, P., Li, J., Chen, J., Song, W., Wang, X.-J., Yang, T., Dehaene, S., Tang, S., Min, B., & Wang, L. (2022). Geometry of sequence working memory in macaque prefrontal cortex. *Science*, *375*(8), 632–639. <https://doi.org/10.1126/science.abm0204>
- Xu, M., Zhang, S., Dan, Y., & Poo, M. (2014). Representation of interval timing by temporally scalable firing patterns in rat prefrontal cortex. *Proceedings of the National Academy of Sciences*, *111*(1), 480–485.
- Xu, R., Bichot, N. P., Takahashi, A., & Desimone, R. (2022). The cortical connectome of primate lateral prefrontal cortex. *Neuron*, *110*(2), 312–327.e7. <https://doi.org/10.1016/j.neuron.2021.10.018>
- Yusif Rodriguez, N. D. R., McKim, T. H., Basu, D., Ahuja, A., & Desrochers, T. M. (2022). Monkey dorsolateral prefrontal cortex represents abstract visual sequences during a no-report task. *BioRxiv*, 2022.09.19.508576. <https://doi.org/10.1101/2022.09.19.508576>
- Zhang, K., Chen, C. D., & Monosov, I. E. (2019). Novelty, Saliency, and Surprise Timing Are Signaled by Neurons in the Basal Forebrain. *Current Biology*, *29*(1), 134–142.e3. <https://doi.org/10.1016/j.cub.2018.11.012>

Zhao, F., Wang, P., Hendrich, K., Ugurbil, K., & Kim, S.-G. (2006). Cortical layer-dependent BOLD and CBV responses measured by spin-echo and gradient-echo fMRI: insights into hemodynamic regulation. *NeuroImage*, 30(4), 1149–1160. <https://doi.org/10.1016/j.neuroimage.2005.11.013>